Investigation of Bond in Unreinforced Interfaces for Partial-Depth Repairs and New Construction

Project Final Report

FINAL REPORT

February 24, 2023
WJE No. 2017.6996.0/2

PREPARED FOR:

ACI Foundation
38800 Country Club Drive
Farmington Hills, MI 48331

Precast/Prestressed Concrete Institute
200 W. Adams St Ste 2100
Chicago, IL 60606

PREPARED BY:

Wiss, Janney, Elstner Associates, Inc.
9511 North Lake Creek Parkway
Austin, Texas 78717
512.257.4800 tel

Investigation of Bond in Unreinforced Interfaces for Partial-Depth Repairs and New Construction

Project Final Report

Maggie E. Becker
Associate II

Jeffrey S. West, PhD, PE
Associate Principal

Carl J. Larosche, PE
Senior Principal

FINAL REPORT
February 24, 2023
WJE No. 2017.6996.0/2

PREPARED FOR:

ACI Foundation
38800 Country Club Drive
Farmington Hills, MI 48331

Precast/Prestressed Concrete Institute
200 W. Adams St Ste 2100
Chicago, IL 60606

PREPARED BY:
Wiss, Janney, Elstner Associates, Inc.
9511 North Lake Creek Parkway
Austin, Texas 78717
512.257.4800 tel

CONTENTS

1. INTRODUCTION

The design for horizontal shear transfer at an interface between concretes placed at two different times occurs in several scenarios in new construction and repair applications. The ACI 318-19 and ACI 562-19 design requirements for interface shear transfer limit the nominal strength of an intentionally roughened, unreinforced interface to 80 psi, and an unreinforced interface without intentional roughening is assumed to have no shear strength. These nominal shear strength limits can be punitive for some applications, such as toppings on precast hollow-core slabs and double-T beams, partial-depth repairs on slabs, and bonded overlays. When interface areas are large, requirements to add interface reinforcement and/or intentional roughening result in considerable time and expense or, in some cases, an alternate approach is needed.

Published research findings suggest that the current 80 psi nominal limit for interface shear stress without interface reinforcement appears to be overly conservative and may be substantially reducing the cost-effectiveness of topping slab designs and partial-depth repair solutions in some situations. The research suggests that ACI standards and related construction practices can benefit from research devoted to redefining nominal interface shear stress limits. As well, the use of various tests, such as the direct shear or guillotine method, to assess the shear bond strength at interfaces should be explored to demonstrate adequate interface shear transfer for quality control purposes.

The research discussed in this progress report has been proposed to study the interface shear transfer in applications for partial-depth concrete repairs and for topping applications on precast elements. This research comprises two phases of laboratory testing. Phase 1 was developed to study the (local) interface bond strength of slab specimens through direct shear tests and direct tensile pull-off tests. Phase 2 comprises flexural tests on beam specimens to assess interface shear strength under combined bending and shear. The beam tests have been designed to represent typical interface shear conditions in practical applications and will allow correlations to be established with common quality control test methods. Ultimately, the research findings are expected to provide the basis for a performance-based design approach for interface bond in topping slab and partial-depth repair applications. The findings may be used to propose modifications to the existing interface bond provisions in ACI 318 and ACI 562.

2. EXPERIMENTAL PROGRAM AND OBJECTIVES

A two-phase experimental program was developed to study the interface shear transfer in topping slabs and partial depth repair applications. The research examined the applicability of the current nominal shear stress limits in ACI 318 and ACI 562 for interfaces without reinforcement. The research established a database of interface shear strength values obtained using guillotine (direct) shear testing. Direct tension pull-off tests, which are the most commonly used method to assess bond capacity at present, were performed on the same specimens to allow comparison with the guillotine shear tests. The research included a testing program using flexural (beam) specimens to assess interface shear strength. These experiments more accurately represent the typical interface shear conditions in practical applications and allowed correlations to be established with common quality control test methods. Ultimately, the research findings were expected to provide the foundation for a performance-based design approach for interface bond in topping slab and partial depth repair applications.

The objectives of this research include the following:

- Summarize previous literature related to concrete-to-concrete interfaces including common roughening practices, roughness quantification methods, past research on localized bond strength methods, past research on composite concrete beams without horizontal shear ties, and the evolution of horizontal shear code provisions.
- Design Phase 1 test specimens to represent concrete surface roughening techniques commonly used in industry practice.
- Establish a database of interface shear strength values obtained using guillotine (direct) shear testing and direct tension pull-off testing. Investigate the correlation, if any, to the two bond test methods.
- Design Phase 2 flexural (beam) specimens to assess interface shear strength. The goal of the beam experiments was to more accurately represent the typical interface shear conditions in practical applications and allow correlations to be established with common quality control test methods (i.e., direct tension pull-off tests and direct shear tests).
- Based on results from the study, recommend future action to improve current code provisions regarding the horizontal shear capacity of composite concrete interfaces without shear ties.

3. LITERATURE REVIEW

The following literature review summarizes several previous research studies investigating horizontal shear in unreinforced concrete-to-concrete interfaces using beam tests, bond tests, and other test methods. Prior to presenting the previous research, analytical methods to calculate horizontal shear demand are summarized and the evolution of interface shear design provisions is discussed.

3.1. Methods to Calculate Interface Shear Demand

Different analytical methods are available to calculate the horizontal shear demand at a composite interface, including the sectional method (mechanics of materials), simplified method, and segment method. The three methods are briefly described in this section.

3.1.1. Sectional Method (Elastic Shear Formula)

The sectional method is based on the Euler-Bernoulli theory for elastic beams. The shear formula, shown in Equation 3-1, is the classic shear stress formula from mechanics of materials. This method assumes elastic behavior and is only an approximation for elastic cracked concrete sections. The sectional shear formula is not valid for concrete members at ultimate conditions and is not included in ACI 318-19 or AASHTO LRFD provisions. However, some research studies (Revesz 1953, Hanson 1960, Saemann and Washa 1964) have used the sectional method to estimate ultimate horizontal shear stress in beam test specimens.

$$v_h = {(V * Q)}/{(I * b_v)} \qquad \text{Equation 3-1}$$

where,

v_h = horizontal shear stress

V = vertical shear force

Q = first moment of area with respect to the neutral axis of the slab

I = moment of inertia of composite section

b_v = width of bonded interface

3.1.2. Simplified Method

The simplified method is based on an idealization of beam theory applied to a segment (length $\Delta\ell$) of a composite beam, as shown in Figure 3-1. The horizontal interface is assumed to coincide with the neutral axis depth in the section. The interface shear force is established based on the equilibrium of the compression resultants above the interface:

$$V_h = C_2 - C_2 = \left[\frac{M_1}{d} + \frac{V_u\,\Delta l}{d}\right] - \left[\frac{M_1}{d}\right]$$

$$V_h = {V_u * \Delta l}/{d}$$

The interface shear stress is calculated based on the shear force and the interface area for the segment:

$$v_u = {V_u}/{A_{cv}} \qquad \text{where } A_{cv} = b_v * \Delta l$$

$$v_u = {}^{V_u}/_{(b_v * d)} \qquad \text{Equation 3-2}$$

where,

v_u = horizontal shear stress at interface

V_h = horizontal shear force at interface

V_u = vertical shear force

Δl = length of beam segment

d = distance from extreme compression fiber for the entire composite section to the centroid of longitudinal tension reinforcement, need not be taken less than 0.80h for prestressed concrete members. Note that AASHTO LRFD defines d as the distance between the centroid of the longitudinal tension reinforcement and the mid-thickness of the slab (denoted as d_v).

b_v = width of the contact surface

The derivation of the simplified method (Equation 3-2) is shown in more detail in Article 5.7.4.5 of AASHTO (2020) and forms the basis of the interface shear provisions in ACI 318-19 Clause 16.4.4. It should be noted this method assumes the thickness of the topping slab is approximately equal to the depth of the composite section neutral axis, and thus the interface coincides with the maximum shear stress at the neutral axis of the composite section. If the thickness of the topping slab does not coincide with the depth of the neutral axis, the interface shear stress will be less than the maximum horizontal shear stress.

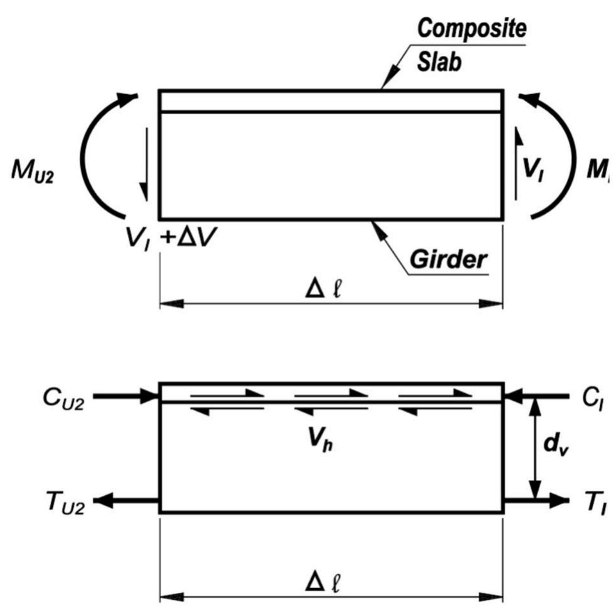

Figure 3-1. Horizontal shear demand – Free-body diagram assumed for simplified method adapted from AASHTO (2020).

3.1.3. Segment Method (Global Force Equilibrium)

The segment method determines the horizontal shear demand along the length of a composite member by analyzing segments of the composite section. Considering equilibrium of the free body diagram of the segment, the force along the interface is taken by the difference between compressive forces in the topping (Figure 3-2). The resulting force is divided by the area of bonded interface within the segment to find the average interface shear stress for the segment, as given by Equation 3-3.

$$v_h = {(C_1 - C_2)}/{(l * b_v)} \qquad \text{Equation 3-3}$$

where,

v_h = horizontal shear stress within segment length

C_1 = resultant compression force in topping acting on one side of the beam segment

C_2 = resultant compression force in topping acting on the opposite side of the beam

l = length of segment considered

b_v = width of interface resisting horizontal shear transfer

The segment method is permitted by ACI 318-19 Clause 16.4.5 as an alternate method to the simplified method shown in the preceding section. The two approaches are based on the same mechanics of a segment of a composite member with the difference that the segment method does not rely on the assumption that the topping thickness corresponds to the neutral axis depth. The segment method is more general, and can be applied to elastic gross section, elastic cracked section, and inelastic (ultimate) section analyses to estimate the compression resultants C_1 and C_2. Consideration must be given to the expected section behavior and limit state considered when selecting the analysis approach to be used to estimate the compression resultants. It should be noted that the segment length used can affect the magnitude of horizontal shear stress if behavior is not linear elastic or if the composite section changes along the length of the member. However, specific requirements or guidelines for the length of the segment are not provided in ACI 318-19.

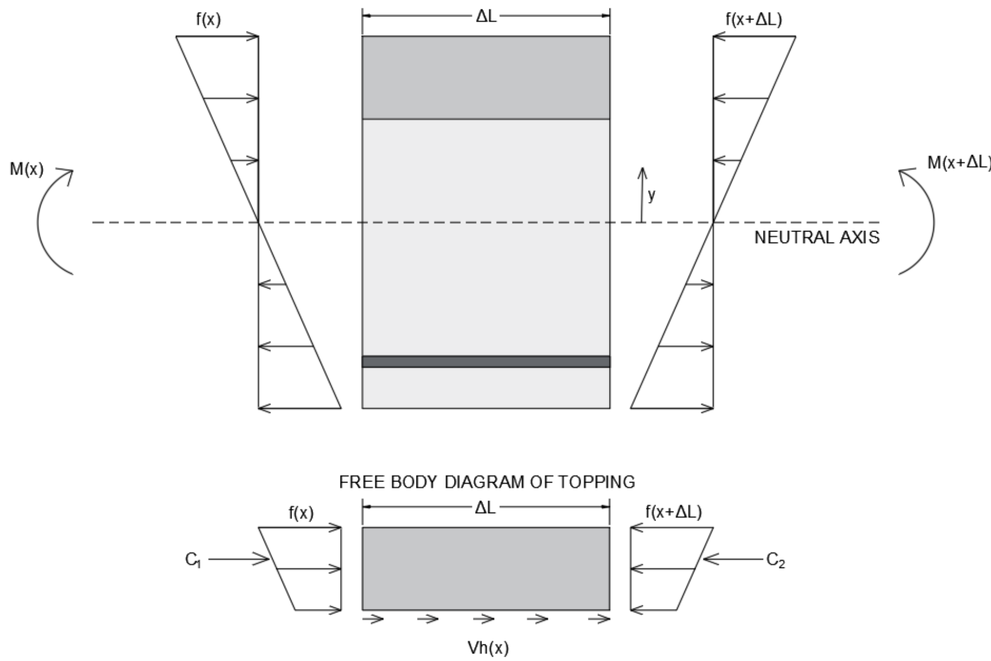

Elastic Uncracked Section

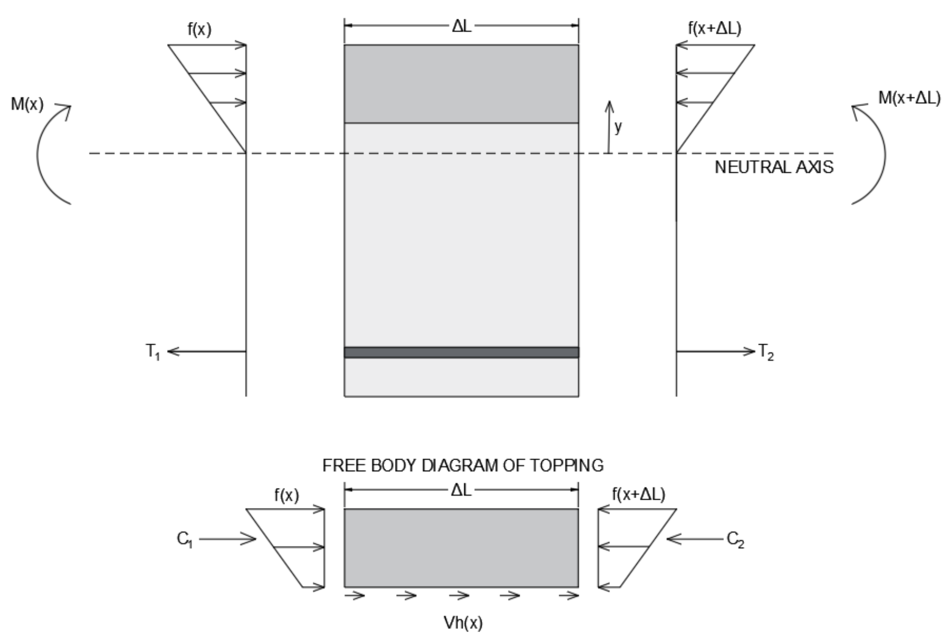

Elastic Cracked Section

Figure 3-2.Horizontal shear demand - Segment method (global force equilibrium).

3.2. Code Provisions to Calculate Horizontal Shear Capacity

3.2.1. Evolution of Horizontal Shear Provisions in ACI 318

Horizontal shear provisions for composite beams and composite girders were first developed by ACI-ASCE Committee 333 in 1960 (ACI-ASCE 1960). The recommendations were based on experimental results reported by Hanson (1960), Ozell and Cochran (1956), Revesz (1953), and Karr, Kriz, and Hognestad (1960).

The committee considered seventy-eight composite beam tests, nine of which failed in horizontal shear at the composite interface. Horizontal shear failure results reported by ACI-ASCE Committee 333 are summarized in Table 3-1. The nine beams had either a smooth or rough interface. Three of the nine beams considered had no reinforcement across the interface, all of which had a smooth interface. Horizontal shear stress at failure ranged from 78 psi to 350 psi for smooth interfaces and 418 psi to 580 psi for rough interfaces. From these test results, the committee recommended allowable bond stresses at working loads of 40 psi for smooth surfaces and 160 for rough surfaces. These recommendations required that a minimum amount of shear ties be present across the interface of the beam to prevent separation of the elements in the direction normal to the contact surface.

Table 3-1. Horizontal Shear Failures of Composite Concrete-Concrete Beams Reported by ACI-ASCE Committee 333.

Reference	Specimen ID	Reinforcement Across the Interface	Interface Roughness Technique	Reported Horizontal Shear Stress at Horizontal Shear Failure (psi)
Hanson (1960)	BS-I	#3 at 6″ O.C.	Smooth	350
Hanson (1960)	BS-II	#3 at 16″ O.C.	Smooth	340
Ozell and Cochran (1956)	A2	None	Smooth	78
Ozell and Cochran (1956)	C2	#4 at 6″ O.C.	Smooth	100
Ozell and Cochran (1956)	A3	None	Smooth	119
Revesz (1953)	J	None	Smooth	122
Hanson (1960)	BRS-1	#3 at 6″ O.C.	Rough	450
Hanson (1960)	BRS-2	#3 at 16″ O.C.	Rough	580
Kaar et al (1960)	III-0.6-1.66	#3 at 6″ O.C.	Rough	418

The basis of the Committee 333 recommendations for allowable interface bond stresses is unknown, and there does not appear to be a direct relationship to the test results reported. As previously discussed, horizontal shear stress at failure was not reported by Hanson (1960). The values reported by the committee for specimens BS-I and BRS-I appear to be the horizontal shear stress when the interface slip begins to increase. These values may be appropriate since an increase in differential ship would indicate an interface failure. This is not the case for BS-II and BRS-II as the reported stress does not appear to relate to any significant events shown in the data provided by Hanson. It is also unclear why specimen BR-1, which had no reinforcement at the interface, was not considered by the committee. The beam specimens referenced by the committee from the Ozell and Cochran (1956) study do not appear in the published paper. None of the beam specimens reported by Ozell and Cochran failed in horizontal shear. Lastly, the horizontal shear stress for specimen J in Revesz (1953) was reported by the committee to be 122 psi when the calculated horizontal shear stress using the sectional method is approximately 137 psi.

The horizontal shear recommendations from Committee 333 were adopted into the ACI 318-63 (ACI 1963) building code. The next change to the horizontal shear provision in the building code was in ACI 318-71 (ACI 1971), where the allowable stresses were rounded up but are essentially the same as those published in ACI 318-63. The code requirement has remained largely unchanged since then, as summarized in Table 3-2.

Table 3-2. Evolution of ACI 318 Horizontal Shear Capacity Provisions

Interface Condition	Interface Reinforcement	Nominal Interface Shear Stress (psi)		
		ACI 318-63	ACI 318-71	ACI 318-19
Intentionally Roughened	None	76*	80	80
Not Intentionally Roughened	Minimum	76*	80	80
Intentionally Roughened	Minimum	304*	350	290**

* *Based on allowable stress reported, multiplied by a factor of 1.9 for capacity of bond at ultimate load.*
** *Based on concrete compressive strength of 4,000 psi.*

3.2.2. Current ACI Code Provisions for Horizontal Shear Capacity

3.2.2.1. ACI 318 – Building Code Requirements for Structural Concrete (ACI 318-19)

The design requirements for horizontal shear transfer in composite concrete flexural members are defined in Clause 16.4 in ACI 318-19. The design strength must satisfy Equation 3-4 at all locations along the contact surface in the composite member.

$$\phi V_{nh} \geq V_u \qquad \text{Equation 3-4}$$

where,

V_{nh} = nominal horizontal shear capacity

V_u = factored vertical shear demand at section of interest

ϕ = strength reduction factor (taken as 0.75 for shear)

For an unreinforced interface, V_{nh} is limited to80 psi as indicated in ACI 318-19 Table 16.4.4.2 and Equation 3-5.

$$\phi V_{nh} = 80 b_v d \qquad \text{Equation 3-5}$$

where,

b_v = width of interface (in.)

d = distance from extreme compression fiber to tension reinforcement but not less 0.80h for prestressed concrete members. (in.)

The code also states that the contact surface must intentionally roughened, clean and free of laitance. The requirements for intentionally roughened unreinforced interfaces do not include a requirement to roughen the surface to a ¼ inch amplitude. This roughness amplitude is required by ACI 318 for interfaces with interface shear reinforcement exceeding the minimum required.

3.2.2.2. ACI 562 – Code Requirements for Assessment, Repair, and Rehabilitation of Existing Concrete Structures and Commentary (ACI 562-21)

ACI 562 provides requirements for interface bond of cementitious repair materials in Clause 7.4. The interface horizontal shear strength requirements are essentially the same as those in ACI 318 for unreinforced interfaces but are presented in terms of interface shear stresses rather than forces. Specifically, where the shear stress demand, v_u, exceeds 60 psi (i.e., ϕ x 80 psi where ϕ is the strength reduction factor for shear and taken as 0.75 for repair design), interface shear reinforcement must be provided.

If the factored shear stress demand, v_u, exceeds 30 psi but does not exceed 60 psi, interface shear reinforcement is not required but quantitative bond strength testing must be performed. The method of quantitative bond testing is not specified, but the Code commentary discusses that it is common to employ tension pull-off testing in accordance with ASTM C1583. ACI 562 does not provide strength requirements for quantitative bond strength testing, although the commentary mentions achievable tensile bond strengths as cited in ICRI Guideline No. 210.3 (2021) and BS EN 1504-10 (2017). The commentary in Clause 7.4 notes "It generally is adequate to assume that the repair to substrate bond will resist an interfacial shear equal to the direct tensile pull-off test result."

If the factored shear stress demand is less than 30 psi, neither interface reinforcement or quantitative bond strength testing are required. Bond integrity testing is intended to confirm that the repair material has not debonded, and can be performed by mechanical sounding, ground-penetrating radar, impact-echo, or other nondestructive evaluation methods.

3.3. Experimental Studies on Shear Capacity of Unreinforced Interfaces – Beam Testing

Several experimental investigations have been conducted to characterize the bond behavior of unreinforced concrete-to-concrete interfaces. The studies presented in this section investigate interface bond strength using beam specimens tested in flexure.

3.3.1. Revesz (1953)

Revesz tested five composite T-beams with unreinforced interfaces to observe behavior in flexure. Four of the beams were prestressed with high tensile strength wire tensioned to various stresses and one specimen was reinforced with non-prestressed bars steel. All specimens had a smooth interface with no reinforcement across the interface. The typical beam cross-section is shown in Figure 3-3. The specimens were loaded at third points of the 14-foot span.

The results of this study are summarized in Table 3-3. Four beams (specimens L, G, F, and N) failed by tension reinforcement fracture or steel yielding, and one beam (specimen J) failed in horizontal shear. The horizontal shear stress at failure for specimen J, using the sectional method, was approximately 137 psi. Based on the test observations, Revesz recommended roughening contact surfaces of composite concrete beams to prevent failure by horizontal shear.

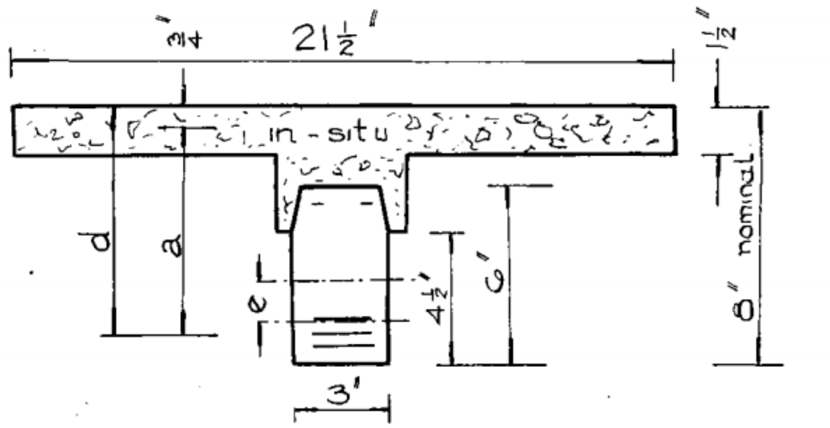

Figure 3-3: Cross-section of T-beam tested by Revesz (1953).

Table 3-3. Results from specimens with unreinforced interfaces from Revesz (1953).

Specimen ID	Reinforcement Across the Interface	Interface Roughness Technique	Failure mode	Method for Calculating Horizontal Shear Stress	Reported Horizontal Shear Stress at Horizontal Shear Failure (psi)
L	None	Smooth	Steel Fracture	-	-
G	None	Smooth	Steel Fracture	-	-
F	None	Smooth	Steel Fracture	-	-
N	None	Smooth	Steel Yield	-	-
J	None	Smooth	Horizontal Shear	Sectional	137

3.3.2. Hanson (1960)

Hanson tested sixty-two composite push-off specimens and ten composite T-shaped girders to study horizontal shear transfer at concrete interfaces. The research program had many variables including interface adhesive bond agents, surface roughness, shear keys, stirrups (interfacial ties), and different bonded contact lengths. The girder tests are discussed in this section and the push-off tests are discussed in Section 3.5.

The composite girders were designed to reach high interface shear stresses before flexural failure. The sectional method was used to find horizontal shear stress, but beam properties were modified to consider the cracked cross section. Ten girders were tested, one of which had an unreinforced interface. The specimen with an unreinforced interface, BR1, had a rough and bonded surface. Rough was defined by scraping the surface to create an amplitude of approximately 1/4 inch and bonded was defined as no attempt to destroy the adhesive bond. The typical cross-section for the girders is shown in Figure 3-4.

The substrate of the girder was cast in plywood forms and consolidated with vibrators. The surface finish conditions were applied and then wet cured for seven days followed by drying for seven days before placement of the top deck. The concrete deck was wet cured for seven days and left to dry for seven additional days before testing. Specimen BR-1 had a 145-inch simple plan with two point loads 25-inches apart in the center of the span. The loading scheme is shown in Figure 3-5.

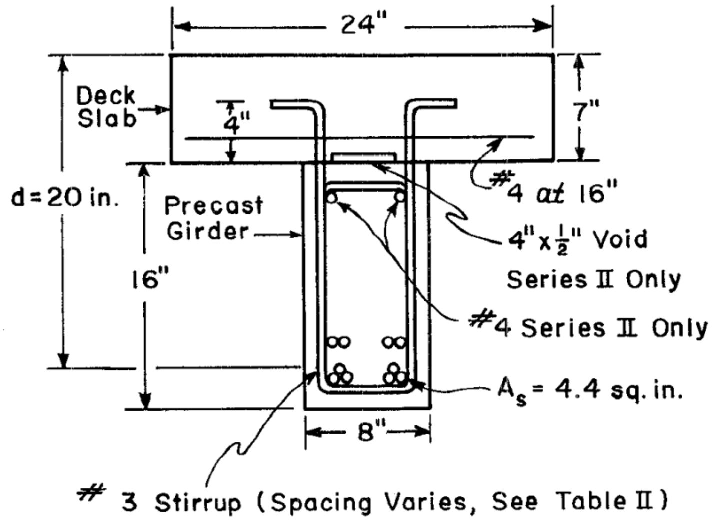

Figure 3-4: Girder specimens tested by Hanson (1960).

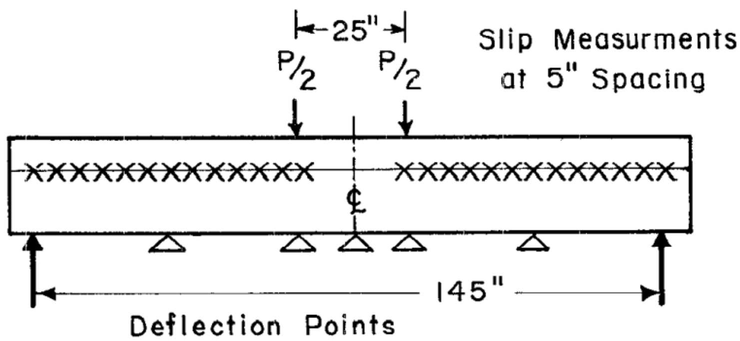

Figure 3-5: Girder loading and elevation by Hanson (1960).

The failure mechanism of girder BR-1 was reported to be a shear-compression failure preceded by loss of composite action. A shear-compression failure was described as flexural cracks that develop and move up toward the point loads with increasing applied load. Once the cracks reach the interface they propagate along the joint for a short distance.

The load or horizontal shear stress at failure was not stated in this study. One conclusion from girder tests was composite action stops when slip between the substrate and topping reach approximately 0.005 inches. The horizontal shear stress of girder BR-1 at a slip of 0.005 inches is approximately 310 psi based on the sectional method. A summary of the results from the beam with an unreinforced interface is provided in Table 3-4.

Hanson (1960) concluded beam and push-off test results indicate that an unreinforced, rough-bonded interface has a horizontal shear capacity of approximately 500 psi and a smooth-bonded interfaced has a horizontal shear capacity of approximately 300 psi. Additionally, the study concluded that 175 psi can be added for each additional percent of reinforcement across the interface.

Table 3-4. Results from specimens with unreinforced interfaces from Hanson (1960).

Specimen ID	Reinforcement Across the Interface	Interface Roughness Technique	Failure mode	Method for Calculating Horizontal Shear Stress	Reported Horizontal Shear Stress at Horizontal Shear Failure (psi)
BR-1	None	Rough & Bonded	Shear-compression	Sectional	310

3.3.3. Saemann and Washa (1964)

Saemann and Washa tested forty-two composite beams, two of which had no reinforcement across the interface (15C and 16C). The cross-section for these beams is shown in Figure 3-6.

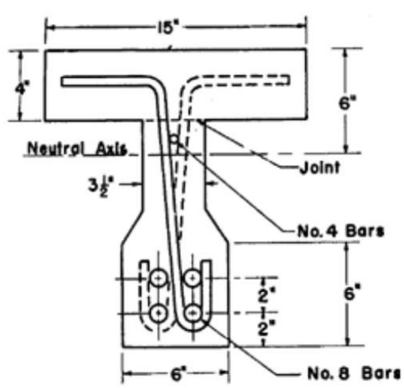

Figure 3-6: Beam cross-section in Saemann and Washa (1964).

The webs were cast and wet cured with burlap for 7 days and then the slab was cast on top. The composite specimen was wet cured again for 7 days and tested 21 days later. The two beams with unreinforced interfaces had intermediate roughness. This roughness was achieved by first screeding off the top surface. A retarding agent was then applied to allow brushing of the mortar between the coarse aggregate. The resulting roughness had an amplitude of approximately 1/8-inch.

Beam 15C was eleven feet long and beam 16C was eight feet long. Both were loaded under flexure by two point loads, each offset one foot from the beam midspan. Both beams reportedly failed in diagonal shear, described as diagonal cracks traveling toward the top-center of the beam. Once the diagonal crack intersected the interface, it propagated along the composite joint. At ultimate loading the shear cracks extended to both ends of the beam. Final failure occurred as crushing of concrete in the web. While the beams did not fail in horizontal shear, the horizontal shear stress at ultimate conditions was reported. Using the sectional method, beam 15C reported a horizontal shear stress of 420 psi and beam 16C reported a horizontal shear stress of 606 psi.

In addition to these horizontal shear stresses at ultimate loading, the paper reports the horizontal shear stress at measured slip of 0.005 inches. The value of 0.005 inches was based on Hanson (1960) and was described to be a critical value for composite beam behavior. The horizonal shear stress for beam 15C and 16C at 0.005-inch slip was 329 psi and 443 psi, respectively. The results of these specimens are summarized in Table 3-5.

Table 3-5. Results from specimens with unreinforced interfaces from Saemann and Washa (1964).

Specimen ID	Reinforcement Across the Interface	Interface Roughness Technique	Failure mode	Method for Calculating Horizontal Shear Stress	Reported Horizontal Shear Stress at Horizontal Shear Failure (psi)
15C	None	Intermediate roughness (1/8" brushing)	Both specimens reported to fail by a shear crack traveling along the interface.	Sectional	420
16C	None	Intermediate roughness (1/8" brushing)		Sectional	606

Saemann and Wahsa (1964) proposed an equation to calculate the horizontal shear capacity based on the findings of their study. This equation (shown below as Equation 3-6) is simplified for unreinforced interfaces.

$$Y = \frac{2700}{X+5} \qquad \text{Equation 3-6}$$

where,

Y = ultimate shear strength (psi)

X = the ratio of shear span to effective depth

This equation provides a significant shear capacity for most unreinforced interfaces; the shear span-to-depth ratio would need to exceed 33 to have a design capacity of 80 psi. Roughness is not considered in this equation, but the paper does conclude that the ultimate shear strength does increase as roughness of the surface is increased.

3.3.4. Concrete Technology Associates Technical Bulletin 74-B6 (1974)

Concrete Technology Associates (CTA) performed a series of beam tests to study the performance of composite beams without ties and determine the relationship between interfacial roughness and the degree of composite action. The study comprised 16 prestressed composite beams without interface ties. Parameters tested included surface roughness (smooth, intermediate, and rough), surface condition before casting the slab (clean and dirty), topping concrete (normal and lightweight), and shear span to effective depth ratio (3.5 and 7.5). The smooth roughness was created by hard-steel trowel finish, the intermediate by wood-float finish, and the rough was created by serrations formed by dragging a sharp object across the wet concrete surface. The cross-section of the CTA beams tested is shown in Figure 3-7.

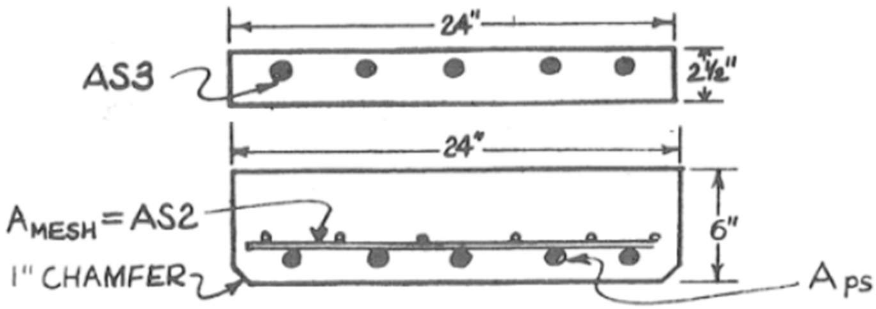

Figure 3-7: Cross section of prestressed beam tested by CTA (1974).

The beams were loaded with a single load at midspan. Two beams failed in horizontal shear: specimen S-7-S (smooth-sandblast-clean) and S-8-S (smooth-cement slurry-clean). The reported horizontal shear stresses for S-7-S and S-7-8 were 429 psi and 398 psi, respectively, using the sectional method (VQ/Ib). The study also reported horizontal shear stresses using the simplified elastic behavior method (V/bd) which was reported to be 453 psi and 442 psi for S-7-S and S-8-S, respectively. A summary of results including the reported horizontal shear stress calculated using the sectional method is provided in Table 3-6.

Table 3-6. Results from specimens with unreinforced interfaces from CTA (1974).

Specimen ID	Reinforcement Across the Interface	Interface Roughness Technique	Failure mode	Method for Calculating Horizontal Shear Stress	Reported Horizontal Shear Stress at Horizontal Shear Failure (psi)
S-1-I	None	Intermediate (wood-float)	Shear	Sectional	302
L-1-I	None	Intermediate (wood-float)	Shear	Sectional	139
S-2-I	None	Intermediate (wood-float)	Shear	Sectional	356
L-2-I	None	Intermediate (wood-float)	Flexure	Sectional	169
S-3-R	None	Rough (serrated)	Shear Flexure	Sectional	477
L-3-R	None	Rough (serrated)	Shear Flexure	Sectional	168
S-4-I	None	Intermediate (wood-float)	Shear Flexure	Sectional	392
L-4-I	None	Intermediate (wood-float)	Flexure	Sectional	150
S-5-I	None	Intermediate (wood-float)	Flexure	Sectional	421
L-5-I	None	Intermediate (wood-float)	Flexure	Sectional	155
S-6-R	None	Rough (serrated)	Shear Flexure	Sectional	411
L-6-R	None	Rough (serrated)	Flexure	Sectional	158
S-7-S	None	Smooth (sandblast)	Horizontal Shear	Sectional	429
L-7-S	None	Smooth (hard trowel)	Flexure	Sectional	164
S-8-S	None	Smooth (cement slurry)	Horizontal Shear	Sectional	398
L-8-S	None	Smooth (cement slurry)	Shear Flexure	Sectional	139

The study concluded that the ACI code at the time may be based on incorrect interpretation of previous research. Previous research indicated the shear strength of concrete-to-concrete bond strength ranged from

140 to 500 psi for smooth to rough contact surfaces. CTA found that for all tests the beams failed at loads above those allowed by the code for monolithic members of the same dimension. CTA also found no apparent correlation between the interface condition (roughness and cleanliness) and the degree of composite action where composite action is measured by the effective moment of inertia of test beams under pre-cracking loads and the ability to achieve full ultimate moment of the composite section.

3.3.5. Seibel and Latham (1988)

Seibel and Latham investigated interface bond on concrete interfaces by testing fourteen shear block tests and twelve slab panel tests (under flexure). The slab panel tests are discussed in this section and the shear block specimens are discussed in section 3.5.2.

The slab panel testing program included four slab panels with unreinforced interfaces (SP-1A, SP-2, SP-3, and SP-4). The specimen number represents the substrate roughness as follows: 1-Monolithic, 2-Lubricated, 3-Surface Rough, and 4-Scarified. The slab panel test reinforcement and setup are shown in Figure 3-8 and Figure 3-9.

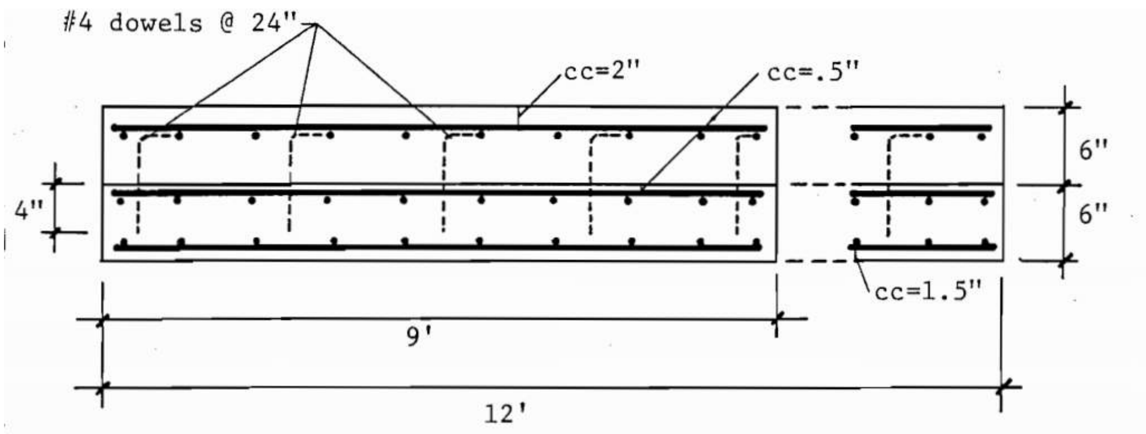

Figure 3-8: Elevation reinforcement layout for slab panel tests by Seibel and Latham (1988).

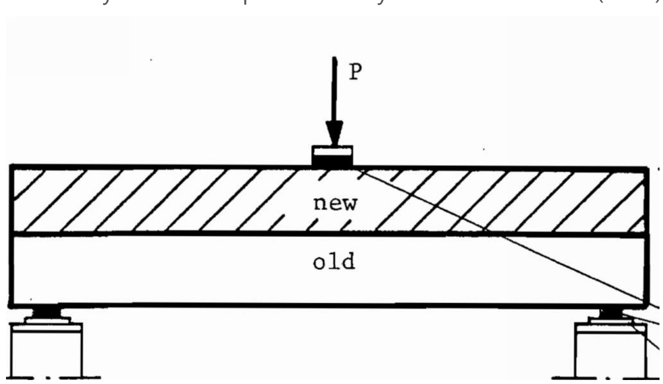

Figure 3-9: Load application for slab panel tests by Seibel and Latham (1988).

The initial behavior of all slab panel specimens was identical to that of a control monolithic specimen except for the lubricated specimen, which failed due to sliding at the horizontal interface. The horizontal shear stress was not stated, but instead the maximum load, load at yield, and load when the interface delamination began. Using the simplified elastic method, the following shear stresses were calculated using the load when interface delamination began (horizontal shear failure). The specimen results are summarized in Table 3-7.

This study concluded that using dowels to reinforce the interface while practicing appropriate placement techniques, such as wet curing, are necessary to avoid horizontal shear failures.

Table 3-7. Results from specimens with unreinforced interfaces from Seibel and Latham (1988).

Specimen ID	Reinforcement Across the Interface	Interface Roughness Technique	Failure mode	Method for Calculating Horizontal Shear Stress	Reported Horizontal Shear Stress at Horizontal Shear Failure (psi)
SP-2	None	Lubricated	Complete interlayer delamination + crushing	Simplified elastic	16.4
SP-3	None	Surface Rough	Interlayer delamination of left side + crushing	Simplified elastic	28.8
SP-4	None	Scarified	Crushing + flexural shear failure	-	-

3.3.6. Kovach and Naito (2008)

Kovach and Naito performed a two-phase study of interface bond in precast beam applications. The study consisted of nineteen composite beams in Phase 1 and twenty-two composite beams in Phase 2, all with unreinforced interfaces.

The first phase investigated the effect of roughness and compressive strength on the horizontal shear stress capacity. The interface roughness types were typical for precast applications including as-placed, broom, 1/4-inch rake, and sheepsfoot. The web was fabricated at a precast/prestressing manufacturer. The slabs were poured one day after the web was poured. Measures were taken to ensure the surface was clean and free of laitance.

The beams were tested in two loading configurations: seven beams were tested under five-point loading (Beams 1 through 7) and twelve beams were tested under two-point loading (Beams 8 through 19). The five-point configuration was intended to represent an approximately uniform loading condition. The interface was unbonded along the edges of the interface of Beams 8-19 to create a higher stress at the bonded region. The cross-section and elevation of the beams used in Phase 1 are shown in Figure 3-10.

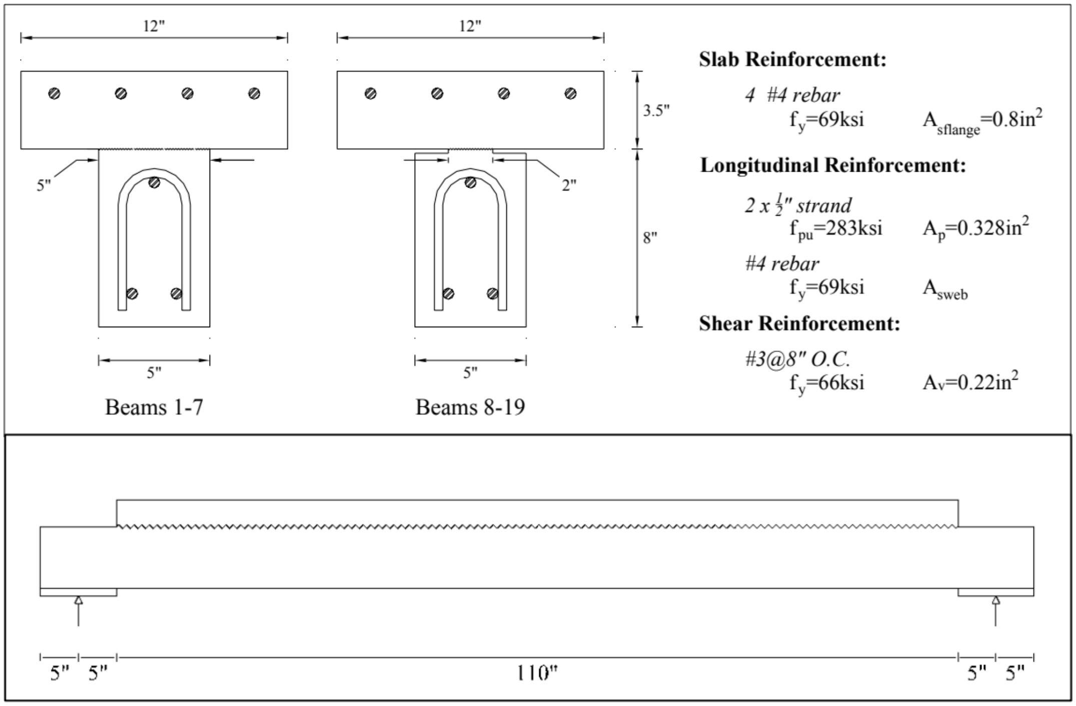

Figure 3-10: Cross-section and elevation of T-beam specimens in Phase 1 tested by Kovach and Naito (2008).

Slip gauges and surface mounted strain gauges were used to measure the beam deformations during testing. Using the strain values from the instrumentation and stress-strain relations from concrete cylinder tests a stress profile was developed at failure. The horizontal shear stress was then calculated using segment method (global force equilibrium). It was not mentioned what length or location of segment was used.

Eleven of the twelve two-point loaded specimens failed in horizontal shear. The horizontal shear stresses for those specimens are shown in Table 3-8. The values presented are found using the strain described earlier. The remaining specimens, including all those tested under five-point loading, failed in flexure or combined flexure-shear, as shown in Table 3-8.

While there was no quantification of the roughness, results from Phase 1 suggest there is a positive correlation between the intensity of the roughness and the horizontal shear strength. For best composite performance, this study suggested using a rake finish.

Phase 2 tested twenty-two composite beams under two-point loading of precast webs with cast-in-place toppings. The typical cross-section for these beams is shown in Figure 3-11. The width of the interface was reduced in these beams by debonding the outer two edges.

Table 3-8. Horizontal shear stress from Phase 1 beams tested by Kovach and Naito (2008).

Specimen ID	Reinforcement Across the Interface	Interface Roughness Technique	Failure mode	Method for Calculating Horizontal Shear Stress	Reported Horizontal Shear Stress at Horizontal Shear Failure (psi)
1	None	As-placed	Flexure-Shear	-	-
2	None	Broom	Flexure-Shear	-	-
3	None	Monolithic	Flexure-Shear	-	-
4	None	Rake	Flexure-Shear	-	-
5	None	Rake	Flexure	-	-
6	None	Rake	Flexure-Shear	-	-
7	None	Sheepsfoot	Flexure-Shear	-	-
8	None	As-Placed	Horizontal Shear	From Strain (C/Lbv)	482
9	None	As-Placed	Horizontal Shear	From Strain (C/Lbv)	814
10	None	Broom	Horizontal Shear	From Strain (C/Lbv)	916
11	None	Monolithic	Horizontal Shear	From Strain (C/Lbv)	1075
12	None	Monolithic	Flexure-Shear	-	-
13	None	Rake	Horizontal Shear	From Strain (C/Lbv)	639
14	None	Rake	Horizontal Shear	From Strain (C/Lbv)	1182
15	None	Rake	Horizontal Shear	From Strain (C/Lbv)	1348
16	None	Rake	Horizontal Shear	From Strain (C/Lbv)	1245
17	None	Rake	Horizontal Shear	From Strain (C/Lbv)	1054
18	None	Rake	Horizontal Shear	From Strain (C/Lbv)	1194
19	None	Smooth	Horizontal Shear	From Strain (C/Lbv)	787

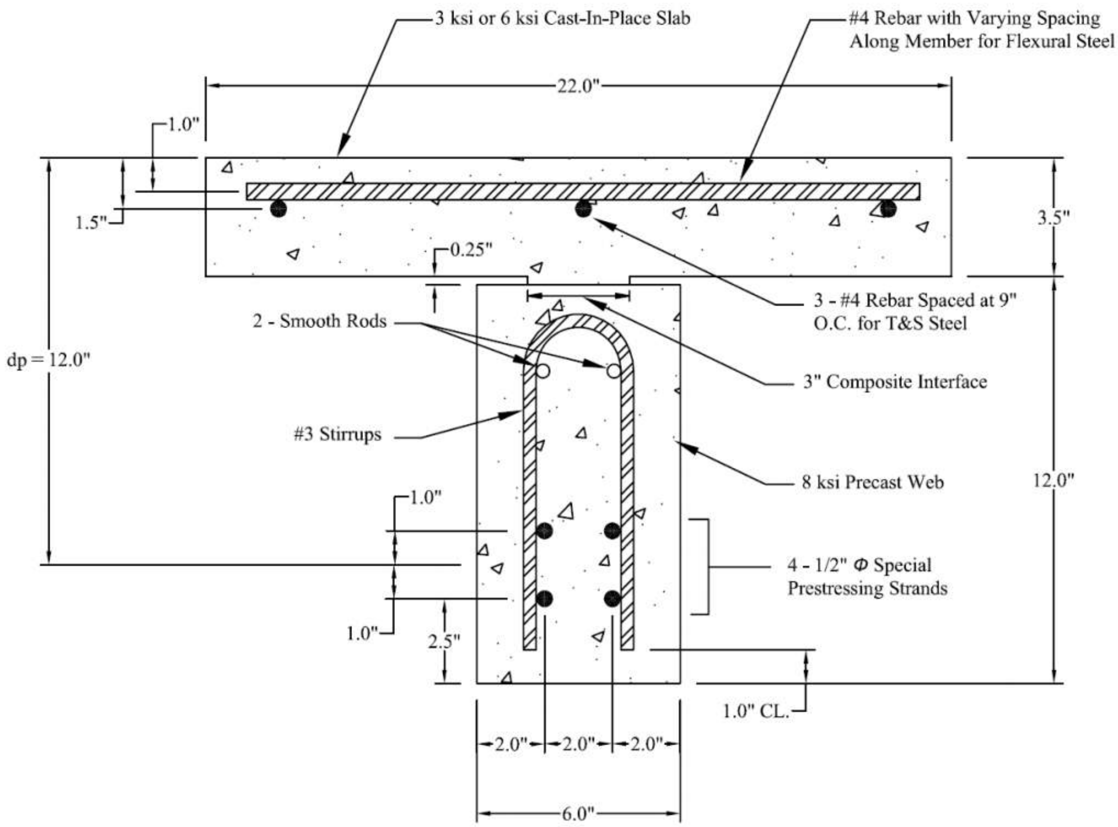

Figure 3-11: Cross-section of T-beam in Phase 2 tested by Kovach and Naito (2008).

Based on the conclusions from the previous phase, Phase 2 reduced the number of variables to obtain more dependable results. The different surface finishes used were smooth, broom, as-placed, and rake. Two different slab concrete compressive strengths were tested: low (3 ksi) and high (6 ksi) strengths.

The beams in Phase 2 were fabricated differently than in Phase 1. There was a several month gap in between placement of the topping slab and the fabrication of the precast/prestressed web. This was done to capture greater differential shrinkage between the two members. The webs were steam cured for three days and let to sit for a few months. The topping slab was poured and vibrated on top of the webs. The slab was wet cured with burlap for seventeen days and then left to air dry for ten days before testing.

Similar to Phase 1, the strain profile was established using strain data from the test. The segment method was used with the measured strains and assumed stress-strain relationships to estimate the compressive forces in the topping. The results of Phase 2 are summarized in Table 3-9.

This study concluded that the horizontal shear strength obtained from beam tests were approximately six to ten times larger than the limit established in the ACI-318 code. The study also concluded that with an increase of surface roughness, the horizontal shear capacity increases.

Table 3-9. Results from Phase 2 beams specimens tested by Kovach and Naito (2008).

Specimen ID	Reinforcement Across the Interface	Interface Roughness Technique	Failure mode	Method for Calculating Horizontal Shear Stress	Reported Horizontal Shear Stress at Horizontal Shear Failure (psi)
6B3-E	None	Broom	Horizontal Shear	From Strain (C/Lbv)	294
6B3-W	None	Broom	Horizontal Shear	From Strain (C/Lbv)	297
6B4-E	None	Broom	Horizontal Shear	From Strain (C/Lbv)	326
6B4-W	None	Broom	Horizontal Shear	From Strain (C/Lbv)	364
6B5-E	None	Broom	Horizontal Shear	From Strain (C/Lbv)	363
6B5-W	None	Broom	Horizontal Shear	From Strain (C/Lbv)	405
6B6-E	None	Broom	Horizontal Shear	From Strain (C/Lbv)	329
6B6-W	None	Broom	Horizontal Shear	From Strain (C/Lbv)	311
3A1-E	None	As-Placed	Horizontal Shear	-	-
3A1-W	None	As-Placed	Horizontal Shear	-	-
3A2-E	None	As-Placed	No-data	-	-
3A2-W	None	As-Placed	Horizontal Shear	From Strain (C/Lbv)	589
6A3-E	None	As-Placed	Horizontal Shear	From Strain (C/Lbv)	502
6A3-W	None	As-Placed	Horizontal Shear	From Strain (C/Lbv)	549
6A4-E	None	As-Placed	Horizontal Shear	From Strain (C/Lbv)	558
6A4-W	None	As-Placed	Horizontal Shear	From Strain (C/Lbv)	550
6A5-E	None	As-Placed	Horizontal Shear	From Strain (C/Lbv)	476
6A5-W	None	As-Placed	Horizontal Shear	From Strain (C/Lbv)	375
6A6-E	None	As-Placed	Horizontal Shear	From Strain (C/Lbv)	555
6A6-W	None	As-Placed	Horizontal Shear	From Strain (C/Lbv)	449

Table 3-9. Results from Phase 2 beams specimens tested by Kovach and Naito (2008). (continued)

Specimen ID	Reinforcement Across the Interface	Interface Roughness Technique	Failure mode	Method for Calculating Horizontal Shear Stress	Reported Horizontal Shear Stress at Horizontal Shear Failure (psi)
6A7-E	None	As-Placed	Horizontal Shear	From Strain (C/Lbv)	409
6A7-W	None	As-Placed	Horizontal Shear	From Strain (C/Lbv)	457
6A8-E	None	As-Placed	Horizontal Shear	From Strain (C/Lbv)	514
6A8-W	None	As-Placed	Horizontal Shear	From Strain (C/Lbv)	592
3R1-E	None	Rake	Horizontal Shear	From Strain (C/Lbv)	782
3R1-W	None	Rake	Horizontal Shear	From Strain (C/Lbv)	668
6R3-E	None	Rake	Horizontal Shear	From Strain (C/Lbv)	560
6R3-W	None	Rake	Horizontal Shear	From Strain (C/Lbv)	603
6R4-E	None	Rake	Horizontal Shear	From Strain (C/Lbv)	579
6R4-W	None	Rake	Horizontal Shear	From Strain (C/Lbv)	742
6R5-E	None	Rake	Horizontal Shear	From Strain (C/Lbv)	487
6R5-W	None	Rake	Horizontal Shear	From Strain (C/Lbv)	476
6R6-E	None	Rake	Horizontal Shear	From Strain (C/Lbv)	664
6R6-W	None	Rake	Horizontal Shear	From Strain (C/Lbv)	664
6R7-E	None	Rake	Horizontal Shear	From Strain (C/Lbv)	652
6R7-W	None	Rake	Horizontal Shear	From Strain (C/Lbv)	665
6R8-E	None	Rake	Horizontal Shear	From Strain (C/Lbv)	478
6R8-W	None	Rake	Horizontal Shear	From Strain (C/Lbv)	567

3.3.7. Swan (2016)

Swan evaluated interface shear strength by testing twelve beams with Iosipescu tests and six beams in three-point flexural tests. All interfaces were unreinforced. The Iosipescu tests are discussed in Section 3.5.4 and the beam tests are discussed herein.

Six beams with three different surface treatments were fabricated for the flexural tests. The surface roughness conditions investigated were described as smooth (CSP 2-3), bush-hammer (CSP 6), jackhammer (CSP 10). Concrete surface profile (CSP) conditions are defined in Section 4.5.1 of this report.

The cross-section of the beams is shown in Figure 3-12. PVC wall paneling was used as a bond breaker on the outer edges. In preparation of the topping layer, the substrate was sprayed with water for saturated surface-dry (SSD) conditions.

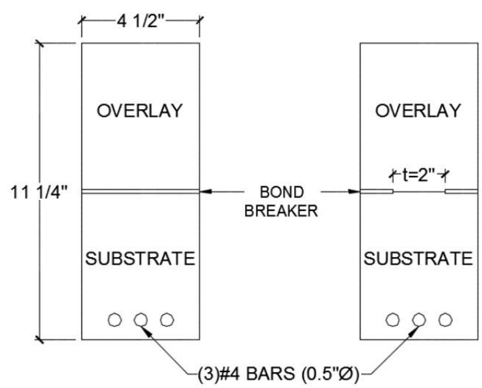

Figure 3-12: Cross-section of beams tested by Swan (2016).

One beam of each roughness was tested in flexural compression (shown on the left of Figure 3-13) and the other in flexural tension (shown on the right of Figure 3-13). This literature review will only discuss the three beams tested in flexural compression.

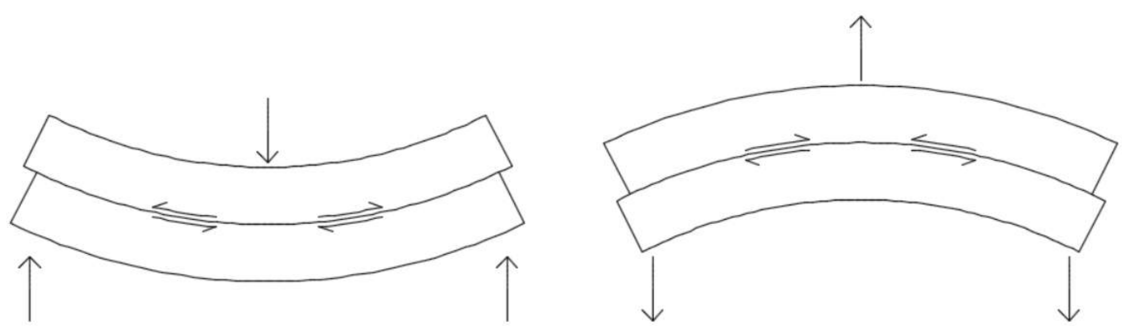

Figure 3-13: Beam loading conditions tested in Swan (2016).

The beams were tested with one point load at midspan, with results as summarized in Table 3-10. Beam 1 and Beam 2 failed in diagonal tension, occurring as a diagonal crack (assumed to be from vertical shear) that traveled across the interface without causing any cracking along the interface. Beam 3 had a flexural crack that traveled up to the interface and then continued along the interface to the edge of the beam causing horizontal shear failure. The sectional method was used to find the horizontal shear stress at failure.

Table 3-10. Results from beams specimens tested by Swan (2016).

Specimen ID	Reinforcement Across the Interface	Interface Roughness Technique	Failure mode	Method for Calculating Horizontal Shear Stress	Reported Horizontal Shear Stress at Horizontal Shear Failure (psi)
1	None	Rake	Diagonal tension	-	-
2	None	Bush Hammer	Diagonal tension	-	-
3	None	Smooth	Flexural Shear	Sectional	637

3.4. Experimental Studies on Shear Capacity of Unreinforced Interfaces – Bond Tests

This section summarizes research studies on the shear strength of concrete-to-concrete interfaces by various small-scale bond test methods. Currently there is no standard test to determine shear bond strength for unreinforced interfaces for partial-depth repair or new construction. Research studies have evaluated various shear test methods including the slant shear test, torsion or friction-transfer test, bi-surface or triplet test, and single-shear tests (e.g., guillotine test), as illustrated schematically in Figure 3-14. This section presents relevant research studies that have investigated one or more of these bond tests.

3.4.1. Silfwerbrand (2003)

Silfwerbrand (2003) performed localized bond tests using two techniques: pull-off testing and torsion testing. The study comprised 49 pull off tests and 33 torsion tests. The tests were performed on composite concrete samples with various surface roughness including waterjet (i.e., hydrodemolition), pneumatic hammer, and sandblasting. Of the 49 pull-off tests, 11 failed at the interface. Of the 33 torsion tests, one failed at the interface.

The study concluded that the shear bond strength is considerably higher than the tensile bond strength. Silfwerbrand (2003) investigated the use of an in-situ torsion test to assess interface shear strength and reported ratios of average shear strength to average tensile bond pull-off strength ranging from 1.9 to 3.1.

3.4.2. Momayez et al. (2005)

Momayez et al. (2005) studied different test methods for evaluating bond strength, including tensile bond pull-off, splitting prism, slant shear and direct shear. The direct shear test used involved lab cast rectangular prisms rather than core samples. Several concrete types were considered, and interface roughness was characterized as low (3 mm to 4 mm amplitude) or high (7 mm to 8 mm amplitude). Momayez et al. reported ratios of direct (single) shear to tensile pull-off bond strength of 1.6 to 2.2 and 1.7 to 2.4 for low and high roughness interfaces, respectively. The slant shear strength results produced higher ratios of shear to tensile pull-off strength of 5.1 to 7.5 and 5.4 to 8.8 for low and high roughness interfaces, respectively. The comparison of shear strength results and splitting tensile strengths rather than pull-off tensile strengths showed similar ratio ranges (i.e. tensile pull-off strengths are similar to splitting tensile strengths).

Momayez et al. (2005) reported ratios of average slant shear strengths to average bi-surface shear strengths ranging from 3.2 to 3.5 and 3.3 to 3.7 for low and high roughness interfaces, respectively. These results indicate that slant shear strengths are consistently higher (on the order of at least three times higher) than direct shear strengths determined using the guillotine test or bi-surface shear test. They also illustrate the significant effect of compression across the interface in the slant shear test on the resulting shear strength. Since many repair and new construction topping applications do not have sustained compression across the unreinforced interface, the use of slant shear tests to establish interface shear strength for design may not be appropriate.

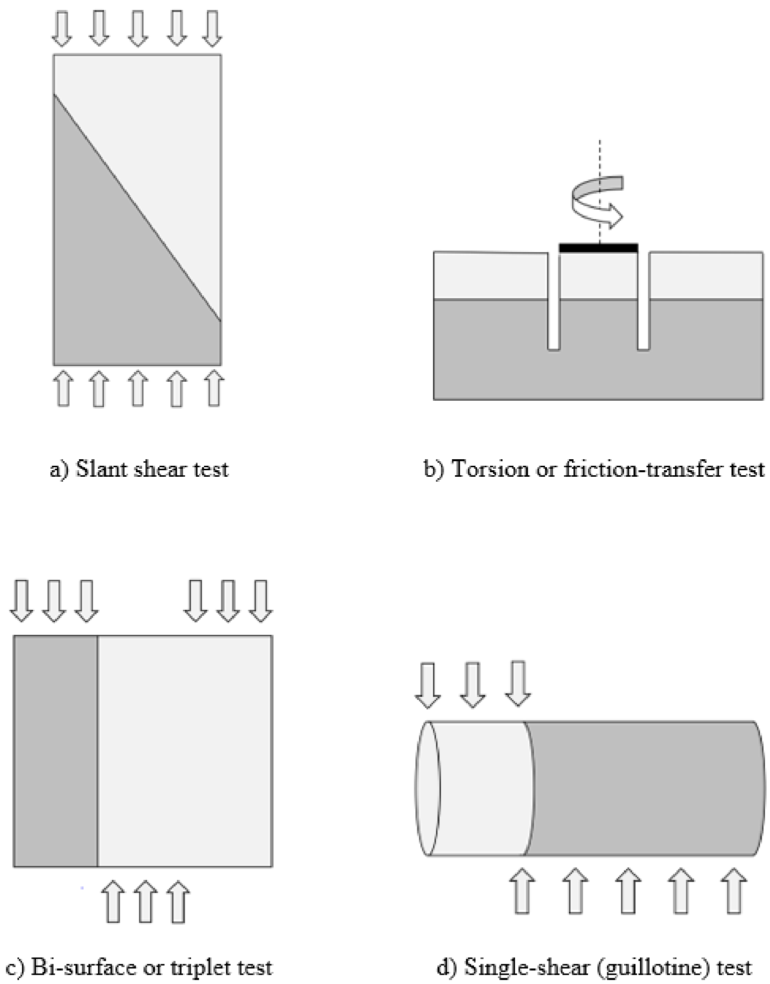

Figure 3-14: Shear test methods.

3.4.3. Santos (2009)

Santos (2009) studied interface bond strength by slant shear and splitting tensile testing in addition to an extensive literature review of horizontal shear strength and characterization of concrete surfaces. The experimental program tested specimens with various time gaps between substrate and topping casting (28-days, 56-days, 84-days) and curing conditions (interior or exterior). Ratios of average slant shear strengths to average splitting tensile strengths range from 5.1 to 6.3.

The study concluded surface roughness proved to have a significant influence on the bond strength of the concrete-to-concrete interfaces. A linear correlation was identified between the roughness parameter, Maximum Valley Depth, and the interface horizontal shear strength. Additionally, curing conditions also had a significant influence on the bond strength. For the same surface preparation and difference of age between concrete layers, the specimens cured under exterior conditions had an average shear strength 19 percent lower than those cast in lab conditions.

3.4.4. Rosen (2016)

Rosen (2016) studied interface bond testing methods including the guillotine test, slant shear test, and tensile pull-off test. Slab specimens were fabricated with various roughening and consolidation techniques. The substrate roughening techniques include broom, rake, and bush hammer. Two specimens of each roughening technique were fabricated, one with a vibrated topping and the other hand consolidated. Rosen reported ratios of average slant shear strengths to average pull-off tensile strength ranging from 7.6 to 10.2. and ratios of average guillotine shear strengths to average pull-off tensile strength ranging from 1.3 to 2.2. Rosen (2016) also reported ratios of average slant shear strengths to average guillotine shear strengths ranging from 3.8 to 6.4.

3.4.5. Sprinkel (2016)

Sprinkel (2016) conducted and evaluated shear tests to provide bond strength values that were representative of the shear bond strength between substrate and topping concrete. Ultimately, the study was intended to correlate direct tension pull-off tests to direct shear tests and to help develop a test method for shear bond strength to be used as an industry standard. The study was conducted on an existing concrete cooling tower structure that received a shotcrete overlay approximately 3.5 to 6.4 inches thick.

Twenty-two tensile bond tests were conducted in accordance with ASTM C1583 on areas that were mechanically blasted or hydroblasted. Seventeen were designated as Test 1 and five as Test 2. The average tensile bond strength test results for Test 1 with the hydroblasted substrate was 145.9 psi with a standard deviation of 58.4 psi. The average for Test 2 was 132.3 psi with a standard deviation of 13.9 psi. The average tensile bond strength test results for Test 1 with the mechanically blasted substrate was 139.8 psi with a standard deviation of 22.1 psi. The result from the single test in Test 2 was 139.1 psi. Seventeen 2.75-inch diameter cores were removed from the cooling tower for guillotine shear tests. The average shear bond strength for hydrodemolition was 1047.7 psi with a standard deviation of 313.3 psi. The average shear bond strength for the mechanically blasted substrate is 972.7 psi with a standard deviation of 245.3 psi.

The ratios of shear to tensile bond strength were similar for both hydrodemolition and mechanically blasted surfaces with ratios of 7.4 and 7.0, respectively. The study reports that there was not a good correlation between tensile and shear bond strength tests.

3.5. Experimental Studies on Shear Capacity of Unreinforced Interfaces – Other Tests Methods

This section includes studies on interface shear strength for concrete-to-concrete interfaces based on tests other than beam tests and basic bond tests. The tests included in this section comprise push-off tests, shear-block tests, and Iosipescu tests. Unlike the bond tests in section 2.3, these tests require unique formwork and test setups. The results are useful for research studies, but the test design is not practical for quality control and assessments in the construction industry.

3.5.1. Hanson (1960)

Hanson tested push-off specimens in addition to the girder specimens discussed in Section 3.3.2. A typical cross-section of the push-off specimens is shown in Figure 3-15. Several variables were tested in this study, one of them being reinforcement across the interface. Nineteen of the sixty-two specimens had no reinforcement across the interface.

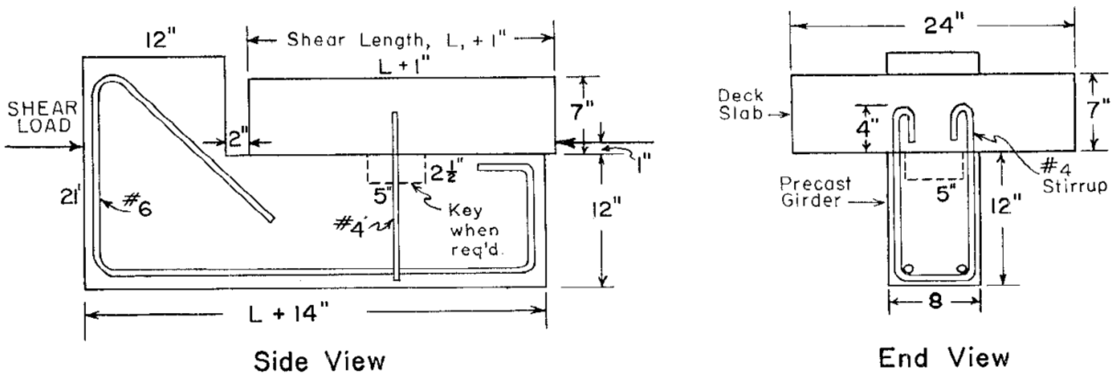

Figure 3-15: Push-off specimens tested by Hanson (1960).

These tests were performed to explore load-deformation characteristics of various contact surfaces subject to a shearing force. Amongst the specimens with no shear reinforcement across the interface, the specimens had other variables such as:

- Interface Length: Length of interface or shear length, either 6″, 12″, or 24″
- Smooth: Contact surface troweled
- Rough: Contact surface roughness by scraping with steel, approximate roughness amplitude of ¼″
- Bond: No attempt made to destroy adhesive bond
- Unbonded: Contact surface coated with silicone
- Smooth Aggregate Bare: After trowel, a retarding compound applied leaving aggregate bare
- Rough Aggregate Bare: After roughening with scraping with steel, the surface paste was prevented from setting and removed with a water jet 24-hours later
- Keys: The keys were 2-1/2-inch deep divots into the substrate surface and 5-inches long along the shearing surface forming an interlocking hole that the topping layer will form into.

The results from the push-off tests are summarized in Table 3-11. Specimens with keys indicated that bond must be destroyed for the keys to be engaged therefore it was concluded that it was desirable to avoid the use of keys and to rely on a combination of bond and surface roughness (and stirrups for reinforced interfaces) to have sufficient interface bond strength. The results show a consistent increase in strength when the surface is roughened to a ¼-inch amplitude.

Table 3-11. Push-off specimen results from tests by Hanson (1960).

Specimen ID	Reinforcement Across the Interface	Interface Roughness Technique	Failure mode	Method for Calculating Horizontal Shear Stress	Reported Horizontal Shear Stress at Horizontal Shear Failure (psi)
BR12-1	None	Rough and Bonded	Interface Failure	0.005" Slip	416
BR12-2	None	Rough and Bonded	Interface Failure	0.005" Slip	555
BR12-3	None	Rough and Bonded	Interface Failure	0.005" Slip	455
BR12-4	None	Rough and Bonded	Interface Failure	0.005" Slip	350
BR12-5	None	Rough and Bonded	Interface Failure	0.005" Slip	362
BR12-6	None	Rough and Bonded	Interface Failure	0.005" Slip	410
BR12-7	None	Rough and Bonded	Interface Failure	0.005" Slip	408
BR12-8	None	Rough and Bonded	Interface Failure	0.005" Slip	405
B12-1	None	Bond Only	Interface Failure	Before 0.005" Slip	125
B12-2	None	Bond Only	Interface Failure	Before 0.005" Slip	230
B12-3	None	Bond Only	Interface Failure	Before 0.005" Slip	130
B12-4	None	Bond Only	Interface Failure	Before 0.005" Slip	90
B12-5	None	Bond Only	Interface Failure	Before 0.005" Slip	120
B24-1	None	Bond Only	Interface Failure	Before 0.005" Slip	109
B24-2	None	Bond Only	Interface Failure	Before 0.005" Slip	94
B24-3	None	Bond Only	Interface Failure	Before 0.005" Slip	100
RSK12-1	None	Rough	Interface Failure	0.005" Slip	270
BRK12-1	None	Keys in Rough and Bonded	Interface Failure	0.005" Slip	420
BRK12-2	None	Keys in Rough and Bonded	Interface Failure	-	-

3.5.2. Seibel and Latham (1988)

Seibel and Latham study tested shear block specimens in addition to the flexural specimens discussed in Section 3.3.5. The shear block test setup included two interface planes as shown in Figure 3-16. A total of eight unreinforced shear block specimens were tested: specimens 1A, 1B, 2A, 2B, 3A, 3B, 4A, and 4B. The numbering is the same as defined in Section 3.3.5 and the letter represents the first (A) and second (B) test of that interface type. The shear stress is calculated by force at failure divided by the area of both interface surfaces between "new" and "old" material. The reported ultimate shear stresses are shown in Table 3-12.

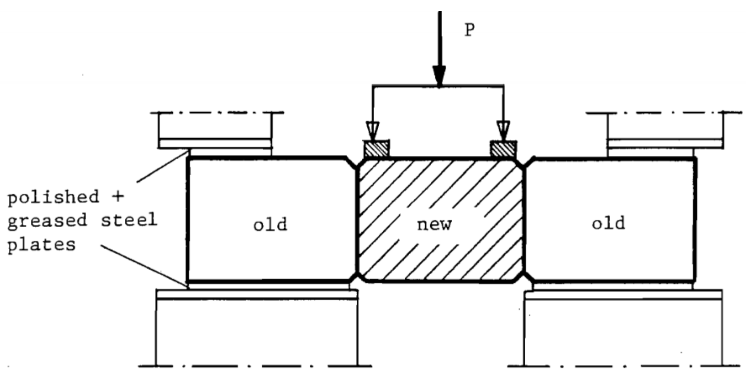

Figure 3-16: Load application of shear block tests by Seibel and Latham (1988).

Table 3-12. Push-off specimen results from Seibel and Latham (1988).

Specimen ID	Reinforcement Across the Interface	Interface Roughness Technique	Failure mode	Method for Calculating Horizontal Shear Stress	Reported Horizontal Shear Stress at Horizontal Shear Failure (psi)
1A	None	Monolithic	-	-	-
1B	None	Monolithic	-	-	-
2A	None	Lubricated	Horizontal Shear	Force/ Interface Area	6
2B	None	Lubricated	Horizontal Shear	Force/ Interface Area	28
3A	None	Surface Rough	Horizontal Shear	Force/ Interface Area	33
3B	None	Surface Rough	Horizontal Shear	Force/ Interface Area	79
4A	None	Scarified	Horizontal Shear	Force/ Interface Area	99
4B	None	Scarified	Horizontal Shear	Force/ Interface Area	110

3.5.3. Mones and Brena (2013)

Mones and Brena investigated the influence of surface preparation techniques on interface shear strength between hollow-core slabs and cast-in-place concrete toppings. The experimental program consisted of twenty-four specimens representing two methods of hollow core construction. Testing was conducted on push-off specimens consisting of two blocks of concrete cast at different times. The geometry of the specimens is shown in Figure 3-17. Mones and Brena tested many different interface roughness conditions representative of precast construction including machine finished, sandblasted, longitudinally raked, longitudinally raked and grouted, longitudinally broomed, longitudinally broomed and grouted, and transversely broomed. Results from the push-off tests are summarized in Table 3-13.

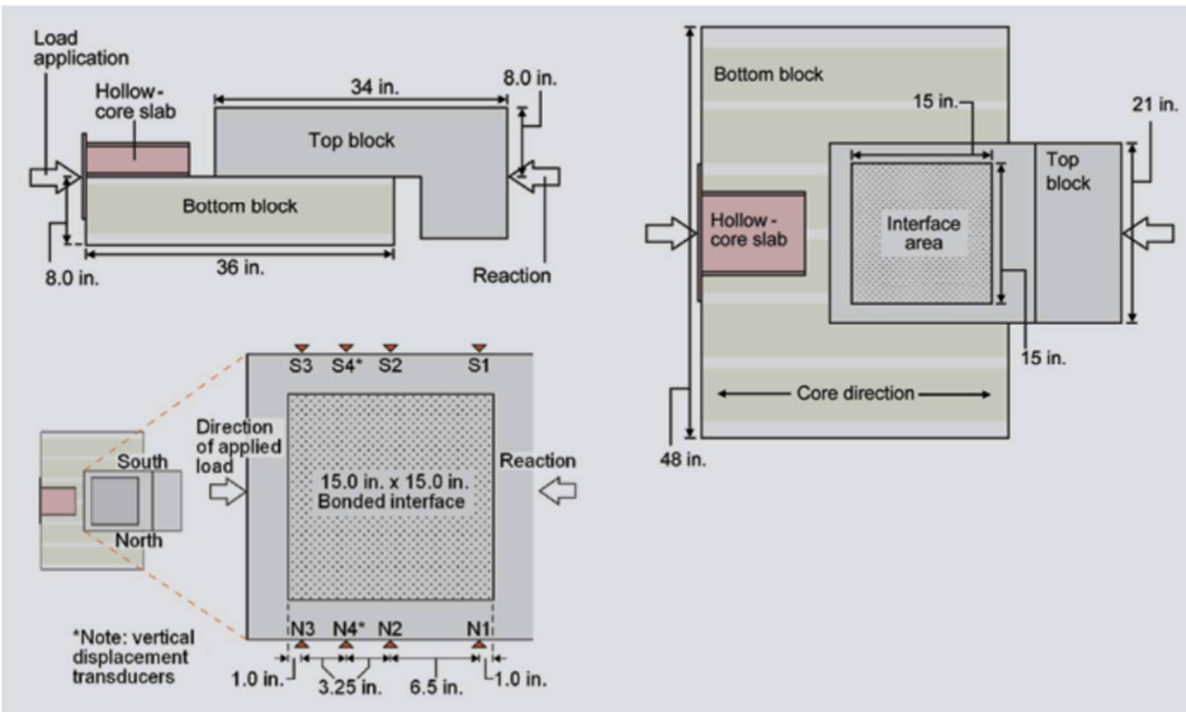

Figure 3-17. Dimensions of push-off specimens and instrumentation locations by Mones and Brena (2013).

The study quantified surface roughness using Mean Texture Depth (MTD). The MTD was determined using ASTM E965 which compares a known volume of sand to the average diameter of a circular sand patch. This method is discussed further in Section 4.5.2 of this report.

The study concluded the following:

- Interfacial shear stress limit of 80 psi for intentionally roughened surfaces is conservative for all surface conditions tested.
- For dry-mix samples, a strong positive linear correlation was observed between surface roughness and interfacial shear strength and horizontal slip capacity. Based on observations, the interfacial shear strength of wet-mix hollow-core slabs was related to both surface roughness and the presence of laitance.
- Sandblasting removed a laitance layer from wet-mix hollow-core slabs and increased interfacial shear strength by providing a higher quality cohesive bond.

- Roughened interfaced developed higher strength and horizontal slip capacity than machine-finished interfaced.
- Roughening was most effective when grooves were perpendicular to the applied shear force.

Table 3-13. Push-off specimen results from Mones and Brena (2013).

Specimen ID	Reinforcement Across the Interface	Interface Roughness Technique	Failure mode	Method for Calculating Horizontal Shear Stress	Reported Horizontal Shear Stress at Horizontal Shear Failure (psi)
DRY-MFX-1	None	Machine Finished	-	Force / Interface Area	207
DRY-MFX-2	None	Machine Finished		Force / Interface Area	152
DRY-SBX-1	None	Sandblasted		Force / Interface Area	162
DRY-SBX-2	None	Sandblasted		Force / Interface Area	215
DRY-LRX-1	None	Longitudinally Raked		Force / Interface Area	223
DRY-LRX-2	None	Longitudinally Raked		Force / Interface Area	205
DRY-TBX-1	None	Transversely Broomed		Force / Interface Area	288
DRY-TBX-2	None	Transversely Broomed		Force / Interface Area	319
DRY-MFG-1	None	Machine Finished, Grouted		Force / Interface Area	276
DRY-MFG-2	None	Machine Finished, Grouted		Force / Interface Area	377
DRY-LRG-1	None	Longitudinally Raked, Grouted		Force / Interface Area	276
DRY-LRG-2	None	Longitudinally Raked, Grouted		Force / Interface Area	266
WET-MFX-1	None	Machine Finished		Force / Interface Area	198
WET-MFX-2	None	Machine Finished		Force / Interface Area	128
WET-SBX-1	None	Sandblasted		Force / Interface Area	268
WET-SBX-2	None	Sandblasted		Force / Interface Area	225
WET-LBX-1	None	Longitudinally Broomed		Force / Interface Area	222
WET-LBX-2	None	Longitudinally Broomed		Force / Interface Area	144
WET-TBX-1	None	Transversely Broomed		Force / Interface Area	257
WET-TBX-2	None	Transversely Broomed		Force / Interface Area	248
WET-MFG-1	None	Machine Finished, Grouted		Force / Interface Area	157
WET-MFG-2	None	Machine Finished, Grouted		Force / Interface Area	165
WET-LBG-1	None	Longitudinally Broomed, Grouted		Force / Interface Area	247
WET-LBG-2	None	Longitudinally Broomed, Grouted		Force / Interface Area	218

3.5.4. Swan (2016)

The Swan study tested Iosipescu specimens in addition to the flexural specimens discussed previously in this literature review. The Iosipescu apparatus is shown in Figure 3-18, and is a type of direct shear test. Steel rods are placed on the bottom and top of the specimen both on opposite sides of the interface and a transverse force is applied to create direct shear across an interface.

For the Iosipescu specimens, the substate was cast in plywood forms, vibrated, and cured for 28 days. In preparation of topping placement, the surface was moistened to SSD conditions. The topping was vibrated and left to cure 28 days before testing. Four Iosipescu specimens were tested for each interface roughness. The average horizontal shear stress at failure is shown in Table 3-14.

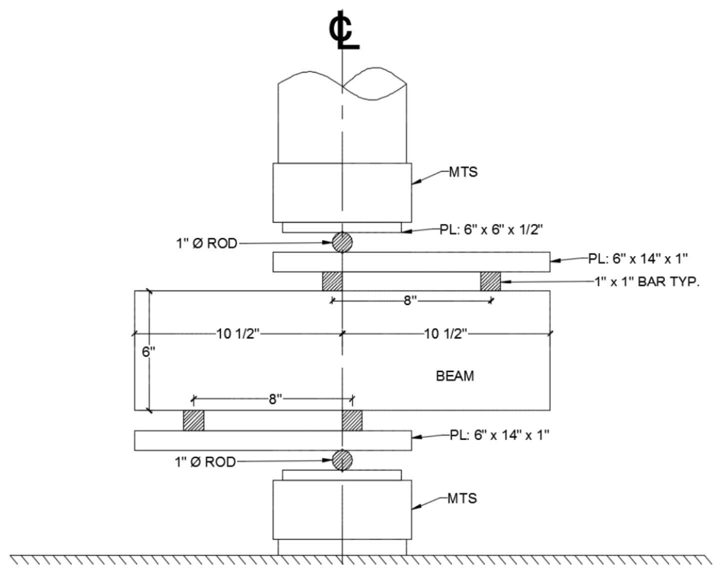

Figure 3-18: Iosipescu test setup in Swan (2016).

Table 3-14. Average shear stresses from Iosipescu specimens tested by Swan (2016).

Substrate Roughness	Average Horizontal Shear Stress (psi)
Smooth	303
Bush Hammer	354
Jackhammer	404

4. PHASE 1 - SLAB SPECIMEN EXPERIMENTAL PROGRAM

4.1. Overview

The Phase 1 specimens were designed to produce a data set of direct shear bond strengths and tensile bond strengths for a range of interface conditions in precast topping and concrete repair applications. The data were used to examine the following:

- Interface bond shear strengths on core specimens as measured by guillotine shear test
- Correlation between interface bond shear strength and tensile bond pull-off strength
- Correlation between interface bond shear strength and a range of interface surface conditions
- Correlation between interface tensile bond strength and a range of interface surface conditions
- Different approaches for characterizing interface surface conditions (i.e., texture/roughness)

4.2. Specimen Design and Variables

A total of twenty composite slabs (two slabs of each variable) with unreinforced interfaces were fabricated and tested. Parameter combinations for each specimen are described in Table 4-1. Interface preparation techniques were selected to provide a range of conditions expected to influence bond strength for both precast topping slab applications and partial-depth repair applications. The following interface preparation conditions were selected to represent new precast construction: smooth (float), tining-raked, and broomed. The following interface preparation conditions were selected to represent concrete repair surface preparation techniques and conditions: sandblasting, mechanical removal followed by sandblasting, and hydrodemolition. The three repair techniques were intended to produce concrete surface profiles (CSP) of CSP 2-3, CSP 5-7, and CSP 9-10, respectively, according to International Concrete Repair Institute (ICRI) No. 310.2R (2013). Concrete material characteristics including workability and consolidation method are discussed in Section 4.3. Interface conditions are discussed in detail in Section 4.4.

The composite slab dimensions were approximately 3 feet by 3 feet, with a thickness of 8.5 inches (2.5-inch topping cast on top of a 6-inch substrate). Direct tensile pull-off tests were conducted on the composite slabs, and direct shear (guillotine) tests were conducted on cores extracted from the slabs. Approximately twelve direct shear tests were performed on cores from each slab, and six direct tensile pull-off tests were performed at locations on each slab. The general slab dimension and testing layout are shown schematically in Figure 4-1.

Table 4-1. Phase 1 slab specimen labels and testing program matrix.

Slab Category	Substrate Interface Preparation Technique	Concrete Placement Technique		Specimen ID
		Concrete Workability (Slump)	Consolidation Technique	
Repair	Sandblast	Moderate	Hand Consolidated	A
Repair	Bush Hammer + Sandblast	Moderate	Hand Consolidated	B
Repair	Hydrodemolition	Moderate	Hand Consolidated	C
Precast	Float	Lower	Screed Only	D
Precast	Broom	Lower	Screed Only	E
Precast	Tine	Lower	Screed Only	F
Precast	Broom	Moderate	Hand Consolidated	G
Precast	Tine	Moderate	Hand Consolidated	H
Precast	Broom	Moderate	Vibrated	I
Precast	Tine	Moderate	Vibrated	J

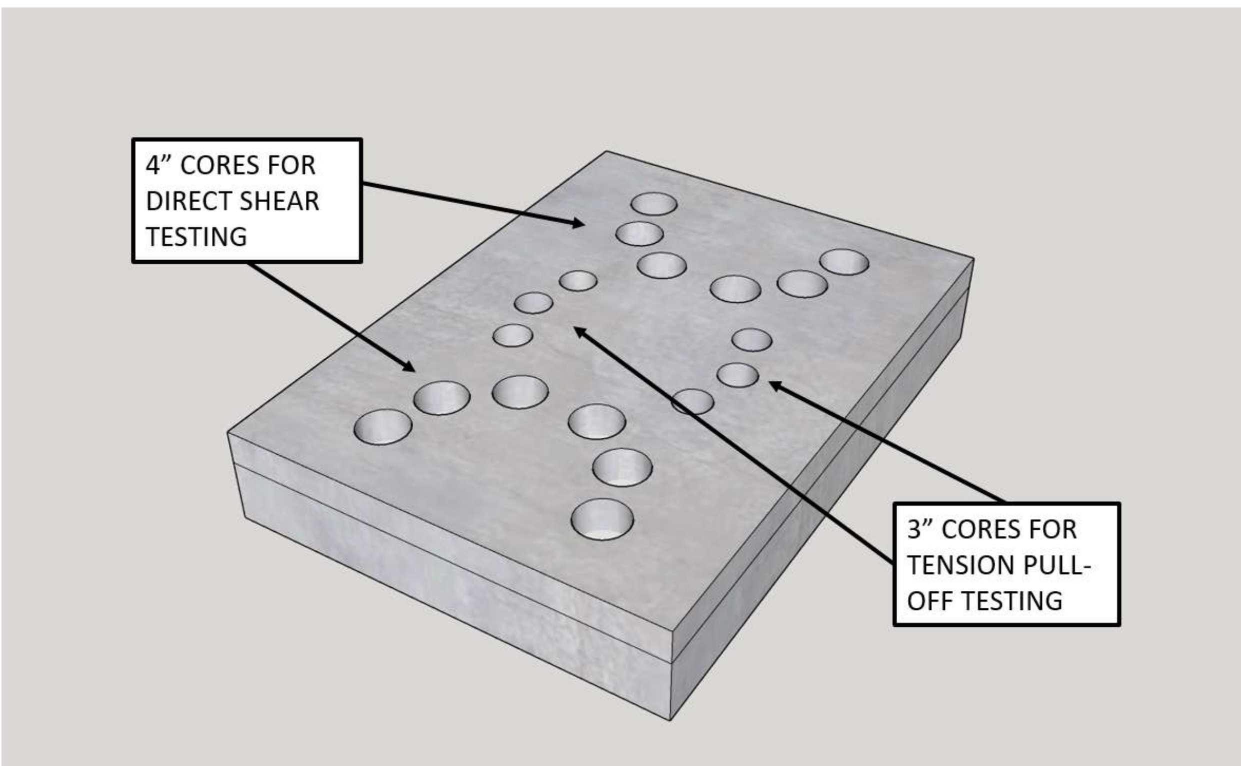

Figure 4-1: Slab specimen general layout.

4.3. Concrete Mixtures and Placement Procedures

Concrete mixtures for the slabs were chosen to be representative of typical design and concrete repair applications. Two different mixtures were initially considered for the overlay concrete representing repair and new construction topping applications. Ultimately, it was decided to use the same concrete for both the topping slab and partial-depth repair applications to limit the number of variables in the testing program and allow the interface condition to be the primary focus when interpreting the shear and tensile bond strength results. Ready-mixed concrete was used for all slab specimens (substrate, repair, and topping concrete). All concrete had a specified 28-day compressive strength of 4,000 psi and a maximum coarse aggregate size of 3/4 inch.

The substrate slabs and topping concrete were fabricated with concrete from one supplier, while the repair concrete was provided by a second supplier. The substrate slabs were placed with a slump of 3 to 6 inches. All concrete substrate placements were consolidated using hand tools followed by wooden screed (hand consolidation).

The concrete for the partial-depth repair specimens was placed at a slump of at least 5 inches (termed moderate workability herein). All partial-depth repair placements were consolidated on the substrate slab by placing in two lifts followed by wooden screed (hand consolidation). The first lift was worked into the substrate by hand using trowels, while the second lift was worked into the first using hand tools (shovels and trowels) followed by screeding.

The precast topping specimens investigated topping workability and placement technique as research parameters. Two workability levels were considered: lower workability with a slump less than 4 inches, and moderate workability with a slump greater than 5 inches. Three placement techniques were investigated: screed only, hand consolidated (same technique as described above for repair series specimens), and vibrated. The last condition was performed using a pencil vibrator inserted in the topping concrete on a 6-inch (approximate) grid pattern, followed by screeding. The concrete workability and placement techniques are summarized in Table 4-2.

Table 4-2. Concrete workability and placement techniques.

Series	Repair or Topping Concrete Workability	Consolidation Method
Repair	Moderate (Slump 5″)	Hand consolidation (HC): two lifts followed by wooden screed
Precast	Lower (Slump < 4″)	Screed only (SC): one lift followed by wooden screed
	Moderate (Slump > 5″)	Hand consolidation (HC): two lifts followed by wooden screed
	Moderate (Slump > 5″)	Vibrated (V): two lifts vibrated followed by wooden screed

The concrete surface treatment immediately prior to placement of the repair concrete or topping concrete may affect the shear and tensile bond strength. Other researchers have compared dry or untreated surfaces to those that are saturated-surface dry, as well as the use of bonding agents. The surface treatment was not considered a variable in the current study; all substrate slabs were prepared to produce saturated-surface dry conditions prior to placement of the repair or topping concrete. First, the surface was cleaned to remove any dust, laitance, or loose material using compressed air. The cleaning was followed by wetting of the substrate concrete approximately 24 hours prior to repair or topping placement and covering with wet burlap. The concrete surface was exposed to drying by evaporation over a period of approximately 1 hour prior to concrete placement, and compressed air was used to ensure that there was no standing water on the substrate surface.

4.4. Interface Preparation Techniques

The interface preparation techniques were selected to represent common surface preparation practices used in industry. For new precast construction, this included substrates that are smooth (floated), tined (raked), and broomed before the concrete has set. The tining-rake and stiff-bristle broom used are shown in Figure 4-2 and Figure 4-4. The substrates with the new construction roughening techniques are shown in Figure 4-3 and Figure 4-5.

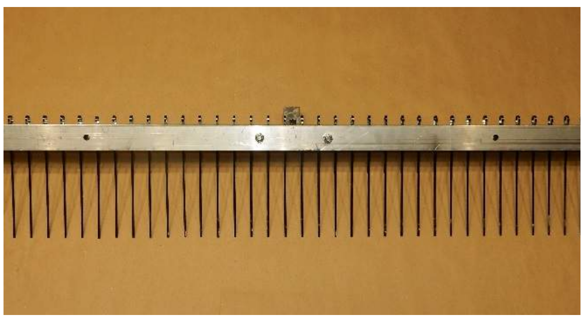

Figure 4-2. Tining rake.

Figure 4-3. Substrate roughened with tining rake.

Figure 4-4. Stiff-bristle broom.

Figure 4-5. Substrate roughened with broom.

For repair construction, the two main practices for surface roughening are hydrodemolition and mechanical removal. Mechanical removal can damage the surface, causing microcracking or "bruising;" therefore, it is commonly specified to be followed by an abrasive blasting technique such as sandblasting. This research project applied three different surfaces with the following range of CSP roughness values:

- Hydrodemolition - CSP of 9 to 10
- Mechanical removal by bush hammer followed by sandblasting - CSP of 6 to 7
- Sandblasting only - CSP of 2 to 3

Although sandblasting alone is not a common surface preparation practice for concrete repair, a range of CSP values was desired for research purposes and sandblasting was included to provide a lower bound of surface roughness. An experienced repair contractor was engaged to perform the surface preparation by sandblasting, bush-hammering, and hydrodemolition. Photographs of each repair surface preparation technique are shown in Figure 4-6 through Figure 4-11.

Figure 4-6. Typical repair surface prepared by hydrodemolition (CSP 9-10).

Figure 4-7. Hydrodemolition technician.

Figure 4-8. Typical repair surface condition prepared by mechanical abrasion (bush hammer followed by sand blasting – CSP 6-7).

Figure 4-9. Bush hammer bit.

Figure 4-10. Typical repair surface prepared by sandblast only (CSP 3).

Figure 4-11. Sandblast technician.

4.5. Surface Roughness Characterization

Previous research and practice have shown that surface roughness has an influence on the interface bond strength. ACI 318 and ACI 562 Code requirements for design of horizontal shear transfer at interfaces require intentional roughening of the substrate surface. To characterize the surface conditions considered in the current study, the following qualitative (visual) and quantitative approaches were used:

- CSP by Visual Comparison to ICRI CSP Comparators
- Mean Texture Depth by Sand Patch Test (ASTM E965)
- Mean Texture Depth by Analysis of 3D Data from Line Laser Scanner (LLS)

4.5.1. CSP by Visual Comparison

ICRI provides a means of visually comparing a concrete surface to ten CSP comparators (ICRI 310.2R-2013) shown in Figure 4-12. The prepared surfaces of the repair specimens were visually matched to the CSP comparators to characterize the surface roughness.

Figure 4-12. ICRI CSP comparators.

4.5.2. Mean Texture Depth by Sand Patch Test

The mean texture depth (MTD) is a measure of surface texture using a volumetric technique. A common approach to measure MTD is performing a sand patch test (SPT) following ASTM E965. This technique was developed to measure the macrotexture depth of concrete pavement surfaces. The technique involves spreading a known volume of sand in a circular manner as uniformly as possible. Once the sand does not spread further, four diameter measurements are taken. These steps are shown in Figure 4-13 and Figure 4-14. The MTD is calculated based on the volume and diameter of the sand patch using the following equation:

$$MTD = \frac{4V}{\pi D^2}$$

where,
V= Volume of sand
D=Average measured diameter

The sand patch test is not commonly used to characterize surface preparation in repair or new construction for structures. Furthermore, there are no established correlations between MTD determined by the sand patch test and shear or tensile bond strength of concrete repairs or topping slab applications. However, since it provides a quantitative indication of surface roughness, the sand patch test was included in the current study as a means of obtaining a quantitative comparison between the surface roughness of the interface types considered.

Figure 4-13. Measuring volume of sand for ASTM E965 Sand Patch Test.

Figure 4-14. Measuring diameter of sand circle after spreading onto concrete surface per ASTM E965.

4.5.3. Mean Texture Depth by Analysis of 3D Data from Line Laser Scanner

Research at the University of Texas at Austin (El Hachem (2019), not related to the current study) was exploring measurement of MTD using a line laser scanner (LLS). The LLS, shown in Figure 4-15, measures surface height (elevation) data over a selected area to create a 3D representation of the surface. An example of a 3D surface plot is shown in Figure 4-16. The 3D data are used along with an algorithm developed by the UT-Austin researchers to calculate an equivalent MTD.

The LLS was used in the current study to scan all substrates (precast and repair surfaces). The 3D data were used to calculate equivalent MTD values for each surface condition. Further surface characterization approaches using the scan data will be explored with the intent of quantitatively correlating surface condition with tested bond strength.

Figure 4-15. Line Laser Scanner (LLS) on the tined substrate specimen.

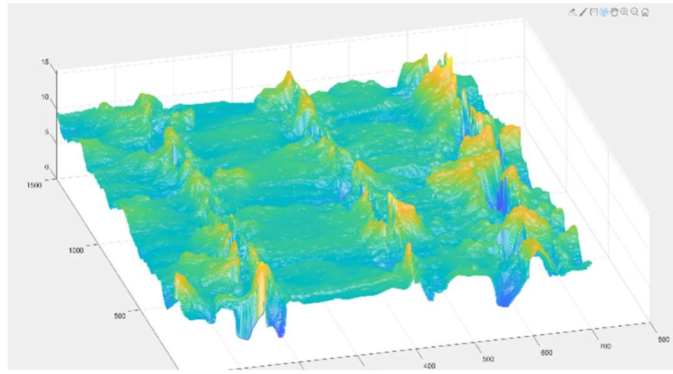

Figure 4-16. Sample LLS 3D scan data for tined substrate specimen.

4.6. Bond Strength Testing Methods

The interface bond strengths were assessed using direct shear (guillotine) tests conducted on cores extracted from the slabs and direct tensile pull-off tests conducted on the slabs.

4.6.1. Direct Shear (Guillotine) Testing

Direct shear testing was performed using 4-inch diameter cores extracted from the slabs. The core specimens were subjected to direct shear loading using a guillotine shear jig, as shown in Figure 4-17 and Figure 4-18. The core samples are inserted into the circular opening of the jig, and thin metal shim sheets are used to ensure a snug fit and maintain the correct alignment of the core sample during testing. The core sample is placed in the jig such that the interface between the substrate and topping is aligned with the line of applied direct shear force. Once the core sample is secured in the jig, a loading block is placed into the jig against the sample and the entire assembly is placed into a concrete compression testing machine. Since the guillotine test is not standardized, there is no specified loading rate for the test method. A loading rate of 5 ± 2 psi per second was used based on the rate specified in ASTM C1583 for direct tensile pull-off tests.

Figure 4-17. Guillotine shear jig – side view.

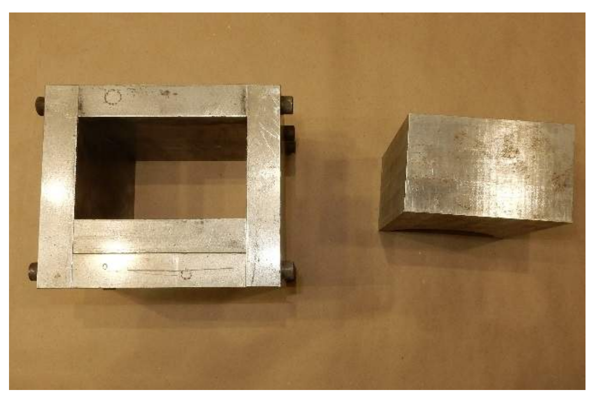

Figure 4-18. Guillotine shear jig – top view.

Figure 4-19. Core sample inside guillotine jig placed within concrete compression testing machine.

Figure 4-20. Core sample shear failure interface after testing (loading head removed).

4.6.2. Direct Tensile Pull-off Testing

Direct tensile pull-off testing was performed in general accordance with ASTM C1583. Preparation for the test involves making a circular cut, or coring, into the slab to a depth of approximately 1-inch below the interface level and attachment of a metal disk to the concrete surface at the cored location using epoxy. Once the epoxy has cured, a pull-off force is applied perpendicular to the interface to measure the interface bond strength in tension. All pull-off tests were performed using a Proceq DY-216 automated pull-off tester.

ASTM C1583 specifies the use of a 2-inch core and metal disk for direct tensile pull-off testing. Preliminary tests in the current study using the standard disk size showed highly variable results, possibly due to the 2-inch core diameter relative to the 2.5-inch interface depth. ASTM C1583 specifies a circular cut or core depth of at least 0.5 inches below the interface between the substrate and overlay, requiring a minimum 3-inch core depth for the specimens in this study. It is possible that stresses due to friction inside the core barrel or core barrel wobble affected the integrity of bond at the interface, increasing the variability of the apparent tensile strength result. It is expected that the effect of barrel twist is more significant as the depth of coring is increased for thicker topping or repair material placements, such as in the case of the 3-inch core depth required in the current study. ASTM C1583 does not provide guidance on this matter, nor does it address disk sizes other than 2 inches. For the purposes of the current study, the test method was changed to use a 3-inch core and disk, which resulted in more consistent test results. All data reported herein are based on a 3-inch core and disk.

Figure 4-21. Direct tensile pull-off testing device.


Figure 4-22. Direct tensile pull-off testing sample.

5. PHASE 1 - SLAB SPECIMEN RESULTS

Results from Phase 1 include material data, surface roughness characterizations, horizontal interface shear strength data from guillotine tests, and interface tensile strengths from direct tensile pull-off tests.

5.1. Material Data

The slab specimens for Phase 1 were fabricated and tested in three groups; each group had a separate concrete placement for the substrate and topping. The complete slab specimen program is shown in Table 5-1, including casting order.

All substrate slabs were cured for 28 days prior to placement of the topping or repair material. This duration was selected to provide a balance between the maturity of the substrate concrete, early-age drying shrinkage and the project schedule. The three topping placements occurred four to six weeks after the substrate was cast.

Each concrete placement (substrate or topping) was moist cured for 7 days using saturated burlap covered by a plastic sheet to seal in the moisture. The specimens were then placed outdoors for the remainder of the 28-day curing period. Both direct tensile and direct shear testing were performed after the topping or repair material reached 28-day strengths.

Table 5-1: Slab specimen parameters.

Cast Number	Slab Category	Interface Preparation Technique	Topping Workability (Slump) Level	Topping Consolidation Technique	Specimen ID
Cast 1 (Substrate) / Cast 2 (Topping)	Repair	Sandblast	Medium	HC	A
Cast 1 (Substrate) / Cast 2 (Topping)	Repair	Bush Hammer + Sandblast	Medium	HC	B
Cast 1 (Substrate) / Cast 2 (Topping)	Repair	Hydrodemolition	Medium	HC	C
Cast 3 (Substrate) / Cast 4 (Topping)	Precast	Float	Low	SC	D
Cast 3 (Substrate) / Cast 4 (Topping)	Precast	Broom	Low	SC	E
Cast 3 (Substrate) / Cast 4 (Topping)	Precast	Tine	Low	SC	F
Cast 5 (Substrate) / Cast 6 (Topping)	Precast	Broom	Medium	HC	G
Cast 5 (Substrate) / Cast 6 (Topping	Precast	Tine	Medium	HC	H
Cast 5 (Substrate) / Cast 6 (Topping	Precast	Broom	Medium	V	I
Cast 5 (Substrate) / Cast 6 (Topping	Precast	Tine	Medium	V	J

SC: Screed Only
HC: Hand Consolidated
V: Vibrated

5.1.1. Concrete Slump

The concrete slump was measured for each concrete placement in accordance with ASTM C143; results are listed in Table 5-2. As described previously, two levels of concrete workability were considered for the topping used on the precast specimens. These are termed lower workability and moderate workability for the purposes of presenting and discussing results herein. While the difference in the measured slump values for these concrete placements was modest, it is noted that a statistically significant difference in interface strength was indicated by the Phase 1 results.

Table 5-2. Measured concrete slump.

Cast Number	Slump
Cast 1 (Substrate)	2.75″
Cast 2 (Topping - Partial-depth Repair)	5″
Cast 3 (Substrate)	4″
Cast 4 (Topping - Lower workability precast topping)	3.75″
Cast 5 (Substrate)	6″
Cast 6 (Topping - Moderate workability precast topping)	5.5″

5.1.2. Compressive Strength

Concrete compressive strength tests were conducted using 4-inch by 8-inch cylinders in accordance with ASTM C39. The strength was tested at 7 and 28 days after casting as well as on the day of shear/tensile testing of specimens. The compressive strengths for each concrete cast are shown in Table 5-3.

Table 5-3. Concrete compressive strength results.

Cast Number	7-Day (psi)	28-Day (psi)	Day of Testing (psi)
Cast 1 (Substrate)	3550	5550	5700
Cast 2 (Topping - Partial-depth repair)	4450	5400	5400
Cast 3 (Substrate)	4400	5750	6700
Cast 4 (Topping - Lower workability precast topping)	4600	5400	5700
Cast 5 (Substrate)	4100	5200	5100
Cast 6 (Topping - Moderate workability precast topping)	4150	5350	5950

5.1.3. Splitting Tensile Strength

Concrete splitting tensile strength tests were conducted using 4-inch by 8-inch cylinders in accordance with ASTM C496. The strength was tested at 7 and 28 days after casting as well as the day of shear/tensile testing of specimens. The splitting tensile strengths for each cast are shown in Table 5-4.

Table 5-4: Splitting tensile strength results.

Cast Number	7-Day (psi)	28-Day (psi)	Day of Testing (psi)
Cast 1 (Substrate)	470	550	-
Cast 2 (Topping - Partial-depth repair)	520	540	-
Cast 3 (Substrate)	510	590	-
Cast 4 (Topping - Lower workability precast topping)	510	550	-
Cast 5 (Substrate)	510	540	540
Cast 6 (Topping - Moderate workability precast topping)	460	580	660

5.2. Surface Roughness Characterization Results

As described previously, three surface roughness characterization techniques were used to define the roughness of each interface preparation condition:

- CSP by Visual Comparison to ICRI CSP Comparators
- Mean Texture Depth by Sand Patch Test (ASTM E965)
- Mean Texture Depth by Analysis of 3D Data from Line Laser Scanner (LLS)

5.2.1. CSP by Visual Comparison Results

The ICRI CSP comparators were only used on repair specimens. The CSP results are summarized in Table 5-5. The surface preparation techniques investigated resulted in CSP values across nearly the full range of CSP comparators.

Table 5-5: ICRI CSP values for repair interface conditions.

Interface Condition	CSP Range
Sandblast	2-3
Bush Hammer + Sandblast	7-8
Hydrodemolition	9-10

5.2.2. Mean Texture Depth by Sand Patch Test and Line Laser Scanner

The SPT was performed on selected substrate specimens with repair interface conditions, followed by use of the Line Laser Scanner (LLS) on the same specimens. As shown in Table 5-6, the MTD values were similar for the two methods. Since the LLS is quicker, cleaner, and has shown to be more repeatable than the SPT, the LLS was the only method used to determine MTD for the remaining slabs. Each slab had measurements of MTD by LLS at four different locations. The complete summary of MTD values for all specimens based on LLS is shown in Table 5-7.

Hypothesis testing using a Student's t-test statistical analysis indicates that there is a statistically significant difference (95 percent confidence) between the MTD values found by LLS for the three repair surfaces (hydrodemolition versus bush hammer + sandblast, and bush hammer + sandblast versus sandblast only). Hypothesis testing also showed a statistically significant difference between MTD average of the broom and tined surfaces. These results indicate that MTD can differentiate between the different surface preparation techniques investigated in this study.

Table 5-6: Comparison of MTD from line laser scanner and sand patch test.

Interface Preparation Technique	MTD Average from LLS (mm)	MTD Average from SPT (mm)
Sandblast	0.20	-
Bush Hammer + Sandblast	0.82	0.83
Hydrodemolition	1.33	1.40

Table 5-7: Average MTD for each interface preparation condition based on LLS measurements.

Interface Preparation Technique	MTD Average from LLS (mm)	Standard Deviation (mm)	Coefficient of Variation	Sample Size
Broom	1.14	0.21	18%	16
Tine (Rake)	2.23	0.44	20%	16
Sandblast	0.2	0.012	6%	8
Bush Hammer + Sandblast	0.82	0.10	12%	8
Hydrodemolition	1.33	0.13	10%	8

5.3. Direct Shear (Guillotine) Results

The direct shear test results for all Phase 1 specimens are shown in Table 5-8 and Figure 5-1. Most of the tested cores failed at the interface bond line. In some cases the failure plane was straight across the bond line, as shown in Figure 5-2 and Figure 5-3, while in other cases the failure plane initiated at the interface and propagated into the topping or substrate, as shown in Figure 5-4 and Figure 5-5. A limited number of cores did not fail in shear at the interface, but rather failed in flexure near the mid-length of the core. These results are not included in the data set provided in this report.

Table 5-8. Phase 1 direct shear strength results.

Slab Category	Interface Preparation Technique	Topping Workability Level	Topping Consolidation Technique	Direct Shear Strength			
				Average (psi)	Std. Dev. (psi)	CoV	Sample Size
Repair	Sandblast	Moderate	HC	815	209	26%	19
Repair	Bush Hammer + Sandblast	Moderate	HC	682	237	35%	18
Repair	Hydro-demolition	Moderate	HC	1009	214	21%	24
Precast	Float	Lower	SC	415	308	74%	2
Precast	Broom	Lower	SC	454	285	63%	31
Precast	Tine	Lower	SC	433	330	73%	32
Precast	Broom	Moderate	HC	848	194	23%	10
Precast	Tine	Moderate	HC	731	258	35%	20
Precast	Broom	Moderate	V	834	214	25%	21
Precast	Tine	Moderate	V	670	210	31%	17

HC: Hand Consolidated
V: Vibrated
SC: Screed Only
Std. Dev.: Sample standard deviation
CoV: Coefficient of variation

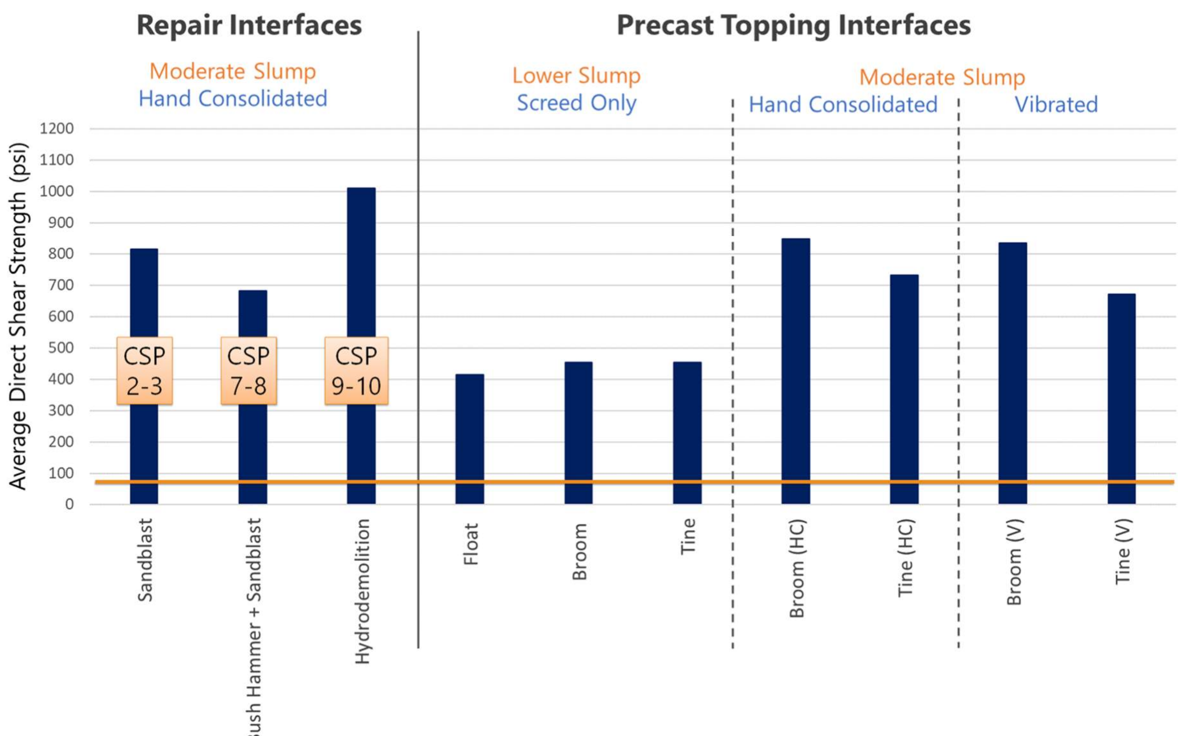

Figure 5-1: Average direct shear (guillotine) strength results. Note current ACI interface nominal shear strength for design is 80 psi (orange line).

Figure 5-2. Direct shear failure plane at interface bond line (whole specimen).

Figure 5-3. Direct shear failure plane at interface bond line (only substrate portion of core shown).

Figure 5-4. Direct shear failure plane propagating into topping layer (whole specimen).

Figure 5-5. Direct shear failure plane propagating into topping layer (only substrate portion of core shown).

5.4. Direct Tensile Pull-off Results

The Phase 1 direct tensile pull-off test results are presented in Table 5-9 and Figure 5-6. The precast series specimens with lower slump topping placed by screed only did not produce valid test results due to separation (debonding) of the topping from the substrate during coring in preparation for pull-off testing. This may have resulted from the limited bond between the topping and the substrate due to the lower slump topping and limited consolidation for these specimens, or the possible effect of differential shrinkage at the interface, or both. The coring action (i.e., shear stress due to torsion while coring or barrel wobble) to prepare for the pull-off test caused debonding of the topping. Therefore, pull-off test results for the precast series presented and discussed herein are only those for moderate slump concrete placed by hand consolidation or vibration. Note that all pull-off tension tests were performed with 3-inch diameter disks as described previously.

Table 5-9: Phase 1 direct tensile pull-off strength results.

Slab Category	Interface Preparation Technique	Topping Workability Level	Topping Consolidation Technique	Direct Tensile Pull-off Strength			
				Average (psi)	Std. Dev. (psi)	CoV	Sample Size
Repair	Sandblast	Moderate	HC	300	65	22%	11
Repair	Bush Hammer + Sandblast	Moderate	HC	191	47	25%	11
Repair	Hydro-demolition	Moderate	HC	422	37	9%	11
Precast	Float	Lower	SC	-	-	-	-
Precast	Broom	Lower	SC	-	-	-	-
Precast	Tine	Lower	SC	-	-	-	-
Precast	Broom	Moderate	HC	339	85	25%	12
Precast	Tine	Moderate	HC	327	65	20%	12
Precast	Broom	Moderate	V	360	77	22%	12
Precast	Tine	Moderate	V	351	39	11%	12

HC: Hand Consolidated
V: Vibrated
SC: Screed Only

Std. Dev.: Sample standard deviation
CoV: Coefficient of variation

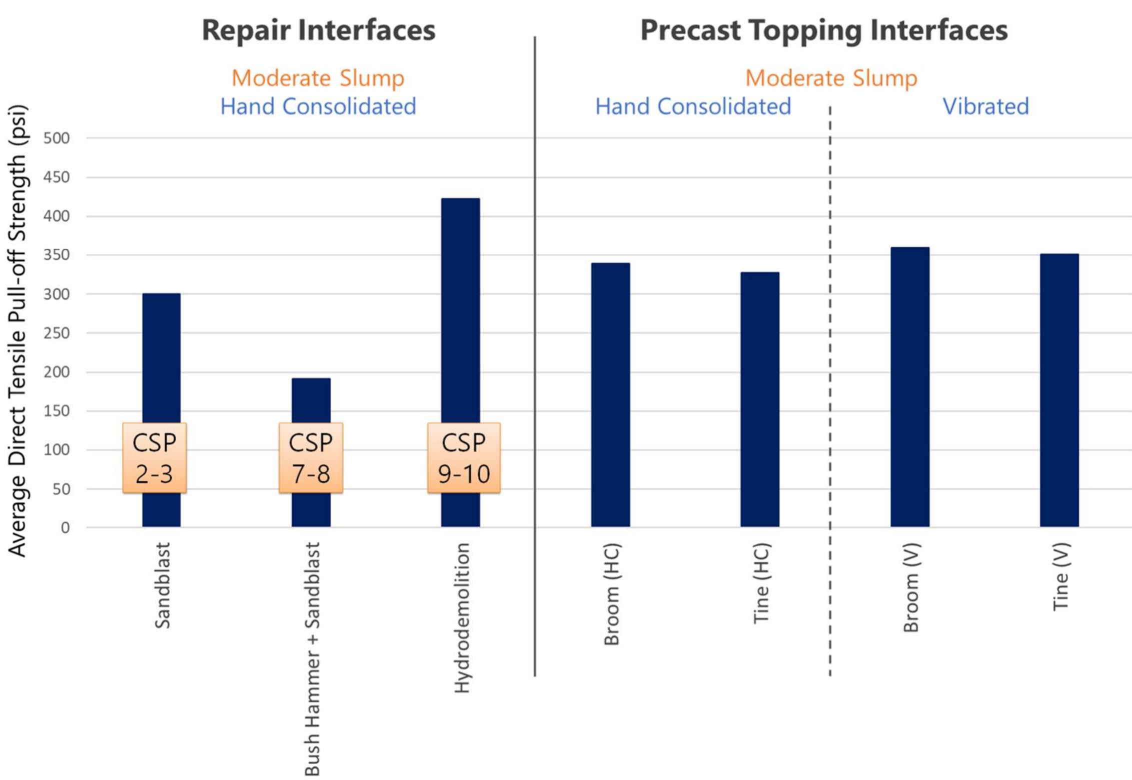

Figure 5-6: Average direct tensile pull-off results (psi).

5.5. Discussion of Phase 1 Results

5.5.1. Influence of Investigation Parameters on Direct Shear Strength

The hydrodemolition interface had the highest average shear bond strength of the three repair interfaces investigated at 1009 psi; this was the highest measured shear strength of all interfaces (repair and precast) considered in the current study. Hypothesis testing using a Student's t-test indicated a statistically significant difference between the mean shear bond strengths of the three repair interfaces. The lowest shear strength in the repair series was obtained for the bush hammer + sandblast interface, which had an average shear strength of 682 psi in comparison to 815 psi for sandblast alone. This suggests that mechanical removal using a bush hammer may be damaging or "bruising" the concrete substrate to a degree that cannot be compensated for by follow-up sandblasting; this is a known concern related to the use of bush hammering for concrete removal. It is also notable that the bush hammer + sandblast had the greatest variability of shear test results for the three repair interfaces, with a coefficient of variation (CoV) of 35 percent in comparison to 26 percent and 21 percent for the sandblast and hydrodemolition interfaces, respectively.

The precast series investigated topping concretes with two different workability levels (termed lower and moderate) as well as different placement techniques as described previously. As expected, a pronounced difference was measured for shear strengths of precast samples with topping placed with lower slump and consolidated by screed only in comparison to topping with moderate slump and hand consolidated or vibrated. The average shear strengths of the float, broom, and tined interfaces with lower slump/screed only placement did not show a significant effect of interface preparation and exhibited very high variability with coefficients of variation ranging from 63 percent to 73 percent. Furthermore, the average strengths for these specimens were on the order of 35 percent to 45 percent lower than the strengths of the same interfaces where the topping was placed with a moderate slump and hand consolidation or vibration.

The difference between the workability levels and placement techniques was visually apparent at the bond interface observed after testing, as illustrated in Figure 5-7. Incomplete consolidation of the topping against the substrate concrete was visually apparent in specimens with lower slump topping placed by screed only. Where moderate slump topping was consolidated by hand or vibration, instances of entrapped air or incomplete consolidation at the interface were significantly reduced. As well, filling of tine grooves in the substrate by the topping was improved such that the groove lines were much less visible after testing to failure.

The precast series specimens with moderate slump concrete had shear strengths comparable to the bush hammer + sandblast and sandblast only specimens from the repair series. The broom-hand consolidated and broom-vibrated had average direct shear strengths of 848 psi and 834 psi, respectively, while the tine-hand consolidated and tine-vibrated specimens had shear strengths of 731 psi and 670 psi, respectively. On average, the shear strengths of the broom finish were approximately 20 percent higher than those of the tine finish; hypothesis testing using a Student's t-test indicates that this difference between the means is statistically significant. Furthermore, hypothesis testing indicates that there is no statistical difference between the means from hand consolidation and vibrated placement conditions for either the broom or tine surface.

The precast series specimens with moderate slump concrete were tested both parallel and perpendicular to the broom/tine direction as illustrated in Figure 5-8 and Figure 5-9. The average direct shear strengths for broom finish when loaded parallel and perpendicular were 893 psi and 787 psi, respectively (results for both vibrated and hand consolidated combined). For tine finish, the average direct shear strengths for parallel and perpendicular loading were 711 psi and 695 psi, respectively (combined results from both consolidation techniques). Hypothesis testing using Student's t-test indicates that the differences between the average direct shear strengths for the two loading directions are not statistically significant when both consolidation techniques are grouped.

The broom-vibrated parallel tests and broom-vibrated perpendicular tests had average direct shear strengths of 957 psi and 722 psi, respectively. The average direct shear strength of loading parallel to the roughening direction is approximately 30 percent higher than when loaded perpendicular for the broom-vibrated specimens. Hypothesis testing using Student's t-test shows this difference in average strength is statistically significant. No other combination of consolidation or roughening technique indicated that the differences between mean strengths were statistically significant.

5.5.2. Influence of Investigation Parameters on Direct Tensile Pull-off Strength

The direct tensile pull-off test results exhibited the same overall trends in strength as shown in the direct shear strength results. In the repair series, hydrodemolition of the interface resulted in the highest tensile bond strength with an average of 422 psi, followed by sandblast alone at 300 psi and bush hammer + sandblast at 191 psi. Hypothesis testing (Student's t-test) indicates that the differences between the average tensile bond strengths for the three repair interfaces were statistically significant. The variability of the test results from the hydrodemolition interfaces was significantly lower than that of the other repair interfaces, indicating more consistent interface conditions and improved tensile bond strength.

The precast series specimens with moderate slump concrete had lower tensile pull-off strengths than the hydrodemolition specimens from the repair series but had higher strengths than the sandblast alone and bush hammer + sandblast repair specimens. The broom-hand consolidated and broom-vibrated specimens had average direct tensile strengths of 339 psi and 360 psi, respectively, while the tine-hand consolidated and tine-vibrated specimens had tensile strengths of 327 psi and 351 psi, respectively. Hypothesis testing indicates that the differences between the tensile bond strength results for the broom and tine finishes are not statistically significant. Similarly, there difference in mean tensile strength between the hand consolidation and vibrated placement conditions is not statistically significant.


Substrate
Topping

Tined surface, lower slump topping with screed only placement.


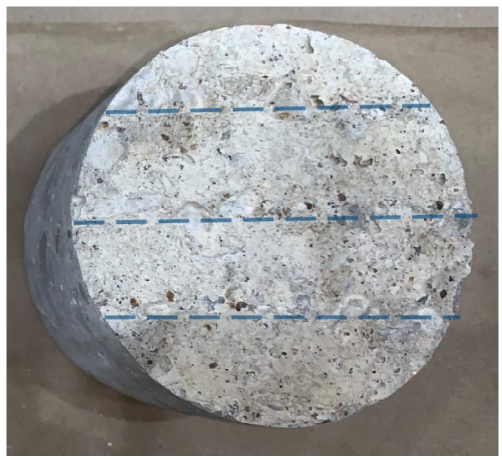

Substrate
Topping

Tined surface, moderate slump topping with hand consolidated placement (note tining lines have been accented using dashed lines in the figure).

Figure 5-7. Visual comparison of interface conditions for precast specimens with topping concrete placed under different conditions.

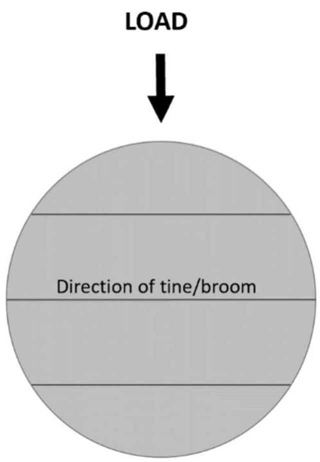

Figure 5-8. Direct shear test orientation for precast specimen loaded perpendicular to the roughening direction.

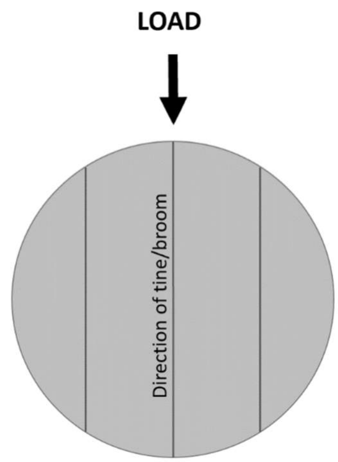

Figure 5-9. Direct shear test orientation for precast specimen loaded parallel to the roughening direction.

5.5.3. Effectiveness of Interface Preparation Techniques

The primary objectives of the research were to explore the use of direct shear (guillotine) strength tests on cores removed from partial-depth repair and precast topping slab specimens, as well as to determine whether the nominal shear strength for design of unreinforced interfaces should be reconsidered. While the objectives were not explicitly intended to determine the most effective surface preparation techniques, the test results reinforce the findings of previous research in this subject area and provide additional insight into the requirements for improving shear and tensile bond strength at unreinforced interfaces. The following sections discuss the apparent effectiveness of the surface preparation techniques investigated based on the Phase 1 results. An overall discussion of results for Phases 1 and 2 is included in Section 8.

5.5.3.1. Repair Interfaces

As expected, the substrate prepared by hydrodemolition provided the highest direct shear and tensile pull-off strengths in the repair series specimens. The hydrodemolition achieved a CSP of 9-10 based on the ICRI CSP comparators and had the highest MTD of the repair series specimens as determined by LLS. Hydrodemolition is a widely used method for concrete removal and can produce a surface profile with a high degree of surface roughness with a low risk for microcracking or bruising.

The bush hammer + sandblast interface had the lowest shear and tensile bond strengths in the repair series. The use of a hand-held bush hammer is a form of scabbling for concrete removal. While removal by bush hammer can produce a concrete profile of CSP 7 to 9 (a CSP of 7 to 8 was achieved in this project), the scabbling action can cause microfractures in the cement paste and loosening of the coarse aggregate at the substrate surface, creating a weakened or bruised layer. The use of abrasive blasting (sandblasting) after concrete removal by bush hammering is intended to remove the weakened layer. Despite having a CSP 7-8 surface profile, the low shear and tensile bond strength test results for the bush hammer + sandblast specimen suggest that microcracking was present and that the sandblasting was unable to remove weakened surface layer at the interface. This surface preparation type had the highest ratio of shear-to-tensile bond strength of all interfaces investigated, suggesting that the (presumed) presence of microcracking had a more significant effect on the tensile pull-off strength than on the direct shear strength.

The sandblast only interface was included to provide a lower bound for surface roughness; a surface profile of CSP 2-3 was achieved in this study. The sandblast only surface could be considered to meet the ACI 318-19 Cl. 16.4.4.2 surface preparation definition of "intentionally roughened" but would not meet the requirement for "intentionally roughened to a full amplitude of approximately 1/4-inch." This latter condition is only required for design conditions with interface shear reinforcement. In spite of this lower degree of surface roughness, the sandblast only interface achieved higher direct shear and tensile pull-off strengths than the bush hammer + sandblast interface and had comparable strength results to the broom and tine interfaces in the precast series. These results illustrate the benefits of limited "intentional roughening" that removes laitance and minor surface defects while opening the paste pore structure at the repair interface.

5.5.3.2. Precast Interfaces

The precast series with float surface preparation and lower slump topping were not able to achieve consistent measurable results in either the direct shear or tensile bond pull-off tests, and thus are excluded from further discussion. This combination of surface preparation and concrete placement was included for comparison purposes to represent a lower bound condition in the precast series. It is not used in practice, nor is it recommended for use in precast or other construction with unreinforced interfaces.

The Phase 1 test results for the precast series indicate that the differences in interface direct shear and tensile bond strength for topping placed by hand consolidation and by vibration were not statistically significant. Accordingly, the data sets for hand consolidated and vibrated precast series specimens have been combined for the purposes of the following discussion.

The broom interface developed an average direct shear strength approximately 20 percent higher than the tine interface (considering all data for moderate slump concrete placed by hand consolidation and moderate slump concrete consolidated by vibrating). The average tensile pull-off strength was similar for the two interfaces (i.e., the differences in the test data were determined to be not statistically significant). The broom interface shear strength results were slightly less variable than the results for the tine surface, although the opposite trend was noted for the tensile pull-off strength results.

It is generally assumed that a tine or rake finish will provide more surface roughness than a broom finish, and thus the tine finish is expected to provide improved interface bond strength. The direct shear strength results from this study contradict this assumption. Previous research comparing the shear strength of broom and tine or rake finishes has also been contradictory. As discussed in Section 3.5, Mones and Breña (2013) performed push-off tests for twenty-four specimens with two hollow-core slab concrete types and six different slab finishes, including broom and raked. The highest shear strength values were obtained for specimens with transverse broomed finish, at 278 psi, while the longitudinally raked finish with an amplitude of about 1/4 inch had an average strength of 198 psi. While these findings are consistent with the current study, Kovach and Naito (2008) observed the opposite trend in a study involving thirty-two composite T-beam flexural experiments to assess shear transfer. Kovach and Naito observed a strong correlation between shear strength and surface roughness and recommended design horizontal shear strength values of 435 psi for broom finish and 571 psi for rake finish.

The contradictory conclusions regarding the shear bond strength of broom and rake finishes in unreinforced interfaces may result from several factors, including substrate and topping properties and placement procedures, variability in the surface textures created by raking or tining the substrate, and differences in shear test methods.

6. PHASE 2 – FLEXURAL SPECIMENS EXPERIMENTAL PROGRAM

6.1. Overview

The experimental program of Phase 2 comprised five composite RC beams tested under three-point bending to study the horizontal shear capacity of unreinforced interfaces. Each of the beams had a different interface roughness representative of common precast (new construction) and partial-depth repair techniques. A monolithic beam was also tested as a control specimen. In addition to the beams, five composite slabs were fabricated at the same time to obtain samples for guillotine shear and direct tensile pull-off tests for the five different interface roughness conditions.

The data were used to examine the following:

- Correlation between interface bond shear strength and a range of interface surface conditions as indicated from composite beam tests and direct shear (guillotine) tests
- Correlation between interface tensile bond strength and a range of interface surface conditions
- Correlation between interface bond shear strength and tensile bond pull-off strength

This section describes the experimental variables, specimen design and fabrication, test setup and instrumentation for Phase 2.

6.2. Specimen Design and Variables

The interface preparation techniques chosen for the five composite beams were sandblast, hydrodemolition, broom, tine, and float. Five companion plain concrete composite slabs were fabricated with the same interface preparation as the composite beams. The topping workability and consolidation technique were consistent for all the composite specimens using a moderate topping slump and vibrating the topping for consolidation. A monolithic beam with the same geometry and reinforcement as the composite beams was also included in the program. The complete test program of Phase 2 with corresponding cast number is summarized in Table 6-1 and Table 6-2.

The dimensions and reinforcement of the beam specimens are presented in Figure 6-1, Figure 6-2, and Figure 6-3. The specimens were designed so that the horizontal shear capacity of the interface in one span would be exceeded prior to reaching the flexural and vertical shear capacities of the beam. The beam substrates had an 18-inch width and a 13-inch height. The beam toppings had an 18-inch width and 5-inch height. The beam longitudinal reinforcement comprised eight #8 bars as tension reinforcement, four #4 bars at the top of the substrate beam to facilitate stirrup placement, and three #4 bars at mid-height of the topping as compression reinforcement. The transverse reinforcement comprised two overlapping closed stirrups to provide four legs of #3 bars spaced at 4.5 inches in the longitudinal direction of the beam.

To ensure a horizontal shear failure, one shear span of the beam (failure end) had an unreinforced interface with a partially debonded area to increase the horizontal shear stress developed. As shown in Figure 6-1, only the middle 8 inches of the interface across the beam width were bonded at the failure end. The other shear span (non-failure end) had the stirrups extending into the topping slab acting as interface reinforcement and the interface was bonded across the entire width, as shown in Figure 6-2. The toppings were designed to end 18 inches (equivalent to the beam depth) from the center of the support. This was done to prevent potential interface failures caused by propagation of diagonal shear cracks originating at the supports. This approach was originally proposed by Loov and Patnaik (1994) and has been implemented in other relevant horizontal shear beam test studies such as Kovach and Naito (2008).

The same slab specimen design used in Phase 1 was used for Phase 2 companion slabs. The slabs had a 4-inch substrate with a 2.75-inch topping. The specimens were approximately 3 by 3.5 feet to provide adequate space for direct shear samples and direct tensile pull-off tests.

Table 6-1: Phase 2 Beam Specimen Test Matrix

Beam Number	Beam Category	Interface Preparation Technique	Topping Workability (Slump) Level	Topping Consolidation Technique	Concrete Cast Number
B0	-	Monolithic	Medium	Vibrated	Cast 7
B1	Repair	Sandblast	Medium	Vibrated	Cast 7 (Substrate) / Cast 9 (Topping)
B2	Repair	Hydrodemolition	Medium	Vibrated	Cast 7 (Substrate) / Cast 9 (Topping)
B3	Precast	Float	Medium	Vibrated	Cast 7 (Substrate) / Cast 9 (Topping)
B4	Precast	Broom	Medium	Vibrated	Cast 7 (Substrate) / Cast 9 (Topping)
B5	Precast	Tine	Medium	Vibrated	Cast 7 (Substrate) / Cast 9 (Topping)

Table 6-2: Phase 2 Slab Specimen Test Matrix

Slab Number	Slab Category	Interface Preparation Technique	Topping Workability (Slump) Level	Topping Consolidation Technique	Concrete Cast Number
S1	Repair	Sandblast	Medium	Vibrated	Cast 8 (Substrate) / Cast 9 (Topping)
S2	-	Hydrodemolition	Medium	Vibrated	Cast 8 (Substrate) / Cast 9 (Topping)
S3	Repair	Float	Medium	Vibrated	Cast 8 (Substrate) / Cast 9 (Topping)
S4	Repair	Broom	Medium	Vibrated	Cast 8 (Substrate) / Cast 9 (Topping)
S5	Precast	Tine	Medium	Vibrated	Cast 8 (Substrate) / Cast 9 (Topping)

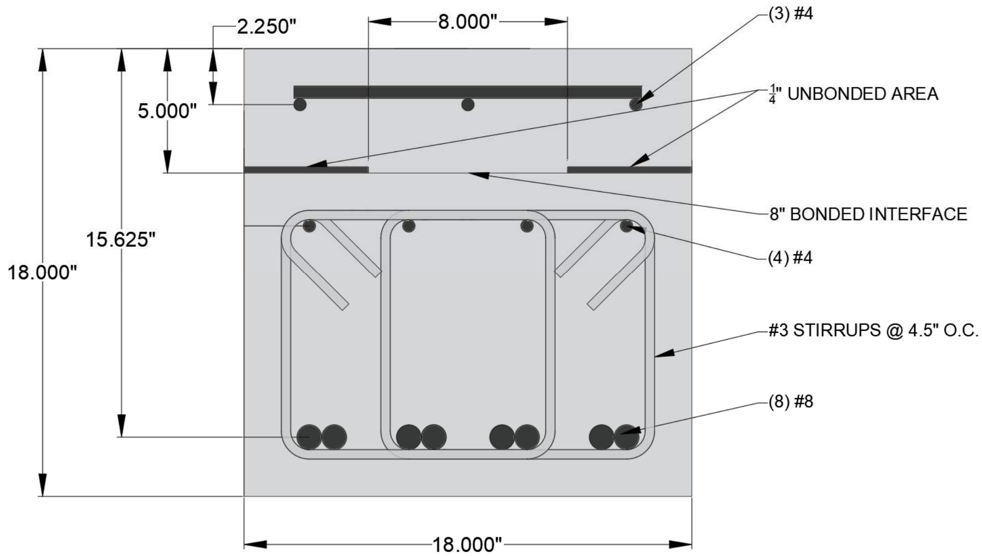

Figure 6-1. Beam specimen cross-section – Failure end.

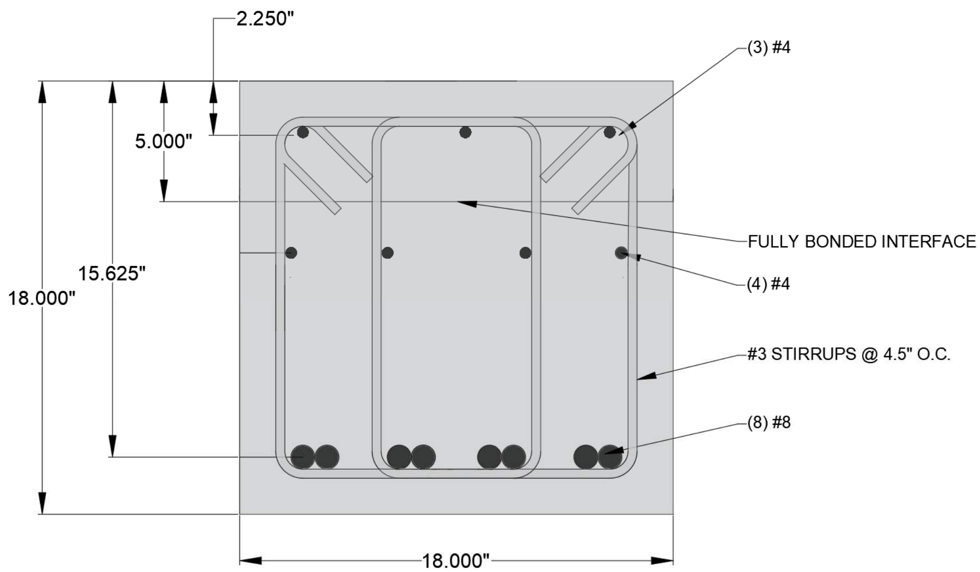

Figure 6-2. Beam specimen cross-section – Non-failure end.

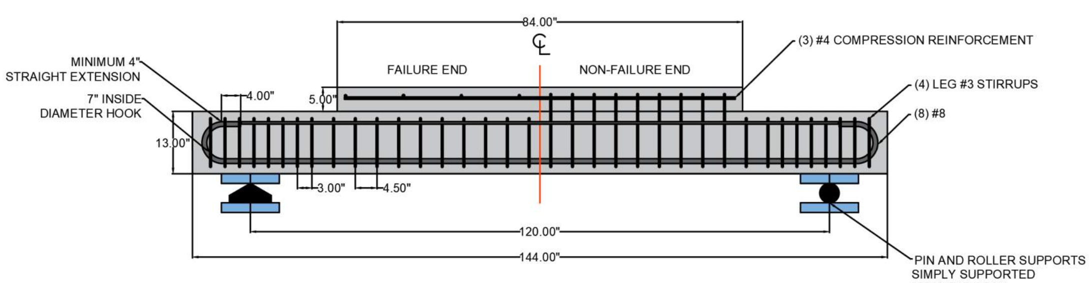

Figure 6-3. Beam specimen reinforcement detail – elevation view.

6.3. Specimen Fabrication

Fabrication of Phase 2 specimens was performed at the Phil M. Ferguson Structural Engineering Laboratory at the University of Texas at Austin.

6.3.1. Concrete Mixtures

The concrete mixture and supplier used for the Phase 2 the substrate and toppings of beam and slab specimens were the same as used in Phase 1 to maintain consistency. The concrete mixture had a 4,000 psi specified compressive strength, 3/4-inch maximum aggregate size, and 4.5-inch design slump.

6.3.2. Substrate Fabrication

The beam specimen (substrate) reinforcement cage was prepared and placed in wood formwork. Prior to casting, all wood surfaces that would be exposed to concrete were coated with form oil. The reinforcement cage and formwork are shown in Figure 6-4 and Figure 6-5.

Figure 6-4. Beam substrate ready for concrete casting.

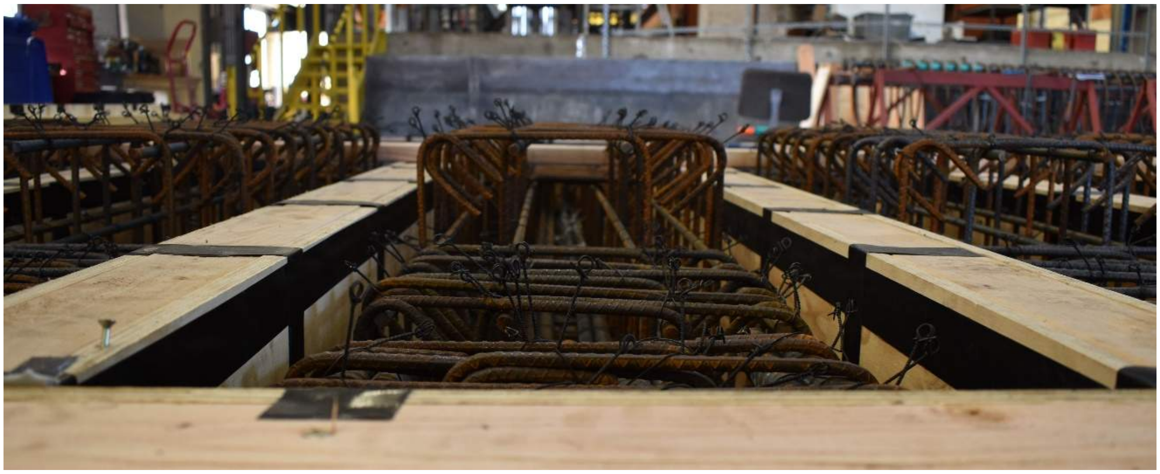

Figure 6-5. Beam substrate showing stirrups on non-failure end that extend into topping as interface reinforcement.

The concrete was placed on August 8, 2020. The specimens were vibrated and screeded for consolidation. Once the concrete had hardened sufficiently, all surfaces were floated on the failure end of the beam. The broom and tine specimens were roughened shortly after the completion of floating. The non-failure end surface was left as-placed. Saturated burlap was placed on the beams and covered with a plastic tarp after finishing was complete. The beams were wet cured for 7 days.

The companion slab substrate elements were cast separately one week later. The same mix design, finishing, roughening, and curing procedures were used.

The sandblast and hydrodemolition interface surface preparation techniques conditions were performed after the beam and slab substrates had cured for at least 28 days. The repair surface preparation was performed by the same repair contractor as in Phase 1.

Once the five interface preparation techniques were completed, roughness measurements were taken using the same line laser scanner used in Phase 1. The 3D data were used to determine mean texture depth (MTD) values for each surface condition.

6.3.3. Method for Limiting Beam Interface Width

As previously described, the beam failure end interface was partially debonded to enforce a higher horizontal shear stress and in turn a horizontal shear failure. A variety of techniques have been used in previous studies to debond portions of concrete interfaces, including plastic wall paneling secured with tape (Swan 2016) and polyethylene foam tape (Kovach and Naito 2008). The debonding material needed to be thick enough to prevent aggregate interlock between the substrate and topping, but also flexible to adhere to the peaks and valleys of each surface. One layer of 1/4-inch thick polyethylene foam tape was used as the debonding material in this study. The polyethylene foam tape installed on the hydrodemolition beam substrate is shown in Figure 6-6.

Figure 6-6. Hydrodemolition substrate with debonding foam tape placed at edges to limit the bonded width to 8 inches.

6.3.4. Topping Placement

The concrete topping for the composite beams and slab specimens was cast on October 6, 2020. The condition of the beam specimens prior to the topping pour are shown in Figure 6-7. Prior to casting, the substrates were wetted and covered with saturated burlap for 24 hours to achieve SSD conditions (Figure 6-8). The burlap was removed and the topping the surfaces were blown clean using compressed air and patted dry about 1 hour before placement of the concrete topping. The topping concrete used was the same concrete mix design from the same supplier as used for the beam and slab substrates. The topping was placed in one layer and was consolidated using a pencil vibrator. The topping was moist cured for 7 days using wet burlap, followed by exposure to the laboratory environment for the duration until testing. Note that the structures laboratory at the University of Texas at Austin is not air conditioned, and ambient temperatures may have exceeded room temperature (70 degrees Fahrenheit).

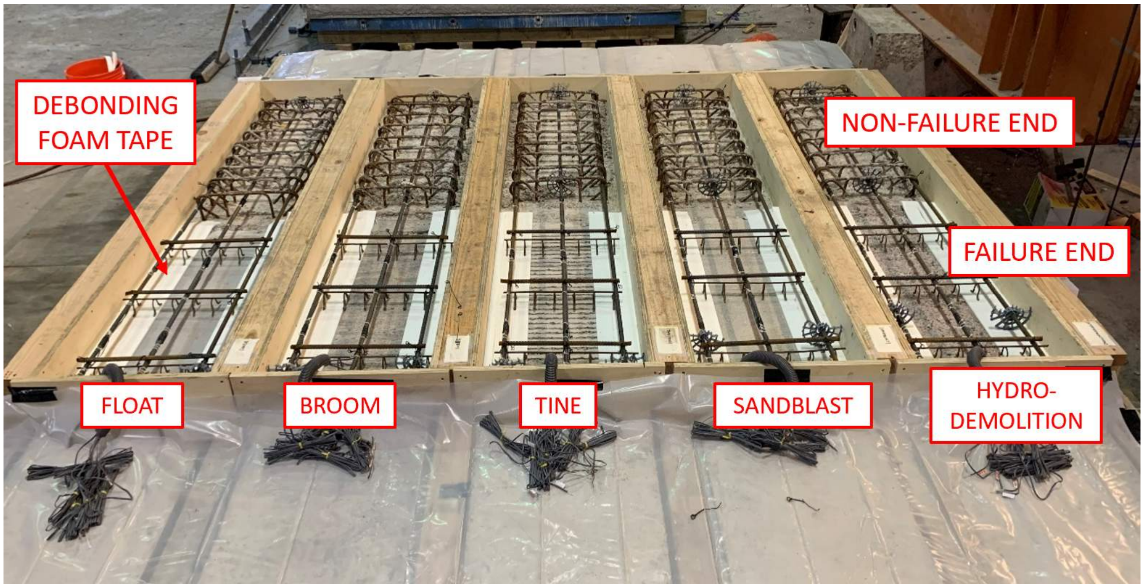

Figure 6-7. Beams ready for concrete topping placement.

Figure 6-8: Wetting of substrates before casting to achieve SSD conditions.

6.4. Beam Test Setup and Loading Protocol

The beams were simply supported and loaded with a single point load at midspan using the test setup shown in Figure 6-9. The supports were fabricated to act as pin and roller boundary conditions. The pin support (Figure 6-10) was created using a tilt saddle placed on top of a load cell to allow rotation in all directions. A steel plate was placed on top of the tilt-saddle to support the beam. The roller support (Figure

6-11) was created by placing a 3-inch diameter steel rod between two steel plates sitting on two load cells for stability. The roller allowed for translation and rotation in the longitudinal direction of the beam.

A 400-kip hydraulic actuator mounted in a structural steel frame was used to apply loading at midspan of the beam. A tilt saddle and steel plates were used to distribute the applied load across the beam width while allowing for rotation. The beam was loaded monotonically to failure with load applied in 10-kip increments. The test was paused at each increment to examine the beam for distress and mark observed cracks.

Figure 6-9. Beam test setup.

Figure 6-10. Pin support.

Figure 6-11. Roller support.

6.5. Beam Test Instrumentation

The response of the beam during testing was monitored using load cells, linear potentiometers, and strain gauges on selected reinforcing bars.

6.5.1. Linear Potentiometers

Linear potentiometers (L-pots) were used to measure midspan deflection (LP01), end slip of the interface (LP02 and LP03), and slip of the interface along one side face of the beam (LP04, LP05, and LP06). The position of the L-pots used to measure deflection and interface slip is indicated in Figure 6-12. The end slip L-pots are shown in Figure 6-13 and the side face L-pot is shown in Figure 6-14.

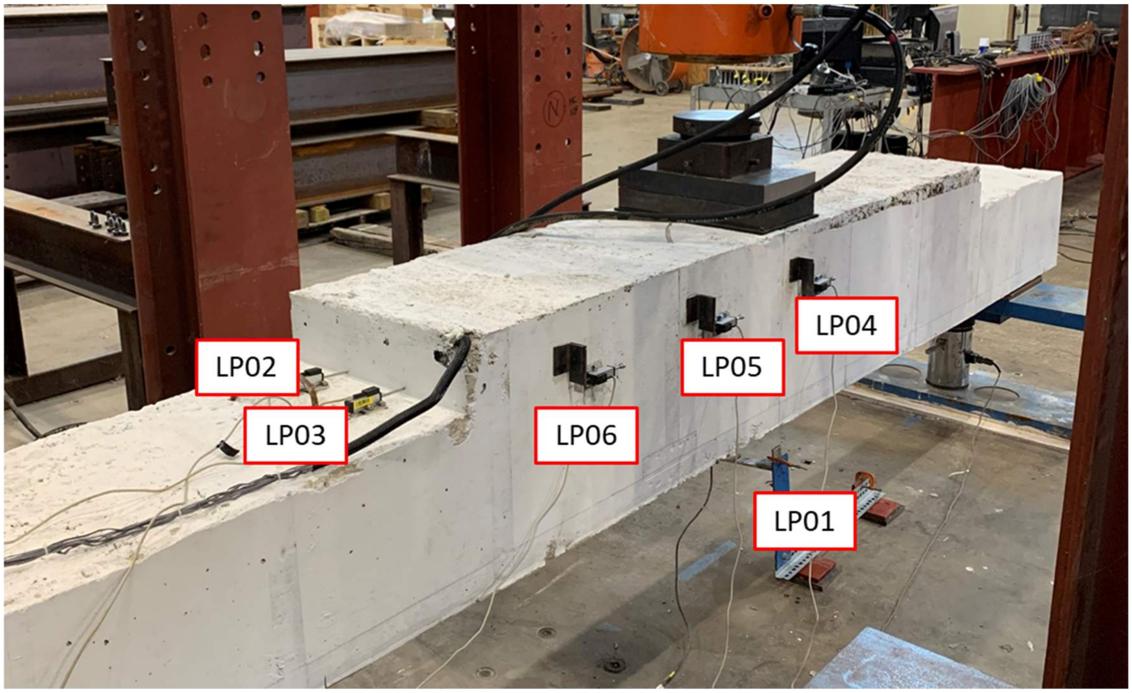

Figure 6-12. Linear potentiometer layout.

Figure 6-13. End slip linear potentiometers.

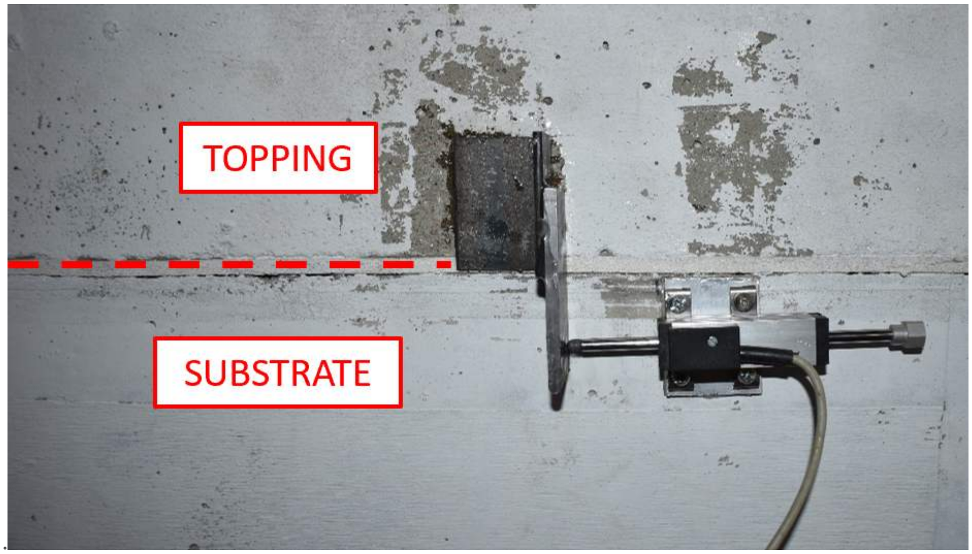

Figure 6-14. Side face linear potentiometer.

6.5.2. Strain Gauges

Each beam specimen was instrumented with nine strain gauges to measure strains in the longitudinal reinforcement. The strain gauges were placed at midspan, 16-inches from midspan, and 32-inches from midspan on one tension bar and two compression bars. The location of strain gauges along the beam length and cross section is shown in Figure 6-15.

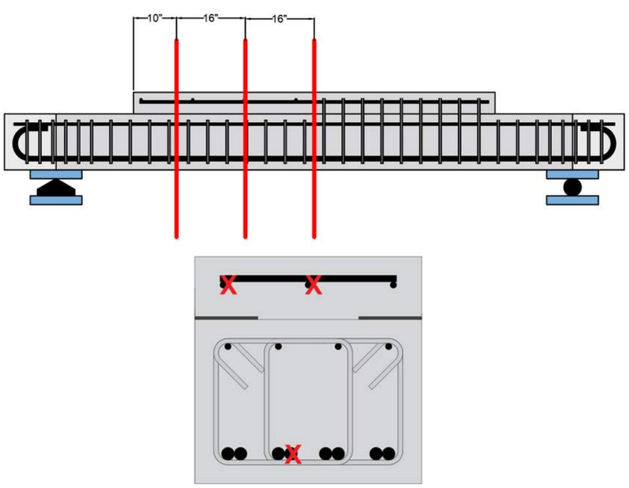

Figure 6-15. Strain gauge layout.

6.6. Companion Slabs for Direct Shear and Tensile Pull-off Testing

The slab specimens were used to provide additional data on interface bond strengths in shear and direct tension for comparison to the beam specimens and the slab specimen results from Phase 1. Nine direct shear (guillotine) tests and six direct tensile pull-off tests were conducted on composite slabs with each of the five interface preparation techniques following the same procedures used in Phase 1 (see Section 4.6). The direct shear testing used 4-inch core samples removed from the slabs. Direct tensile pull-off testing was performed by making a 3-inch core into the slab for comparison with the Phase 1 results.

7. PHASE 2 – BEAM AND COMPANION SLAB SPECIMEN RESULTS

Results from Phase 2 include material test data, surface roughness characterization of slab and beam specimens, flexural testing of beam specimens, and guillotine tests and direct tensile pull-off tests of samples from composite slabs are presented in this section.

7.1. Material Data

Material data for Phase 2 include slump, compressive strength, and splitting tensile strength. The fabrication process including curing and timeline of casting is described previously in this report in section 6.3.

7.1.1. Concrete Slump

The concrete slump was measured for each concrete placement in accordance with ASTM C143; results are listed in Table 7-1. The target slump was intended to represent a typical “moderate” slump in the range of 4 to 5 inches for beam and slab construction and for consistency with the Phase 1 specimens.

Table 7-1. Phase 2 measured concrete slump.

Cast Number	Slump (in.)
Cast 7 (Substrate-Beams)	4.5
Cast 8 (Substrate-Slabs)	4.75
Cast 9 (Topping-Beams and Slabs-Moderate workability)	5.75

7.1.2. Compressive Strength

Concrete compressive strength tests were conducted using 4-inch by 8-inch cylinders in accordance with ASTM C39. The strength was tested 28 days after casting and on the day of beam testing. The compressive strengths for each concrete placement are shown in Table 7-2.

Table 7-2. Concrete compressive strength results.

Cast Number	28-Day (psi)	Day of Beam Test (psi)			
		Monolithic	Broom and Tine	Hydrodemolition	Sandblast and Float
Cast 7 (Beam substrate)	5500	6100	6100	6100	6100
Cast 8 (Slab substrate)	5700	-	-	-	-
Cast 3 (Beam and slab topping)	6000	-	6000	6200	6450

7.1.3. Splitting Tensile Strength

Concrete splitting tensile strength tests were conducted using 4-inch by 8-inch cylinders in accordance with ASTM C496. The strength was tested 28 days after casting and on the day of beam testing. The splitting tensile strengths for each placement are shown in Table 7-3.

Table 7-3: Splitting tensile strength results.

Cast Number	28-Day (psi)	Day of Beam Test (psi)			
		Monolithic	Broom and Tine	Hydrodemolition	Sandblast and Float
Cast 7 (Beam substrate)	550	700	700	700	700
Cast 8 (Slab substrate)	650	-	-	-	
Cast 3 (Beam and slab topping)	650	-	650	700	700

7.2. Surface Roughness Characterization by Mean Texture Depth

The laser line scanner was used to characterize the surface roughness of the repair and precast concrete surface preparation techniques used in the Phase 2 beam and slab specimens. The MTD results from the LLS are presented in Table 7-4 and Figure 7-1. As shown, the MTD values for the float, broom, sandblast, and hydrodemolition surfaces in the beams are similar to the corresponding MTD values for slab surfaces. The tine specimens present a larger disparity, with the tine beam having a 73 percent higher average MTD than the tine slab.

Using the MTD averages, the specimens were grouped into three levels of roughness: high, moderate, and low as shown in Figure 7-1. The hydrodemolition beam, hydrodemolition slab, and tine beam are in the "high roughness" group with MTD averages of 1.46 mm, 1.33 mm, and 1.30 mm, respectively. The broom beam, broom slab, and tine slab are in the "moderate roughness" group with MTD averages of 0.70 mm, 0.60 mm, and 0.75 mm, respectively. The sandblast beam, sandblast slab, float beam, and float slab are in the "low roughness" group with MTD averages of 0.23 mm, 0.20 mm, 0.16 mm, and 0.08 mm, respectively.

These groups were defined by clear distinctions of the averages. Hypothesis testing using a Student's t-test indicated that the difference between the mean MTD value for the specimens in the "high roughness" group (pooled data) and the mean MTD for the "moderate roughness" group (pooled data) is statistically significant. Similarly, the difference between the mean MTD value for the "moderate roughness" group and the "low roughness" group is statistically significant.

Table 7-4. Phase 2 – Mean texture depth obtained from LLS.

Specimen Type	Interface Preparation Technique	Average MTD (mm)	Standard Deviation (mm)	Coefficient of Variation	Sample Size
Slab	Float	0.08	0.011	13%	4
	Broom	0.60	0.072	12%	4
	Tine	0.75	0.118	16%	4
	Sandblast	0.20	0.033	17%	4
	Hydrodemolition	1.33	0.139	10%	4
Beam	Float	0.16	0.038	24%	4
	Broom	0.70	0.065	9%	4
	Tine	1.30	0.145	11%	6
	Sandblast	0.23	0.021	9%	5
	Hydrodemolition	1.46	0.170	12%	4

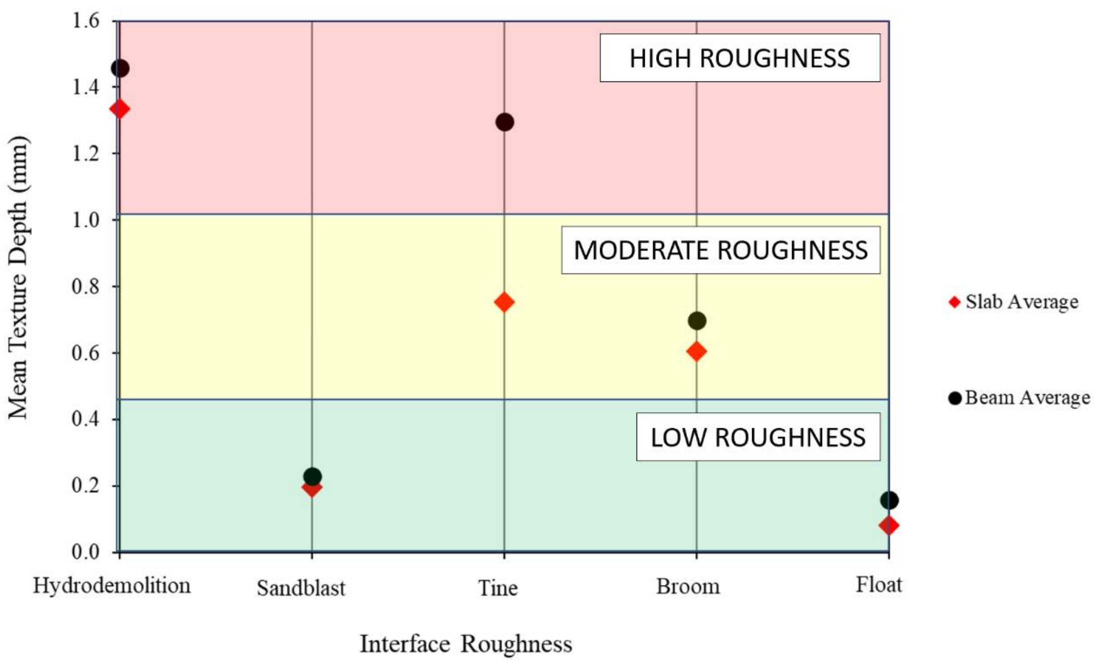

Figure 7-1. MTD results for Phase 2 beam and slab specimens.

7.3. Beam Test Results

Results from the six flexural beam tests (monolithic, float, broom, tine, sandblast, and hydrodemolition) are presented and analyzed in terms of observed damage, load-deflection response, load-slip response, and steel reinforcement strains. The horizontal shear stress at failure was estimated using the experimental results based on different analytical methods.

7.3.1. Interface Debonding Observed Prior to Testing

Debonding at the interface was observed before testing in the float and sandblast slab and beam specimens. Interface debonding in the beams was observed at the end of the topping slab where the bonded interface is visible, as shown in Figure 7-2. The debonding gap observed for the beam with the float interface, shown in Figure 7-3, was approximately 1/16-inch in width. The gap was first observed approximately three weeks after topping placement, but the actual timing of debonding is unknown.

After the debonding was observed, all Phase 2 beams and slabs were scanned using a Proseq Pundit 250 Ultrasonic Array device that can be used to detect voids and delaminations in concrete. The scans indicated the float and sandblast beams were fully delaminated along the unreinforced interface. The corresponding float and sandblast slabs were also fully delaminated. All other beams and slabs did not exhibit delamination in the bonded regions. Due to the delaminated interface, no intact cores could be obtained from the slabs for these interface conditions and therefore no direct shear or direct tensile data was collected. The float and sandblast interface beams were still tested to provide information on the behavior of non-composite beams and for comparison to the composite and monolithic specimens.

Figure 7-2. Observed location of gap at interface indicating debonding of the float and sandblast beam specimens prior to testing.

Figure 7-3. Gap due to debonding at the end of topping in float beam prior to testing.

7.3.2. Conditions Observed During Testing

The beam specimens were tested under a monotonically increasing vertical load applied at mid-span, as described in Section 6.4. The beams behaved in three distinct manners: a) monolithic, b) composite, and c) non-composite.

7.3.2.1. Monolithic Beam

The progression of cracking in the monolithic beam is shown in Figure 7-4. Flexural cracks initiated near midspan at an applied load of 40 kips. As the load was increased, more flexural cracks developed all propagating vertically and inclined toward the location of the point load. As the beam approached yielding of the tension reinforcement at an applied load of 215 kips, flexural-shear cracks were visible, extending from the support locations. The beam failed shortly after yielding at a load of 223 kips. The failure was caused by a flexural-shear crack that developed from the interior face of the support, extended horizontally for a short distance within the region where the stirrups did not extend to the full height of the beam, and then extended inclined to the point load. The crack pattern at failure is shown in Figure 7-5 with the approximate location of the stirrups superimposed on the photograph.

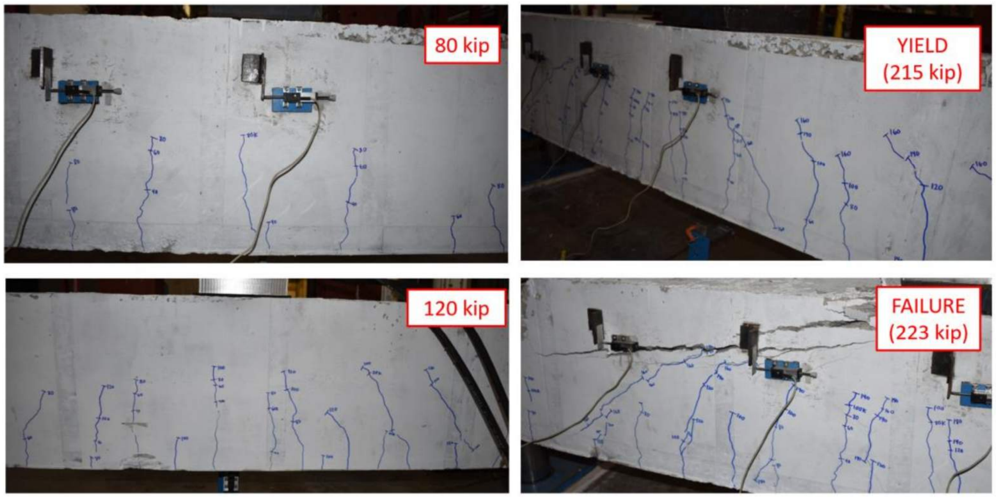

Figure 7-4. Crack progression of the monolithic beam during testing.

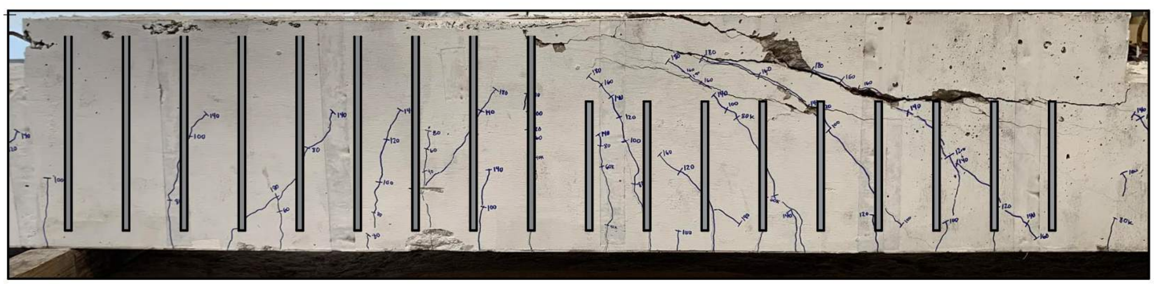

Figure 7-5. Failed monolithic beam with approximate location of stirrups.

7.3.2.2. Composite Beams

The tine, broom, and hydrodemolition beams behaved in a composite manner until failing in horizontal shear at the interface. Following interface failure, the beam was non-composite and the substrate acted as the primary load-resisting member. The tine, broom, and hydrodemolition specimens failed in horizontal shear at the substrate-topping interface at applied load levels of 86 kips, 89 kips, and 86 kips, respectively.

The composite beam behavior until interface shear failure occurred was similar to the monolithic specimen response. The crack progression during testing is shown in Figure 7-6. After loading to 40 kips, flexural cracks were observed near midspan, with additional cracks developing as load increased. All three composite beams failed in horizonal shear failure at applied loads close to 90 kips. The failures were identified by an audible slip or crack, a sudden drop in the lateral load capacity, and a sudden increase in slip at the interface. Immediately after interface failure, cracks were observed at the bottom of the topping slab (Figure 7-7) indicating the bottom of the topping slab was now in tension (due to bending since the topping was now non-composite) and a crack was visible at the interface at the end of the topping (Figure 7-8). Due to the intentional debonding of outer width of the topping at the sides of the section, it was not possible to visually identify longitudinal cracks along the interface. However, increasing slip was measured by the side face linear potentiometers positioned to measure interface slip.

After horizontal shear failure, loading of the composite beams was continued in 10-kip intervals. The beam stiffness was reduced consistent with non-composite behavior. The tests were stopped after the tension steel yielded at an applied load of approximately 160 kips, which coincided with wide flexural cracks near the center of the beam and crushing of the concrete at the top of the substrate near mid-span (Figure 7-9). During loading to failure, a vertical gap opened at the interface (Figure 7-10) due to the non-composite behavior. The gap was visible on the sides of the beam along most of the length of the interface as loading approach flexural failure of the beam.

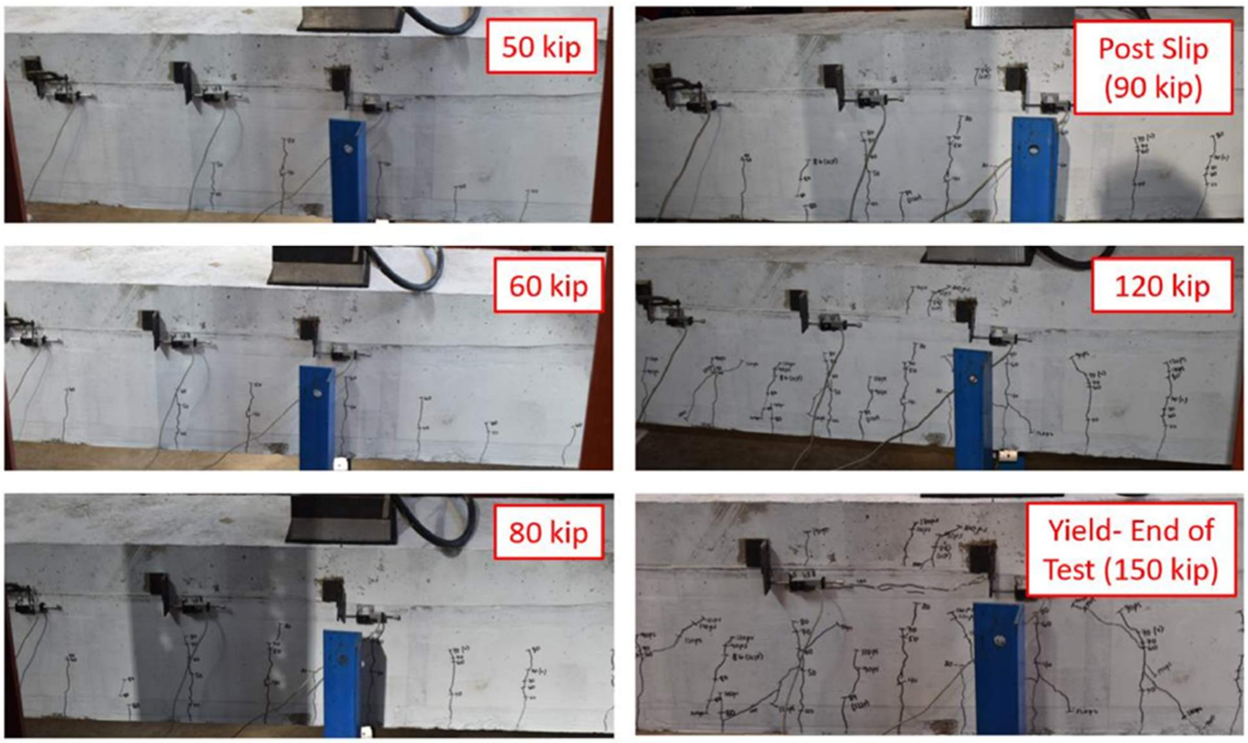

Figure 7-6. Composite beam crack progression during testing (tine beam).

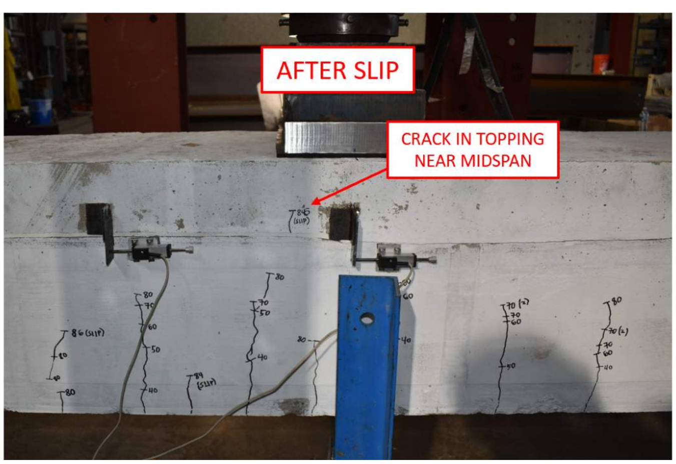

Figure 7-7. Crack pattern after interface slip.

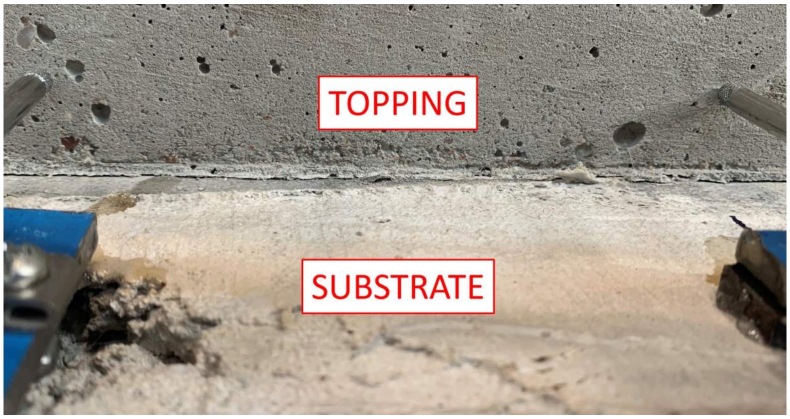

Figure 7-8. Interface crack after slip at end of topping slab.

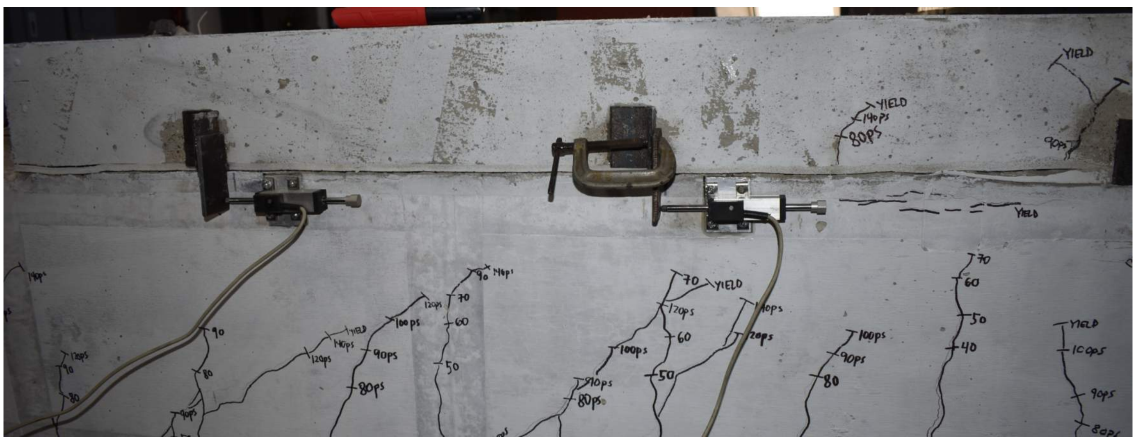

Figure 7-9. Beam crack pattern after yield showing the top of substrate concrete crushing at midspan.

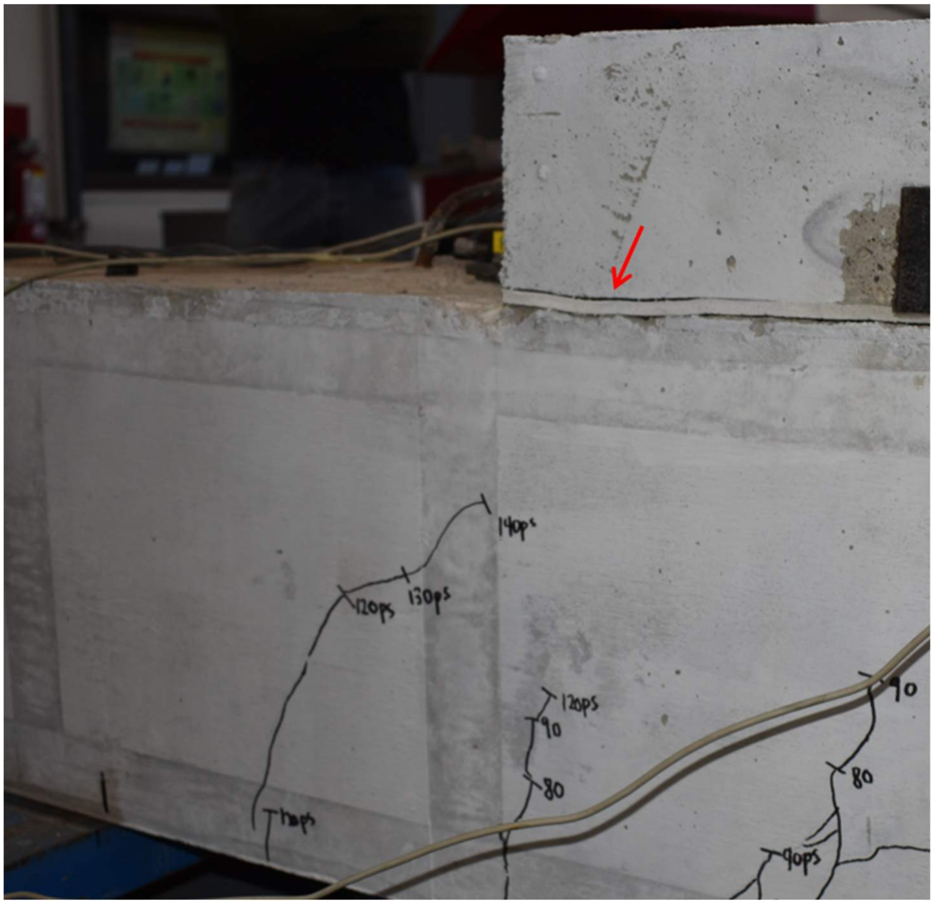

Figure 7-10. Vertical gap at end of topping slab when loaded past interface horizontal shear failure.

7.3.2.3. Non-Composite Beams

The beams with the float and sandblast interfaces exhibited non-composite behavior from the initiation of loading due to debonding of the topping during curing. The crack progression during testing of the sandblast beam is shown in Figure 7-11 (the behavior of the float interface beam was nearly identical). After loading to 30 kips, the specimen exhibited flexural cracking near midspan. After increasing load to 50 kips, more flexural cracks were observed on the bottom of the substrate beam and at the bottom of the topping slab, demonstrating the non-composite behavior and development of flexural tension at the bottom of the topping. As loading progressed, more cracks developed in the topping and substrate with cracks forming farther away from midspan. Neither specimen showed indications of composite behavior. The tests for these beams were stopped when the substrate tension steel yielded at a load of approximately 140 kips.

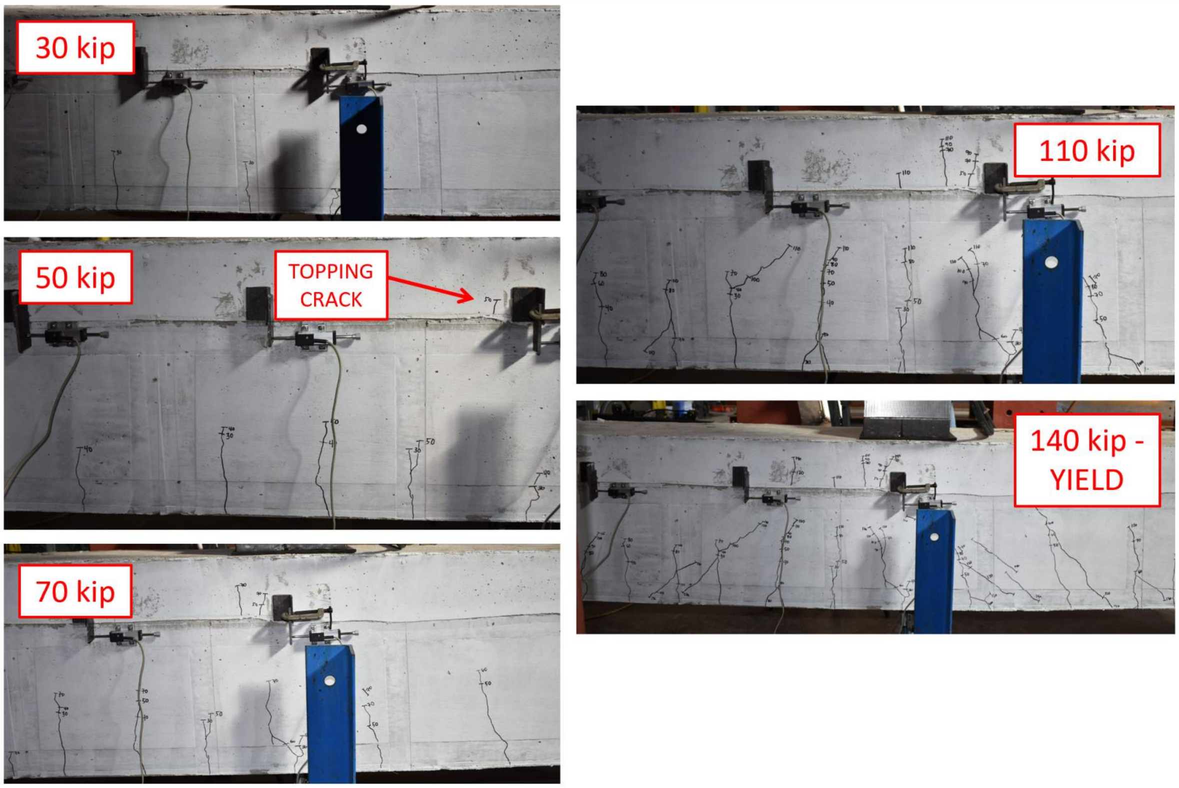

Figure 7-11. Non-composite beam crack progression (sandblast beam).

7.3.3. Load-Deflection Response

The load-midspan deflection responses of the monolithic, broom, tine, hydrodemolition, float, and sandblast specimens are shown in Figure 7-12. The monolithic and composite beams present very similar response until interface shear failure occurs in the composite beams. The horizontal shear failure of the three composite beams occurring at applied loads between 86 kips and 89 kips and was characterized by a sudden drop in load of approximately 20 kips caused by the reduction of stiffness as the beams loses composite action and the substrate and topping start to behave independently at the failure end of the beam. After horizontal shear failure occurred, the three beams had a similar response, with a lower stiffness and strength in comparison to the monolithic beam. The interface shear forces and stresses coinciding with horizontal shear failure are discussed in Section 7.3.6.

After initial flexural cracking, the non-composite specimens (float and sandblast interfaces) appear to follow a similar response to that displayed in the composite beams after interface failure. The load-deflection response of the non-composite beams was relatively linear until yielding of the tension steel occurred. The measured response indicated that there was no evidence of interface shear capacity in the beams with float and sandblast interfaces, as was expected due to the indications of interface debonding prior to testing.

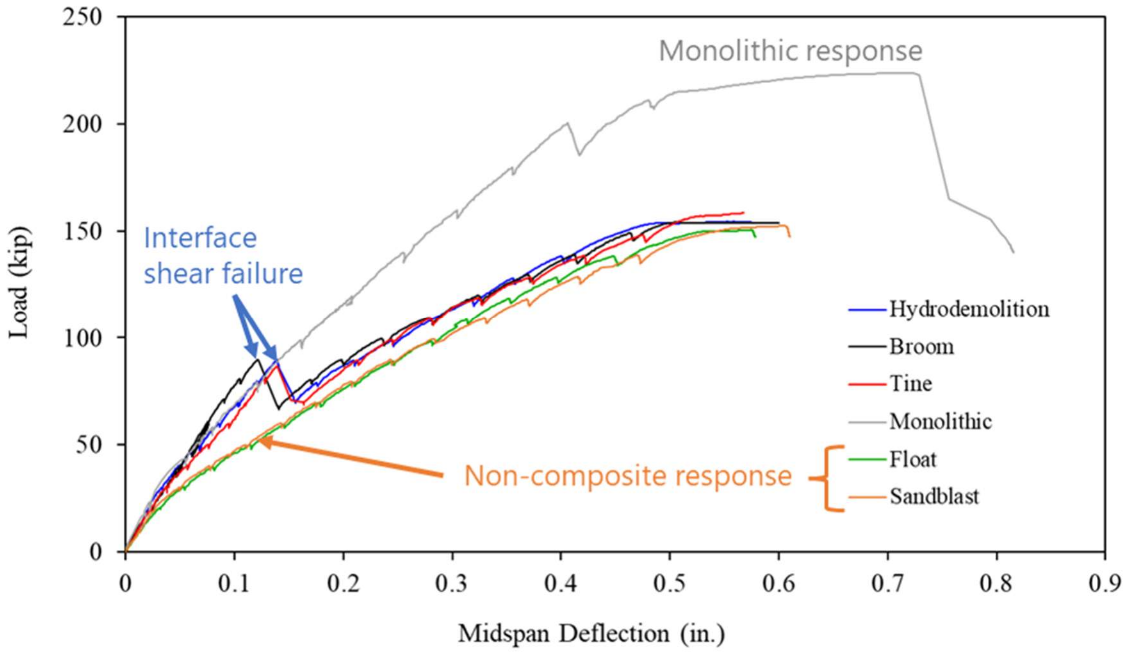

Figure 7-12. Load vs. deflection of hydrodemolition, broom, tine, monolithic, float, and sandblast beam specimens.

7.3.4. Load-Slip Response

The relative horizontal displacement between the topping and the substrate, or interface slip, was measured at midspan, 16 inches from midspan, 32 inches from midspan, and 42 inches from midspan (end of topping slab) as described in section 6.5.1. To interpret the data, positive slip refers to the topping moving away from the load position relative to the substrate as shown in Figure 7-13. The measured slip response at the four measurement locations is plotted for each beam test in Figure 7-14 through Figure 7-17.

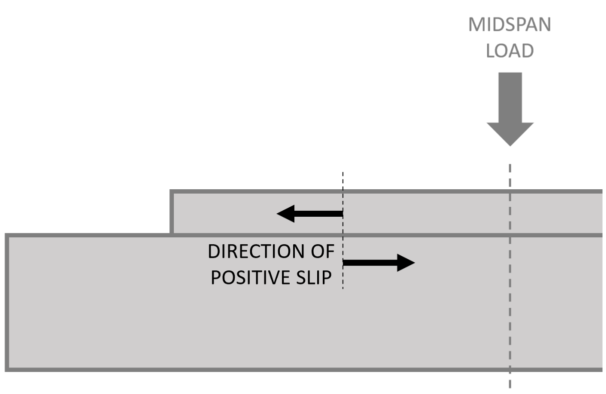

Figure 7-13: Direction of positive slip.

7.3.4.1. Monolithic Beam

Although the monolithic beam does not have an interface between a substrate and topping, displacement transducers (L-Pots) were placed at the same locations as those along the interface in the composite beams for comparison purposes (see Figure 6-12). The slip response indicated by transducers on the side face of the beam was different from that at the end of the “topping” (increased beam depth region); transducers on the side face exhibited negative slip since the top fiber, representative of the topping, is in compression relative to the bottom fiber.

Relative displacement at the end of the topping slab increased linearly at early stages of loading for all the beams, including the monolithic specimen (Figure 7-17). Since it is unlikely the monolithic “topping” was slipping, it is assumed the small displacement is not attributed to slip but to a small differential deformation caused by bending between the two points of measurement.

7.3.4.2. Composite Beams

A sudden increase of slip was measured at the occurrence of bond failure, accompanied by a small reduction in applied load. The measured slip response at midspan, 16 inches from midspan, and 32 inches from midspan showed a relatively small, linearly increasing deformation up to interface bond failure when a large, sudden slip occurred. The magnitude of slip immediately following the occurrence of shear failure increased along the length of the interface, as shown in Figure 7-18 for the three composite beams (hydrodemolition, broom and tine interface surface preparation). Note that the slip occurring after interface failure was calculated by subtracting the deformation (slip) measurement immediately prior to interface failure from the slip measured after bond failure.

7.3.4.3. Non-Composite Beams

The non-composite specimens (float and sandblast interface surface preparation) exhibited significant slip after the beam midspan section reached the cracking moment. The interface slip steadily increased with load up to failure of the beam in bending. The load-slip response of the non-composite beams was similar to that of the composite beams after interface bond failure occurred.

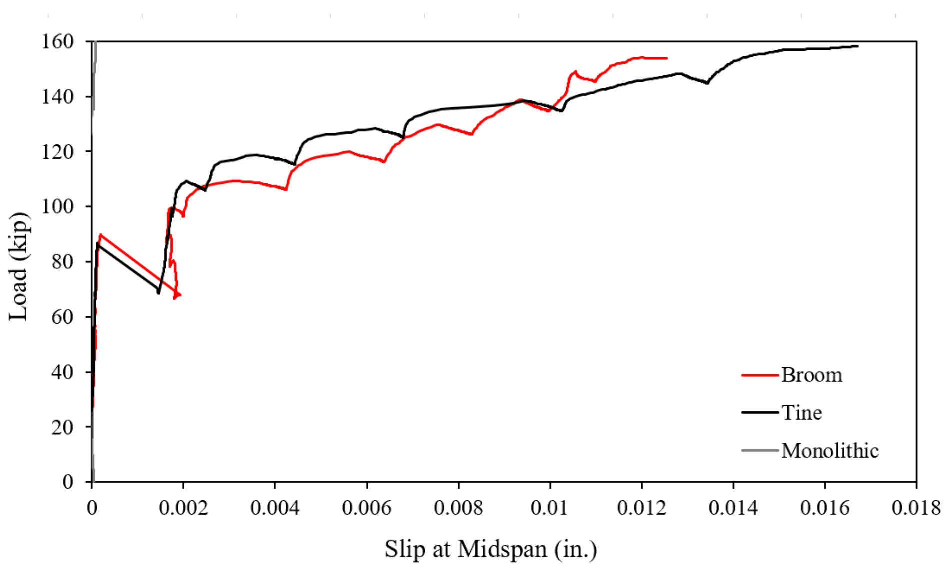

Figure 7-14. Load-slip response: substrate-to-topping slip measured at midspan.

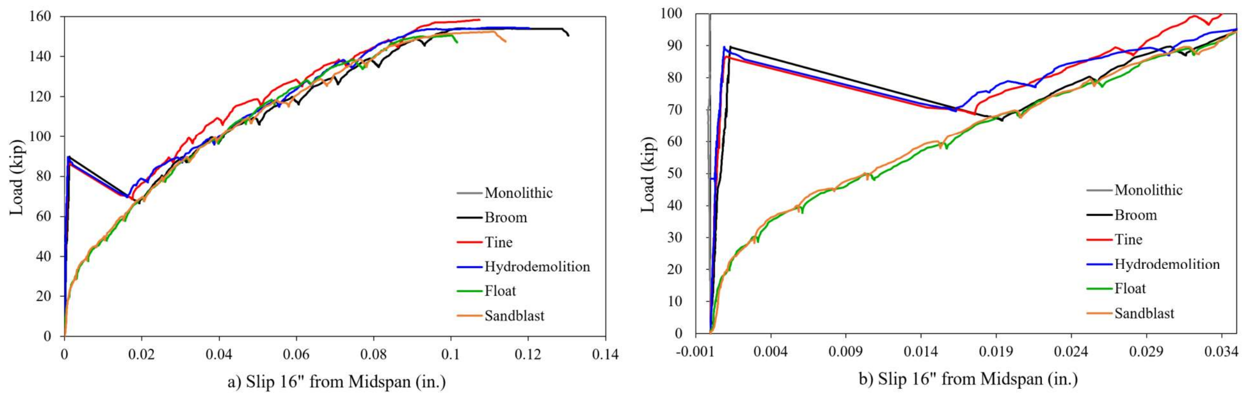

Figure 7-15. Load-slip response: substrate-to-topping slip measured 16 inches from midspan on the failure end: (a) full response, (b) expanded view of slip response during interface failure.

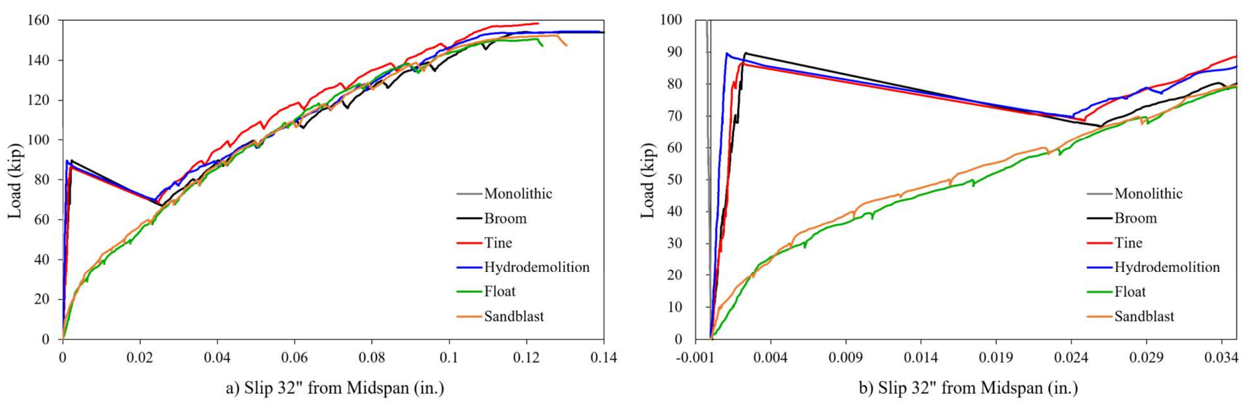

Figure 7-16. Load-slip response: substrate-to-topping slip measured 32 inches from midspan on the failure end: (a) full response, (b) expanded view of slip response during interface failure.

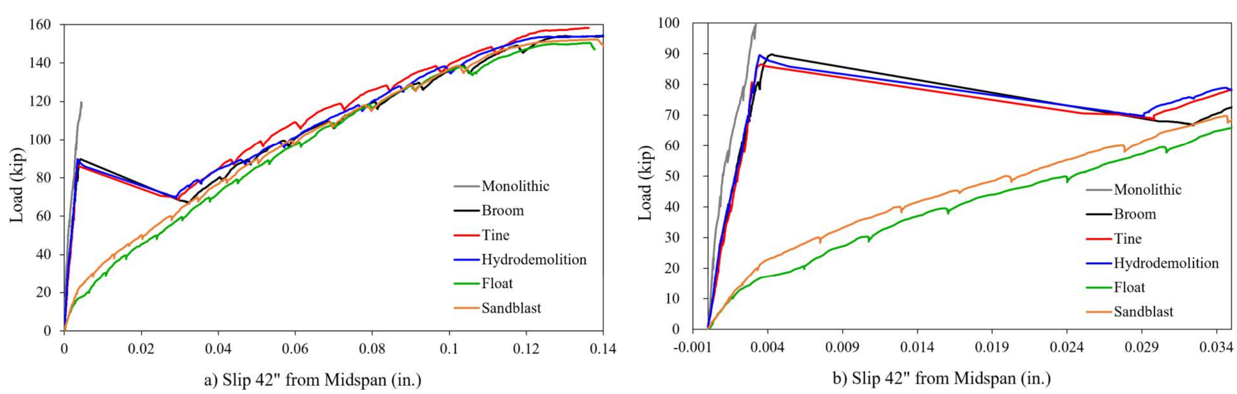

Figure 7-17. Load-slip response: substrate-to-topping slip measured 42 inches from midspan on the failure end: (a) full response, (b) expanded view of slip response during interface failure.

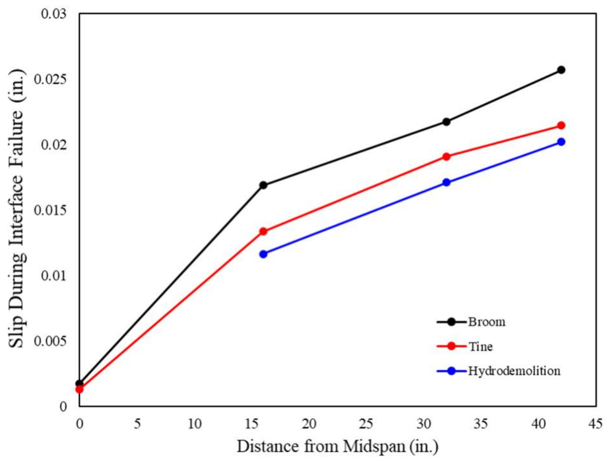

Figure 7-18. Magnitude of slip occurring at interface shear failure as a function of distance from midspan.

7.3.5. Moment-Strain Response

Strain gauge data were recorded for tension and compression reinforcement for all tests. The measured strain response was used to confirm composite behavior and transition to non-composite behavior. Additionally, the reinforcement strains were used to estimate the interface shear stresses as described in Section 7.3.6. A summary of tension and compression reinforcement strains corresponding to the occurrence of interface shear failure is provided in Table 7-5. The measured strain response for all beams is presented in detail by Becker (2020) and is not discussed further in this report.

Table 7-5. Summary of measured reinforcement strains corresponding to interface shear failure.

Interface Preparation Technique	Cross Section Location	Applied Moment at Failure	Tension Reinf. Strain	Average Compression Reinf. Strain
Broom	Midspan	224	0.00105	0.00033
	16″ from Midspan	164	0.00078	0.00026
	32″ from Midspan	104	0.00052	0.00014
Tine	Midspan	217	0.00098	0.00036
	16″ from Midspan	159	0.00073	0.00025
	32″ from Midspan	102	0.00045	0.00013
Hydro-demolition	Midspan	217	0.00104	0.00033
	16″ from Midspan	159	0.00084	0.00023
	32″ from Midspan	102	0.00058	0.00014

Strain Gauge Locations

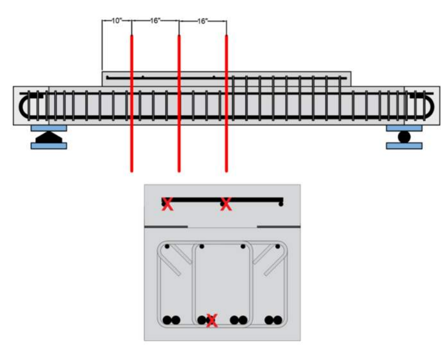

7.3.6. Estimated Interface Shear Stresses at Failure

The horizontal shear stress along the interface was estimated by concrete section analysis using strain data recorded for the compression and tension reinforcement up to the occurrence of interface slip. The analysis approach involved the following steps:

- Determine the strain profile over the section depth for loading immediately prior to interface shear failure. Three different approaches were investigated:
  - Method A: Linear strain profile based directly on measured compression and tension reinforcement strains.
  - Method B: Linear strain profile within compression zone based on measured compression reinforcement strains and equilibrium.
  - Method C: Strain compatibility analysis based on applied load at interface shear failure.
- Estimate the total compression resultant (concrete and steel) and tension resultant based on the strain profiles and assumed material stress-strain models.
- Estimate the compression force resultant acting on the topping slab only.
- Estimate the interface shear stress using the topping compression force resultant.

The applied beam loads at the occurrence of the interface shear failure were reported in the preceding sections and are summarized in Table 7-6 for reference. The midspan moment corresponding to the failure load is also included. These loads and moments were used for the concrete section analyses described in the following sections.

Table 7-6. Summary of peak loads and moments corresponding to interface shear failure in beam specimens.

Interface Preparation Technique	Peak Applied Load at Interface Failure (kips)	Corresponding Moment at Interface Failure (kip-ft)
Broom	89.9	224.6
Tine	86.6	216.5
Hydrodemolition	86.8	217.0

7.3.6.1. Material Stress-Strain Models

The concrete section analysis to estimate the interface shear stresses required the assumption of material stress-strain constitutive relationships. Concrete was modeled with the stress-strain relations for short-term loading in compression proposed in Section 5.1.8.1 of the fib Model Code 2010 (fib 2010). The predicted stress-strain response is shown in Figure 7-19 and compared with the linear response based on the secant modulus based on ACI 318 ($57{,}000 * \sqrt{(f'_c)}$). The steel reinforcing bars were assumed to have an elastic-perfectly plastic stress-strain response with a modulus of elasticity of 29,000 ksi. The section analyses performed in this study were for loading conditions associated with interface shear failure, which occurred at load levels well below the flexural or vertical shear capacity of the beam. As a result, the concrete and steel responses were determined to be within the linear-elastic range.

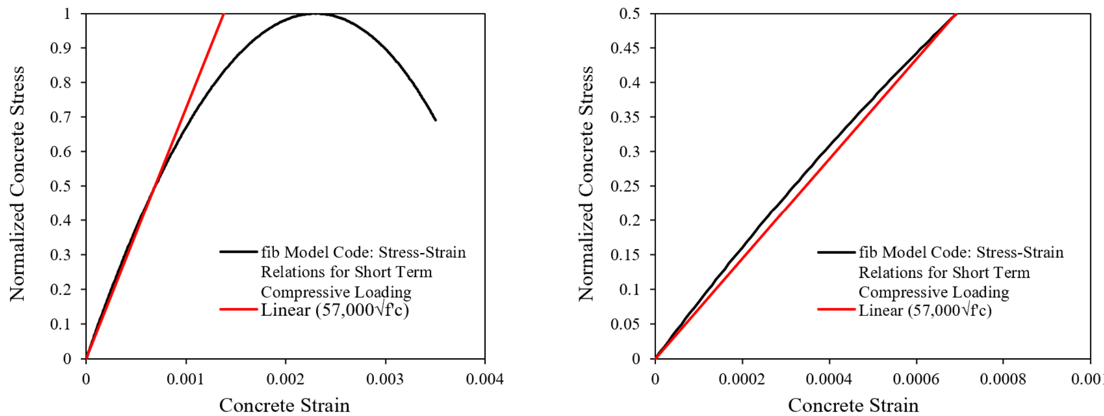

Figure 7-19. Concrete stress-strain model (fib 2010)

7.3.6.2. Method A: Stress Distribution Based on Linear Strain Profiles

Assuming plane sections remain plane in bending, the strain gauge data from the tension and compression reinforcement was used to develop a linear strain profile over the beam depth for cross-sections at midspan, 16 inches from midspan, and 32 inches from midspan. The resulting strain profiles for the broom, tine, and hydrodemolition beams are shown in Figure 7-20.

The stresses distributions in the concrete and steel were calculated based on the assumed material models. The resultant compression and tension forces acting on the section were calculated using the concrete and steel stress distributions and are presented in Table 7-7. In almost all cases, the calculated tension force resultant was larger than the compression force resultant, which does not satisfy section equilibrium. Furthermore, the difference between the tension and compression force resultants increased with increasing distance from midspan.

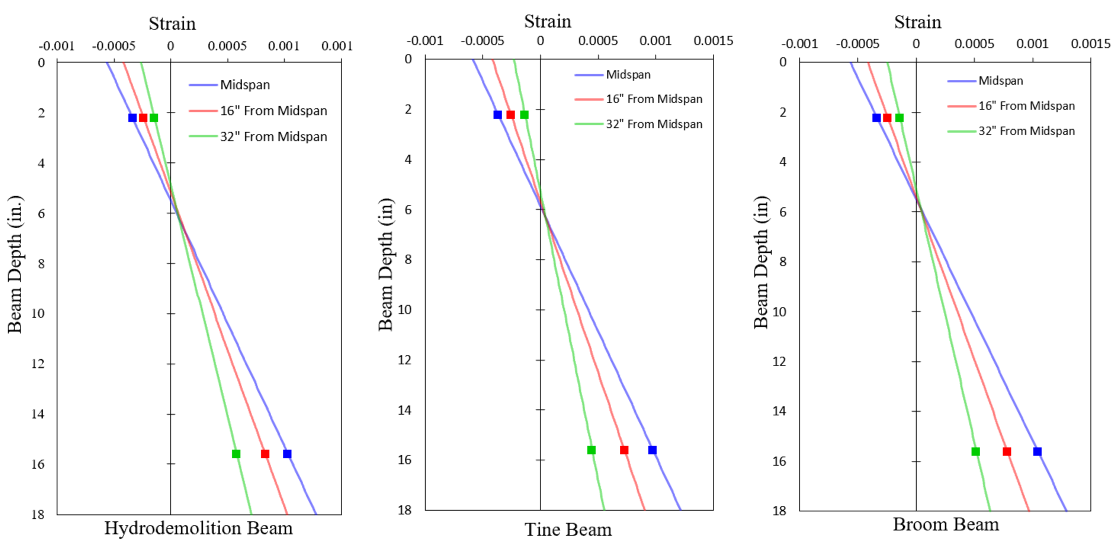

Figure 7-20. Strain profiles from Method A: Linear strain along the entire depth using strain gauge data.

Table 7-7. Tension and compression force resultants assuming a linear strain profile over the beam depth.

Location	Force Resultant	Hydrodemolition	Tine	Broom
Midspan	Compression Force (kips)	168	180	163
	Tension Force (kips)	190	179	192
16″ from Midspan	Compression Force (kips)	115	122	116
	Tension Force (kips)	153	134	144
32″ from Midspan	Compression Force (kips)	67	61	64
	Tension Force (kips)	107	82	95

7.3.6.3. Method B: Linear Strain Profile for Compression Region Only and Enforcing Equilibrium

Based on the differences between the tension and compression force resultants indicated by the strain data using Method A, a second approach was used to estimate the strain profiles assuming a linear strain distribution for the compressive strain region only and enforcing section equilibrium. This method does not enforce linear strain distribution in the tension region, acknowledging that reinforcement strains may vary significantly depending on the location of the strain gauge relative to a crack, particularly at lower load levels. Method B set the compression force resultant equal to the tension force calculated from the measured tension strains in the reinforcement. The neutral axis depth was estimated based on the compression resultant and the measured compression reinforcement strain. The strain profiles for the broom, tine, and hydrodemolition beams obtained from Method B are shown in Figure 7-21. Note that this approach results in increased neutral axis depths as the distance from midspan increases.

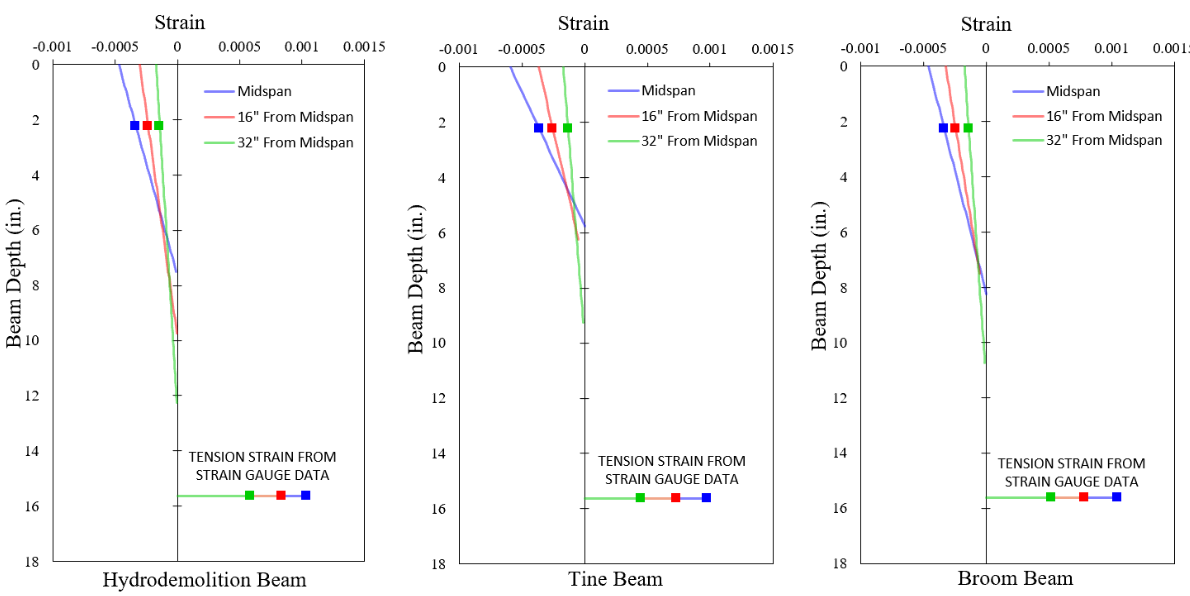

Figure 7-21. Strain profiles from Method B: Linear distribution for compression region but not for tension region. Section equilibrium is enforced.

7.3.6.4. Method C: Strain Profile from Applied Moment and Strain Compatibility Analysis

The third method estimated the beam strain and stress distributions using a strain compatibility analysis at the applied moment corresponding to interface shear failure. This analysis assumed plane sections remain plane and used the concrete and steel constitutive models described previously (the measured strain data were not used). The analytical strain profiles for the hydrodemolition, tine, and broom beam are shown in Figure 7-22. The strain values from this analysis are compared to the test data in Table 7-8. The predicted tension reinforcement strains were close to the measured strains, while the predicted compression reinforcement strains were consistently larger than the measured values. Note that the tension and compression strains estimated using strain compatibility analysis are very close (essentially equal) to the response predicted using linear-elastic cracked section analysis, indicating that the beam sectional response is linear elastic at the load level associated with the occurrence of interface shear failure.

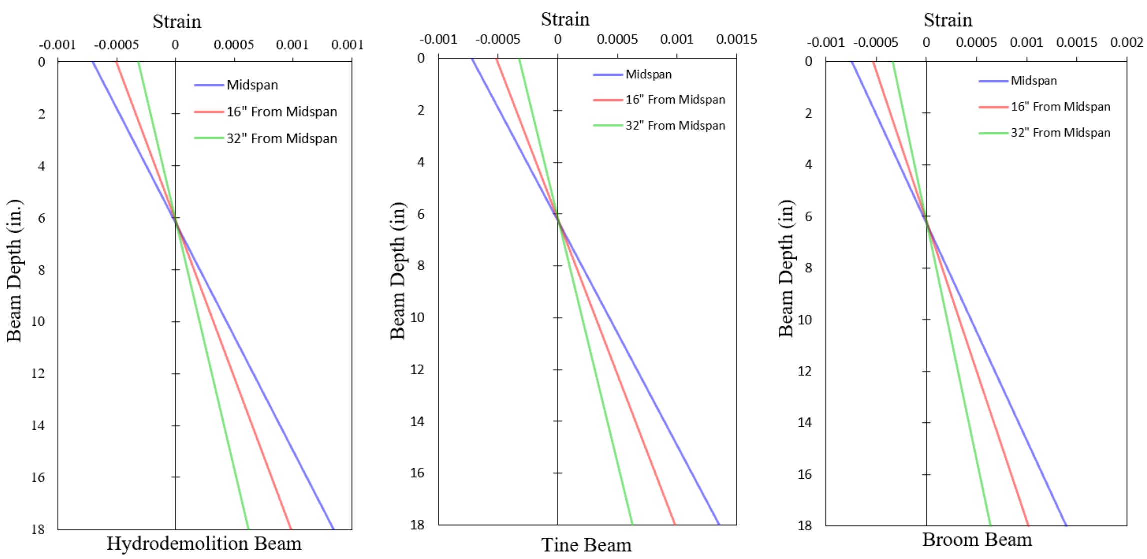

Figure 7-22. Strain distributions from Method C: Strain compatibility analysis.

Table 7-8. Comparison of Strains for Test Data and Strains from Strain Compatibility Analysis (Method C).

Interface Preparation Technique	Cross-Section Location	Tension Strain		Compression Strain	
		Test Data	Strain Compatibility Analysis	Test Data (avg. of 2 gauges)	Strain Compatibility Analysis
Broom	Midspan	0.00105	0.0011	0.00033	0.00045
	16" from Midspan	0.00078	0.0008	0.00023	0.00032
	32" from Midspan	0.00052	0.0005	0.00014	0.00020
Tine	Midspan	0.00098	0.0011	0.00036	0.00046
	16" from Midspan	0.00073	0.0008	0.00025	0.00033
	32" from Midspan	0.00045	0.0005	0.00013	0.00021
Hydro-demolition	Midspan	0.00104	0.0011	0.00033	0.00045
	16" from Midspan	0.00084	0.0008	0.00023	0.00032
	32" from Midspan	0.00058	0.0005	0.00014	0.00020

7.3.6.5. Comparison of Estimated Compression Force in Topping Slab

The three strain profile methods described in the preceding sections use different assumptions to estimate the sectional response prior to interface failure. The resulting strain profiles were used to estimate the compression resultant acting on the topping slab by multiplying the area under the resulting stress distribution in the topping slab by the width of the topping slab and including the compression in the topping reinforcement. The estimated compression resultants in the topping slab are summarized in Table 7-9 for the three strain profile analysis methods.

The strain compatibility analysis (Method C), which does not use the measured strain data, estimates the largest compression force resultant at each of the three sections considered. The estimated compression resultants for Methods A and B are less than the Method C results; this is expected since the measured compression reinforcement strains are less than the strains estimated by strain compatibility analysis. This observation suggests that the actual section response may not be consistent with idealized fully composite behavior, which implies deformation at the interface or the occurrence of slip. Given the brittle nature of concrete-to-concrete bond and the unreinforced interface, it is unlikely that slip deformations (partial debonding) initiated prior to the observed horizontal shear failure. It is also possible that the compression reinforcement strains may not adequately reflect the distribution of compression in the topping slab. It is noted that the measured compression reinforcement strains reported herein are the average strains from gauges located on the center bar and one outer bar of the topping reinforcement. The outer gauge indicated slightly lower strains, likely due to in-plane shear deformation (shear lag) of the topping slab. This also suggests that the actual section response is not consistent with idealized fully composite behavior wherein plane sections remain plane. The actual compression resultant in the topping slab cannot be determined based on the measured data and analyses performed. Since the measured tension reinforcement strains are well predicted using strain compatibility, the Method C results will be used for most of the comparative discussion in the following sections.

Table 7-9. Resultant compression force in topping slab at horizontal shear failure using the three strain profile methods.

Interface Preparation Technique	Cross-Section Location	Linear Strain Distribution Using Strains from Test Data	Linear Strain Distribution for Comp. Region Only	Strain Compatibility Analysis
		Method A	Method B	Method C
		(kips)	(kips)	(kips)
Broom	Midspan	162.6	167.3	190.4
	16″ from Midspan	115.8	120.0	139.6
	32″ from Midspan	64.2	67.9	88.7
Tine	Midspan	177.7	177.5	183.8
	16″ from Midspan	121.2	123.5	134.8
	32″ from Midspan	61.2	64.1	85.8
Hydrodemolition	Midspan	167.1	171.3	184.2
	16″ from Midspan	114.5	119.9	135.2
	32″ from Midspan	67.0	71.4	86.2

7.3.6.6. Horizontal Shear Stress at Interface Failure

The horizontal shear stress along the interface was calculated using the segment method (see Section 3.1.3 and Equation 3-3) considering the three strain profile calculation methods and the compression resultant forces described in the previous section. The compression resultant was determined at the three strain gauge locations and was taken as zero at the end of topping.

Horizontal shear stress was calculated for four segments along the length of the beam with the bond topping, as shown in Figure 7-23 and listed below:

- S1: Midspan to 16 inches from midspan (16-inch length)
- S2: 16 inches from midspan to 32 inches from midspan (16-inch length)
- S3: 32 inches from midspan to end of topping (10-inch length)
- S4: Midspan to end of topping (42-inch length)

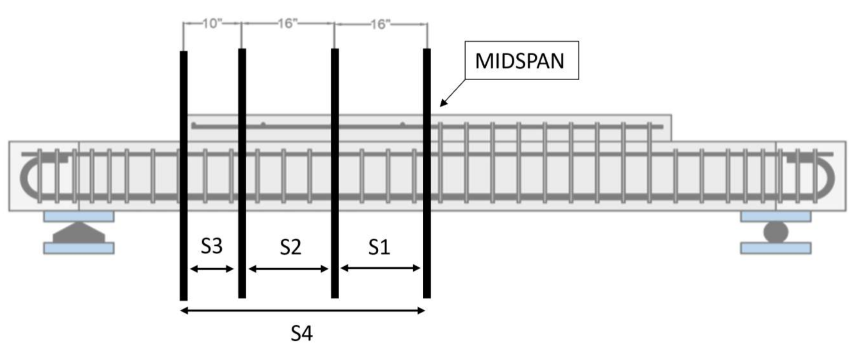

Figure 7-23. Diagram of sections used to calculate horizontal shear stress.

The interface shear (horizontal) stress results for each segment are presented in Table 7-10 and Figure 7-24. As seen in Figure 7-24, horizontal shear stress results for all beams were similar within segments S1 and S2 for all three analytical methods. The horizontal shear stress ranged from approximately 370 psi to 470 psi in segments S1 and S2.

Regarding the average shear stress along the entire interface at failure (based on Segment 4), the three analytical methods provided a similar range of values of approximately 480 to 570 psi for the three composite beams with different interface preparation techniques. For analysis Method B, the broom interface presents a slightly higher average horizontal shear stress (548 psi) than hydrodemolition (529 psi) and tine (528 psi).

The estimated horizontal shear stress at interface shear failure within segment S3 was significantly higher than the shear stress in the other segments for all three analysis methods. The increased stress in this segment is explained by the abrupt ending of the topping where the compression resultant in the topping is zero, but the remaining beam section is still subject to a bending moment. The topping resultant compression force measured 32-inches from midspan is transferred by interface shear over the 10-inch length of segment S3 to where the topping ends. The distribution of interface shear stresses along this length is unknown, however the measured strains and sectional mechanics of the beam indicate that the shear stresses must be higher in this region due to the abrupt change in geometry.

Table 7-10: Horizontal stress results using various sections and strain profile methods.

Interface Preparation Technique	**Segment Along Beam Length Considered**	**Linear Strain Distribution Using Strains from Test Data**	**Linear Strain Distribution for Comp. Region Only**	**Applied Moment – Moment Curvature Analysis**
		Method A	**Method B**	**Method C**
		psi	**psi**	**psi**
Broom	S1	366	370	397
	S2	403	407	397
	S3 (max.)	802	849	1108
	S4 (average)	484	498	567
Tine	S1	442	422	383
	S2	469	464	383
	S3 (max.)	765	801	1073
	S4 (average)	529	528	547
Hydrodemolition	S1	411	401	383
	S2	372	379	383
	S3 (max.)	837	892	1078
	S4 (average)	497	510	548

S1: Midspan to 16 inches from midspan.
S2: 16 inches from midspan to 32 inches from midspan.
S3: 32 inches from midspan to end of topping.
S4: Midspan to end of topping (average along entire unreinforced span).

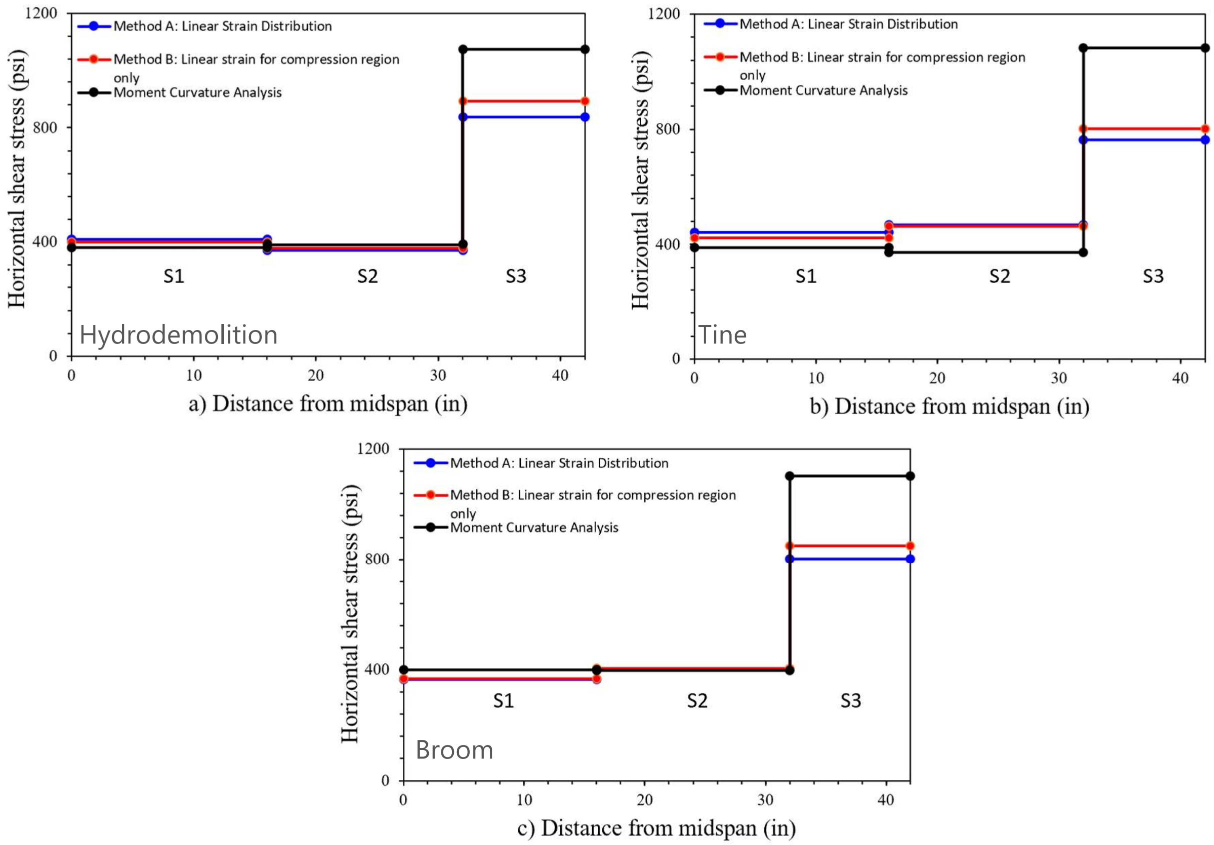

Figure 7-24. Horizontal shear stress for each segment a) Hydrodemolition beam, b) Tine beam, and c) Broom beam.

The three types of interfaces (hydrodemolition, tine, broom) presented a similar maximum horizontal shear stress in segment S3 for each analysis method, although the different analysis methods estimated notably different shear stresses in comparison to one another. Using Method B, the horizontal shear stress for hydrodemolition, broom, and tine are 892 psi, 849 psi, 801 psi, respectively. Results from Method A trend the same with hydrodemolition reaching the highest horizontal shear stress followed by the broom beam, and the tine beam with the lowest with strengths for hydrodemolition, broom, and tine of 837 psi, 802 psi, and 765 psi, respectively. Method C indicates the same relative strengths for the three interface types and estimates the highest interface shear stresses of the three methods, ranging between 1,073 psi and 1,108 psi. Possible explanations for the differences between the three analysis methods were discussed in the preceding section. The results from Method C will primarily be used for the comparative discussion in the following sections.

7.4. Companion Slab Direct Shear and Direct Tensile Pull-off Results

Testing was performed on companion slab specimens to provide additional data on interface bond strengths in shear for comparison to the beam specimens and to provide direct shear and direct tensile pull-off results for comparison with Phase 1 results.

7.4.1. Direct Shear (Guillotine) Test Results

The direct shear (guillotine) results for Phase 2 slabs are presented in Table 7-11 and Figure 7-25. Nine four-inch cores were taken from each slab. All cores failed at the interface with similar behavior to Phase 1 (Figure 5-2 through Figure 5-5).

The hydrodemolition slab had the highest direct shear strength (1208 psi) and the lowest CoV (27 percent). This was the only repair specimen capable of obtaining cores for Phase 2 (the sandblast and float interfaces debonded as described in Section 7.3.1).

The broom and tine specimens had average direct shear strengths of 939 psi and 518 psi, respectively. The broom slab not only had a higher strength average, but also a CoV of 33 percent which is significantly lower than the tine slab CoV of 45 percent. The difference between the mean bond strengths for these surfaces was determined to be statistically significant according to Student's t-test, indicating that the broom surface did provide a meaningful increase in strength relative to the tine surface.

Table 7-11. Phase 2 direct shear (guillotine) results.

Slab Category	Interface Preparation Technique	Topping Workability Level	Topping Consolidation Technique	Direct Shear Strength			
				Average (psi)	Std. Dev. (psi)	CoV	Sample Size
Precast	Broom	Moderate	V	939	311	33%	9
Precast	Tine	Moderate	V	518	231	45%	9
Repair	Hydrodemolition	Moderate	V	1208	324	27%	9

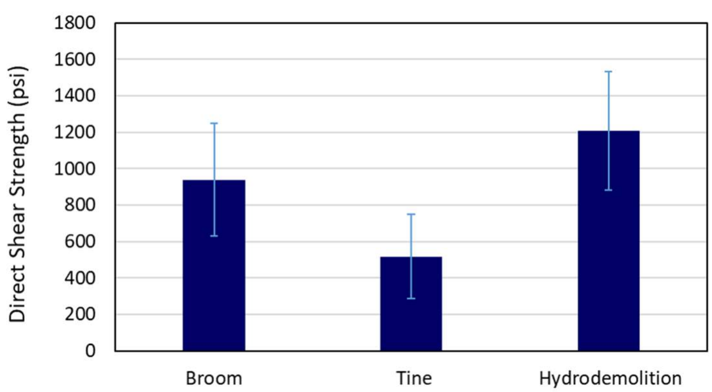

Figure 7-25. Phase 2 direct shear (guillotine) results.

7.4.2. Direct Tensile Pull-off Test Results

The direct tensile pull-off results for Phase 2 slabs are presented in Table 7-12 and Figure 7-26. All samples were tested with 3-inch test disks and circular cuts (cores). The hydrodemolition slab had the highest direct tensile pull-off strength (399 psi) and the lowest CoV (22 percent). This was the only repair specimen capable of direct tensile testing for Phase 2 (the sandblast and float interfaces debonded as described in Section 7.3.1).

Similar to the direct shear results, the direct tensile strengths for the tine interface had higher variability than the broom with CoVs of 54 percent and 41 percent for tine and broom, respectively. The difference between the mean direct tensile strengths for the tine and broom interfaces was not statistically significant.

Table 7-12. Phase 2 direct tensile pull-off test results.

Slab Category	Interface Preparation Technique	Topping Workability Level	Topping Consolidation Technique	Direct Tensile Pull-off Strength			
				Average (psi)	Std. Dev. (psi)	CoV	Sample Size
Precast	Broom	Moderate	V	239	97	41%	9
Precast	Tine	Moderate	V	248	133	54%	6
Repair	Hydrodemolition	Moderate	V	399	89	22%	9

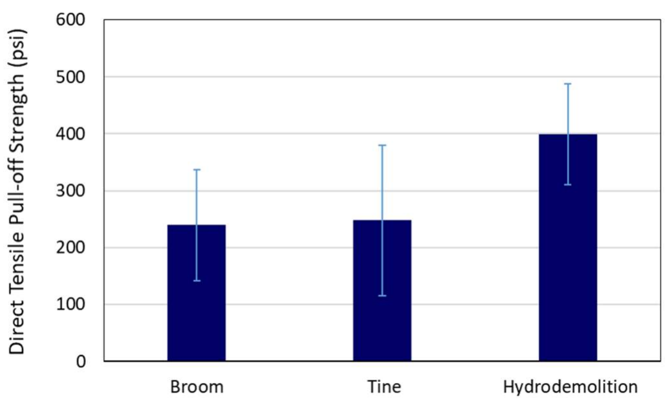

Figure 7-26. Phase 2 direct tensile pull-off results.

7.5. Discussion of Phase 2 Results

The following sections discuss several factors the effectiveness of the surface preparation techniques investigated and compare the shear and tensile strength results from the different test methods employed in Phase 2. An overall comparison of Phase 1 and Phase 2 results and discussion is provided in Section 8.

7.5.1. Effectiveness of Surface Preparation Techniques Investigated

As discussed for the Phase 1 results, the purpose of this research was to study unreinforced concrete interfaces and to develop a method to characterize the strength with better confidence using direct shear (guillotine) testing. The research parameters were selected to provide a range of interface preparation techniques and construction practices commonly used in industry. While the objectives were not explicitly intended to determine the most effective surface preparation techniques, the test results reinforce the findings of previous research in this subject area and provide additional insight into the requirements for improving shear and tensile bond strength at unreinforced interfaces.

Since the sandblast only beam and slab specimens experienced debonding of the repair material (topping) prior to testing, the only interface preparation technique tested in the Phase 2 repair series was hydrodemolition. As such, the Phase 2 results cannot be used to comment on the effectiveness of repair surface preparation techniques.

In the precast series, the beam tests for specimens with tine and broom finishes indicated comparable failure loads and interface shear stresses at failure. The maximum interface shear stress at failure (estimated using analysis Method B (Table 7-10)) was 849 psi and 801 psi for the broom and tine beam specimens, respectively. Since only one test was performed for each condition, statistical analysis of the data is not possible. From a practical perspective, the beam tests would indicate that the interface shear strength of the two interface types was similar.

In contrast, the direct shear (guillotine) tests performed on cores removed from the Phase 2 companion slab specimens indicated that the average direct shear strength of the broom interface was approximately 80 percent higher than the tine interface. The average tensile pull-off strength for the companion slab specimens was comparable for the two interfaces (i.e., the difference between mean strength was not statistically significant). The broom interface shear strength and direct tensile strength results were less variable than the results for the tine surface. Overall, the Phase 2 slab specimen results support the Phase 1 conclusion that the broom finish provides similar or higher interface bond strengths than the tine surface. As noted in Section 5.5.3.2, other researchers have reported the opposite trend, indicating higher interface shear strength for tine finishes in comparison to broom finishes.

The contradictory conclusions regarding the shear bond strength of broom and tine finishes in unreinforced interfaces may result from several factors, including substrate and topping properties and placement procedures, variability in the surface textures created by raking or tining the substrate, and differences in shear test methods.

7.5.2. Comparison of Beam Test Results to Direct Shear and Tensile Pull-off Tests Results

A summary of Phase 2 results from beam tests, direct shear (guillotine) tests, and direct tensile pull-off tests is shown in Table 7-13. The horizontal shear stress results from the beam tests are those calculated using Method B (discussed in section 7.3.6.6), with results shown for the estimated maximum shear stress (based on Segment S3) and average shear stress (based on Segment S4).

Table 7-13. Summary of shear and tensile bond strength results from Phase 2.

Interface Preparation Technique	Horizontal Shear Stress at Failure from Beam Tests* (psi)		Average Guillotine Shear Strength (psi)	Average Tensile Pull-off Strength (psi)	MTD Slab (mm)	MTD Beam (mm)
	Max. (S3)	Average (S4)				
Hydrodemolition	1078	548	1208	399	1.33	1.46
Tine	1073	547	518	239	0.75	1.3
Broom	1108	567	939	248	0.6	0.7

**Note: Based on analysis Method C.*

The broom, tine, and hydrodemolition beams failed in horizontal shear at applied loads between 86 kips and 89 kips. The maximum horizontal shear strengths for these three beams were estimated at between 1073 to 1108 psi based on Method C. The similarities between the failure loads and estimated shear strengths indicated from the beam tests are contradictory to the direct shear and direct tensile results performed using the companion slab specimens that show a more pronounced effect of interface type on bond strength.

7.5.2.1. Direct Shear Comparison

The direct shear (guillotine) results are compared to the horizontal shear strengths from beam tests in Figure 7-27. The hydrodemolition average direct shear strength is 1.12 times the maximum horizontal shear stress at failure and 2.2 times the average horizontal shear stress at failure from the beam test. The broom average direct shear strength is 0.85 times the maximum horizontal shear stress and 1.66 times the average horizontal shear stress. The results from the tine slab specimen indicate a direct shear strength lower than both the maximum and average shear stress from the beam test. It is noted that tine direct shear results from Phase 2 indicated lower and more variable shear strengths than the results from Phase 1, and that the Phase 2 tine slab specimen had a lower surface roughness (MTD) than the Phase 2 beam and Phase 1 slab. As a result, the comparison of the Phase 2 tine slab and beam shear stress results may not be a representative comparison of the beam and direct shear test methods.

The limited results suggest that the maximum horizontal shear stress at the occurrence of interface shear failure for the beam specimens tested is generally comparable to the direct shear strength by guillotine testing. Basic mechanics of bending and shear in elastic composite members indicate that the shear stress should be constant along the horizontal interface between the topping and the beam. However, since the topping does not extend to the end of the beam specimen, the discontinuity in section properties results in increased interface shear stresses near the end of the topping slab. This is demonstrated by sectional analysis (linear elastic or non-linear strain compatibility) and estimation of the interface shear stresses using the segment method (Section 3.1.3). If the number of beam section locations instrumented with strain gauges was increased, thereby decreasing the segment length, an improved estimation of maximum shear stress at interface failure could have been obtained. Based on the data collected, the shear stresses estimated for segment S3 (32-inch from midspan to end of topping) are likely more representative of the peak interface shear stresses developed in the beam specimens and are more comparable to the shear strength determined by the direct shear (guillotine) test.

7.5.2.2. Direct Tensile Pull-off Test Comparison

The direct tensile pull-off results from the companion slab specimens are compared to the horizonal shear strength results estimated using the beam test results in Figure 7-28. For hydrodemolition, the ratio of maximum and average horizontal shear stress at failure from the beam testing to average direct tensile pull-off strength is 2.7 and 1.4, respectively. For the broom interface, the ratio of maximum and average horizontal shear stress to average direct tensile pull-off strength is 4.5 and 2.3, respectively. The strength ratio results from the tine slab specimen are similar to those for the broom slab specimen.

The interface bond strength in tension is consistently lower than the shear strength indicated by the beam tests, however, there does not appear to be a consistent relationship between the two strengths. Specifically, the data indicate higher direct tensile bond strength for the hydrodemolition interface than the tine or broom surfaces, while the maximum shear stresses at interface failure in the beam tests are similar for the three interface conditions. As discussed in the preceding section, this may be influenced by the nature of the interface shear stress distribution in the beam tests, which may make it difficult to distinguish differences in interface shear strength from the beam tests. The comparison of direct shear strength from guillotine tests and direct tensile strength is discussed in Section 8 for data from both phases of slab testing.

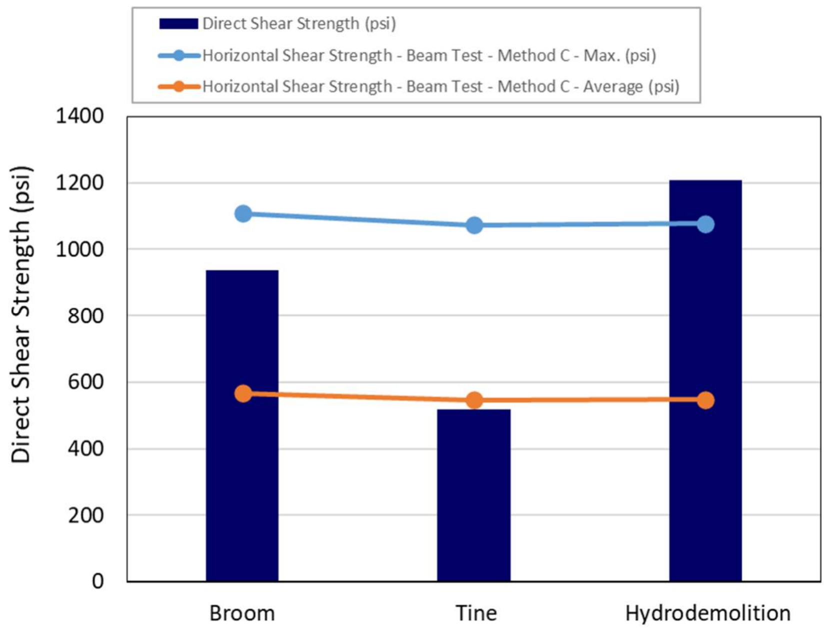

Figure 7-27. Phase 2 direct shear (guillotine) results versus beam horizontal shear stress results.

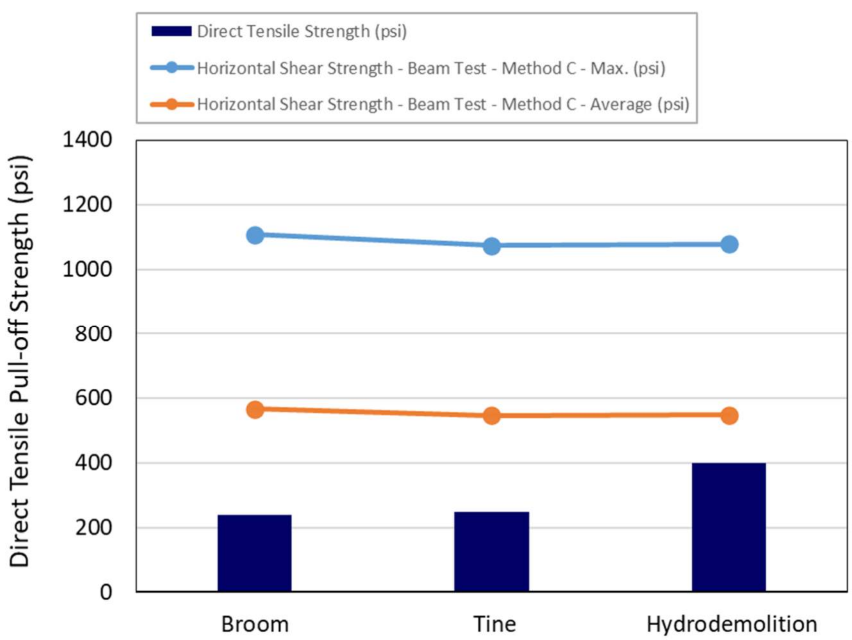

Figure 7-28. Phase 2 direct shear tensile pull-off results versus beam horizontal shear stress results.

8. OVERALL DISCUSSION OF RESULTS (PHASES 1 AND 2)

The primary aspects and parameters of the experimental program, including interface preparation techniques, concrete material characteristics, casting/curing procedures, and testing procedures, were similar between the two phases. The following sections discuss the experimental results and observed behavior for the two phases, including comparisons between the phases were appropriate.

8.1. Variability of Interface Roughness for Different Surface Preparation Techniques

The interface surface roughness results based on MTD are summarized in Table 8-1 and Figure 8-1 for both Phase 1 and Phase 2. Results are shown for repair surfaces prepared by hydrodemolition and sandblasting. Note that results for repair specimens prepared by mechanical removal by bush hammer followed by sandblasting are not presented, as this method was not included in Phase 2. For the precast series, results are shown for interfaces prepared by floating, tine, and broom.

The combined MTD results for the hydrodemolition and sandblast specimens from the repair series had relatively low CoVs of 5 percent and 9 percent, respectively. The repair specimens represent surface preparation techniques that remove the finished, or as-cast, outer layer of concrete while increasing the surface roughness. The repair surface preparation techniques in this study were performed by experienced concrete repair technicians using the same equipment for both phases. The technician performed the surface preparation in increments, after which the surface was compared to a surface profile comparator (CSP) to determine if further concrete removal was necessary. The consistency in application of the surface preparation technique and comparison to the CSP standards is reflected in the low variability of the MTD data. A Student's t-test indicates that the difference between the mean values of the MTD results for the four hydrodemolition specimens (two each from Phases 1 and 2) is not statistically significant. The same conclusion was determined for the four sandblast specimens. These results indicate that repair surface preparation by experienced technicians with good oversight can achieve consistent surface roughness. It is noted that although the apparent surface roughness (MTD) from Phase 1 and Phase 2 repair specimens were statistically the same, the direct shear and direct tensile results were varied between phases, indicating the influence of other factors that affect bond strength.

The combined MTD results for the tine and broom specimens in the precast series were significantly more variable than the repair series, with CoVs for tine and broom of 52 percent and 35 percent, respectively. The float surface also exhibited a high CoV of 44 percent. The variation in MTD for both broom and tine specimens from Phase 1 slabs, Phase 2 slabs, Phase 2 beams suggests intentional roughening during finishing of fresh concrete (representative of new construction) may be variable due to several factors, including:

- Duration after concrete placement and floating before application of tine or broom finish (degree of concrete surface hardness).
- Aggregate size in the substrate (if aggregates are pulled up while roughening using a tining rake).
- Tool used (type and condition of broom or tining rake).
- Technique and amount of pressure applied by the finishing personnel while pulling the boom or tining rake.

Application of the broom and tine finishes was performed using the same tools in both phases, but by different personnel. Additionally, the timing of the finishing process is based on the judgement of the person doing the finishing and is subject to variation. Lastly, there are no reference standards such as CSP cards for broom and tine finishes. While it is likely that the finishing practices will be less variable when performed by experienced personnel at a precast plant, it is possible that these types of finishes may be more prone to variable results than the roughness for surfaces prepared using the repair techniques performed by experienced personnel.

Table 8-1. Summary of MTD results for Phase 1 and Phase 2.

Interface Preparation Technique	Phase 1 Slabs (mm)	Phase 2 Slabs (mm)	Phase 2 Beams (mm)	Average (mm)	Standard Deviation (mm)	CoV
Hydrodemolition	1.33	1.33	1.46	1.37	0.07	5%
Sandblast	0.20	0.20	0.23	0.21	0.02	9%
Tine	2.23	0.75	1.30	1.43	0.75	52%
Broom	1.14	0.60	0.70	0.81	0.29	35%
Float	-	0.08	0.16	0.12	0.05	44%

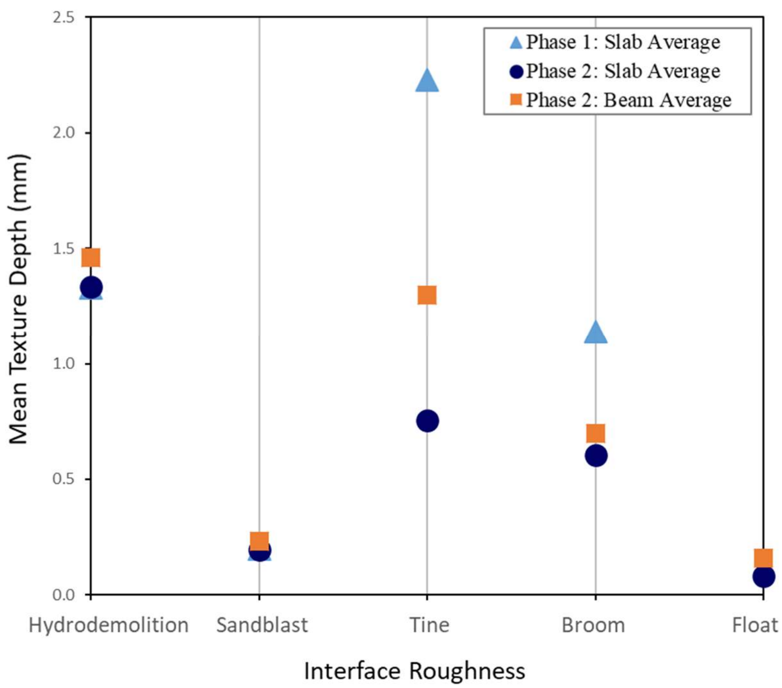

Figure 8-1. Comparison of MTD Results from Phase 1 and Phase 2

8.2. Inconsistency of Bond Strength for Repair Surface Preparation by Sandblast Alone

The surface preparation technique using sandblasting alone produced significantly different bond strength results in Phases 1 and 2. For Phase 1, the sandblast surface had a direct shear strength of 815 psi with a CoV of 26 percent and a direct tensile pull-off strength of 300 psi with a CoV of 22 percent. The shear strength was higher than the average direct shear strength of bush hammer + sandblast and tine slab specimens from Phase 1 and was similar to strength results from the broom surface.

The sandblast results from Phase 1 were initially counter-intuitive since the interface bond strength was relatively high with lower variability while the mean texture depth was much lower than the other surface preparations. These results suggested that the degree of roughness did not have a strong influence on bond strength and that uniform roughening (opening of concrete pore structure) along with good repair or topping placement techniques could achieve good interface bond despite low MTD.

The sandblasting alone preparation technique was applied for beam and slab specimens in Phase 2. In both instances the repair/topping completely delaminated from the substrate before testing, and test results were recorded as zero bond strength. It is likely that increased early-age shrinkage or thermal strains, possibly resulting in curling, of the repair/topping occurred, which developed interface stresses that exceeded the early-age bond strength. Several factors may have affected debonding due to differential shrinkage in the Phase 2 specimens:

Interface Surface Texture

- The surface roughness characterized by MTD was presented in Sections 5.2.2 and 7.2 for the Phase 1 and Phase 2 specimens, respectively.
- The MTD values for Phase 2 specimens were classified as low, moderate, and high roughness based on MTD values (Figure 7-1). The float and sandblast interfaces were both considered as low roughness with MTD values on the order of 0.1 to 0.2 mm, possibly indicating that the debonding of these specimens was related low surface roughness. However, this is inconsistent with the Phase 1 results, where the slab specimen with sandblast interface had a comparable average MTD of 0.2 mm but did not experience debonding. Furthermore, the Phase 1 sandblast specimen exhibited shear and tensile bond strengths comparable to specimens with broom and tine interface preparation with higher MTD.
- Collectively, the Phase 1 and Phase 2 results indicate lower MTD may have contributed to debonding of the Phase 2 float and sandblast specimens, but that other factors likely also contributed to the debonding.

Topping Material Properties

- One batch of concrete was used for the beam and slab topping for all Phase 2 specimens. This indicates that topping material properties were not likely a factor in the debonding of the float and sandblast specimens relative to the other Phase 2 interface types.
- The same concrete mixture and ready-mix supplier were used for Phase 1 and Phase 2 topping (and substrate) concrete, although cast on different dates; batch-to-batch variability may be a factor for comparison of Phase 1 and 2 results.

Topping Placement	▪ The Phase 1 results demonstrated that the topping placement and consolidation procedures can influence interface bond (Section 5.5.3.2). ▪ The topping for all Phase 2 beams and slabs was placed on the same day using the same procedures for all specimens, including substrate surface cleaning, substrate soaking/drying time for SSD conditions, topping consolidation technique, and personnel performing each task. ▪ The consistency of procedures rules out topping placement as a likely factor for debonding of the float and sandblast interface specimens compared to other Phase 2 specimens.
Topping Curing	▪ The topping on the Phase 2 beam and slab specimens was moist cured for 7 days using wet burlap, followed by exposure to the laboratory environment for the remaining curing period prior to testing. These curing conditions were similar to those in Phase 1. ▪ The curing conditions were the same for all Phase 2 specimens, suggesting that curing is not likely a factor for debonding of the float and sandblast interface specimens compared to other Phase 2 specimens.
Specimen Type	▪ The bonded interface area in the beam may be more prone to differential shrinkage than the slab specimens or other configurations. The beam specimen design had an unreinforced interface at the failure end (8 inches wide by 42 inches long) and a reinforced interface at the non-failure end. This may have caused non-uniform interface shear stresses due to restrained shrinkage; larger interface shear stresses may have occurred at the free end of the unreinforced region, possibly initiating debonding there. The initiation of debonding may have been exacerbated by curling of the topping due to non-uniform shrinkage and restraint. ▪ Although the beam specimens may be more prone to debonding, the occurrence of debonding on the companion slab specimens suggests that specimen type is not a factor for debonding of the Phase 2 sandblast specimens (beam and slab) relative to the Phase 1 slab specimens.

The preceding discussion does not lead to definitive explanation for the debonding of the float and sandblast specimens in Phase 2; the materials, construction, and other conditions appear to be essentially the same between Phase 1 and Phase 2 and within Phase 2. The performance of the Phase 2 specimens relative to each other suggests that the lower surface roughness for the float and sandblast specimens is the most likely reason why those samples debonded while the hydrodemolition, broom, and tine specimens did not; the lower roughness may make these interfaces more prone to debonding due to restrained shrinkage and curling effects. Moreover, it is possible that unknown differences in topping material properties, curing conditions, or thermal exposures resulted in increased restrained shrinkage or thermal volume changes in the Phase 2 sandblast specimens causing debonding while the Phase 1 sandblast specimens showed good bond strengths.

The occurrence of premature debonding of composite specimens with low surface roughness was also noted by Kovach and Naito (2008) where composite beams with unreinforced interfaces exhibited debonding before testing. These results indicated smooth or low roughness interfaces were incapable of developing bond sufficient to resist the restrained shrinkage that occurred.

The different results between Phase 1 and Phase 2 indicate that although good bond strength can be achieved by sandblast alone under some conditions, the risk of premature debonding and delamination may be increased for interfaces with low surface roughness. Typical repair and precasting practices would not permit the use of sandblast alone as surface preparation. The results from the current study indicate that these practices should be maintained.

8.3. Correlation Between Bond Strength and Interface Mean Texture Depth

The mean texture depths of the various substrate surface preparations were presented in Sections 5.2 and 7.2, and are summarized in Figure 8-2. The average direct shear and tensile bond strengths are also included in the figure. The relationships between MTD and direct tensile pull-off strength, and MTD and direct shear strengths, are shown in Figure 8-3 and Figure 8-4, respectively.

The test results indicate that there does not appear to be a consistent correlation between interface bond strength and MTD. Notably, the precast tine surface in Phase 1 had the highest MTD due to the large grooves in the surface macrotexture created by the tining rake, although this surface did not have the highest shear or tensile bond strength. The precast tine surface from Phase 2 had a significantly lower MTD than the Phase 1 tine surface, but the shear and tensile bond strengths were not proportionally lower. The repair hydrodemolition interface had the highest average shear and tensile bond strength in both phases but had an average MTD of about 60 percent of the MTD for the Phase 1 precast tine surface. The repair bush hammer + sandblast surface preparation achieved the second lowest shear bond strength and lowest tensile bond strength of all interface types but had a higher MTD than the sandblast only interface and Phase 2 tine interface. The Phase 1 broom interface MTD was nearly twice the Phase 2 broom MTD, while the tensile strengths were comparable, and the Phase 2 shear strength was higher than Phase 1.

The MTD for the Phase 1 precast tine surface and the corresponding bond strength results are particularly different from those of the other interface types. The high MTD for the tine interface results from the deep, narrow grooves created by the tining rake. The grooves are pronounced but are spaced further apart than the surface undulations created by the broom. Examination of the tine grooves from a Phase 1 specimen under optical microscope (Figure 8-5) shows that the mortar from the topping concrete may not be fully consolidated in the substrate grooves. This condition, in combination with the wide spacing of the grooves, does not appear to provide improved bond in comparison to the broom substrate finish in spite of having a high MTD. The more uniform and shallower surface roughness of the other surfaces investigated, including the precast series broom finish, may facilitate more thorough consolidation of the topping concrete at the interface, resulting in improved bond.

Published research typically shows a strong correlation between shear strength and surface roughness, although most studies do not quantitatively characterize surface roughness. From a qualitative perspective, there is a subtle correlation between surface texture roughness and interface shear strength in the repair series; the increased surface roughness (higher CSP) of the hydrodemolition interface provided a significant increase in shear and tensile bond strength in comparison to the sandblast only and bush hammer + sandblast interfaces, which have lower surface roughness (CSP values). However, the comparison of the bush hammer + sandblast and sandblast only interfaces provides a contradictory conclusion, most likely due to microcracking or bruising of the substrate due to concrete removal by bush hammer that may have reduced bond strength.

The combined Phase 1 and 2 results indicate that for the interface types and topping placement conditions investigated, the shear and tensile bond strength of an unreinforced interface do not appear to be influenced by the degree of surface macrotexture roughness measured by MTD. This contrasts with most published research, although the published correlations are primarily qualitative indications of relative surface roughness rather than the quantitative measure of MTD used in the current study. The results in the current study suggest that the interface bond strength in shear may be less dependent on degree or magnitude of surface roughness and more dependent on having a uniformly roughened surface that is sound (i.e., no laitance or surface defects) and having well consolidated repair or topping concrete.

The limited influence of surface roughness on shear and tensile bond strength results for the unreinforced interfaces considered in this study contrasts with shear transfer mechanisms where friction is engaged. For example, surface roughness is known to have a significant influence on shear transfer by shear friction across interfaces with reinforcement, or for unreinforced interfaces subjected to a permanent normal force such that friction can develop.

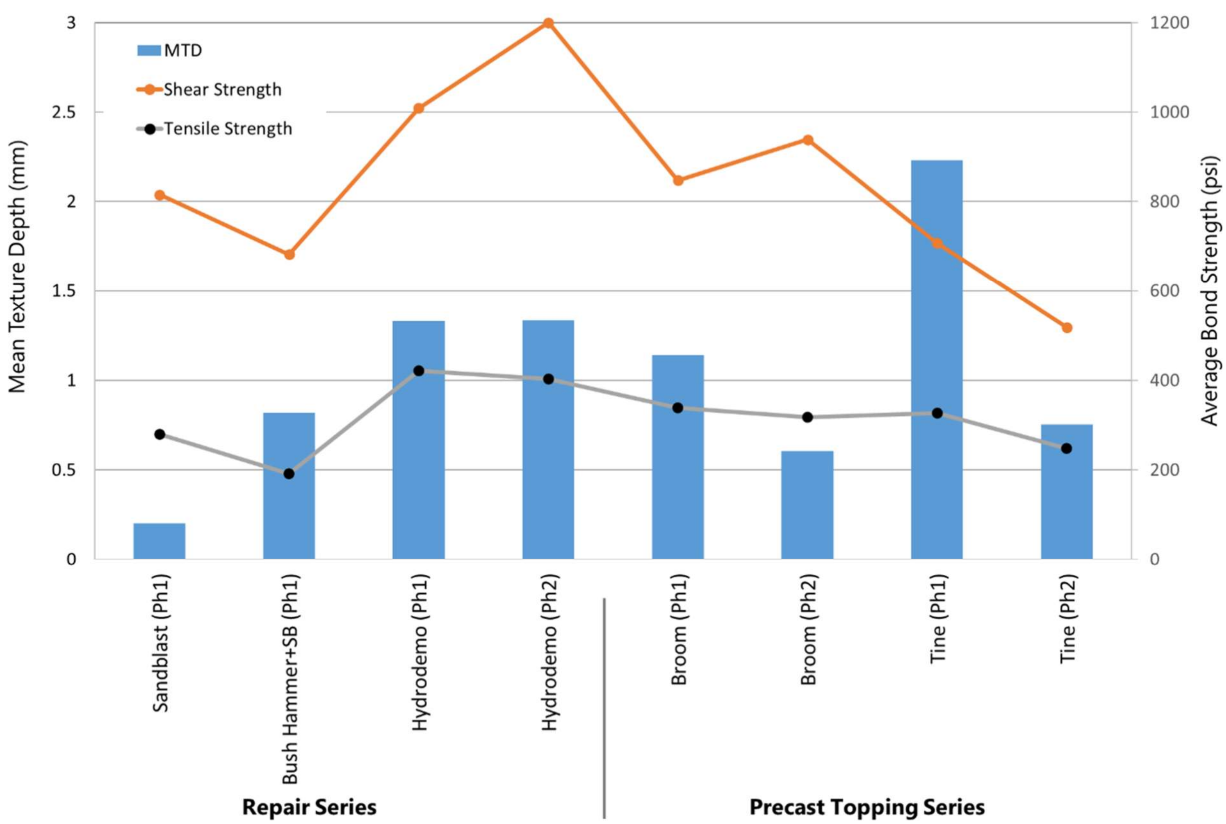

Figure 8-2. Measured mean texture depths and direct shear (guillotine) and direct tensile bond strengths for different surface preparation techniques (Phase 1 and 2 data).

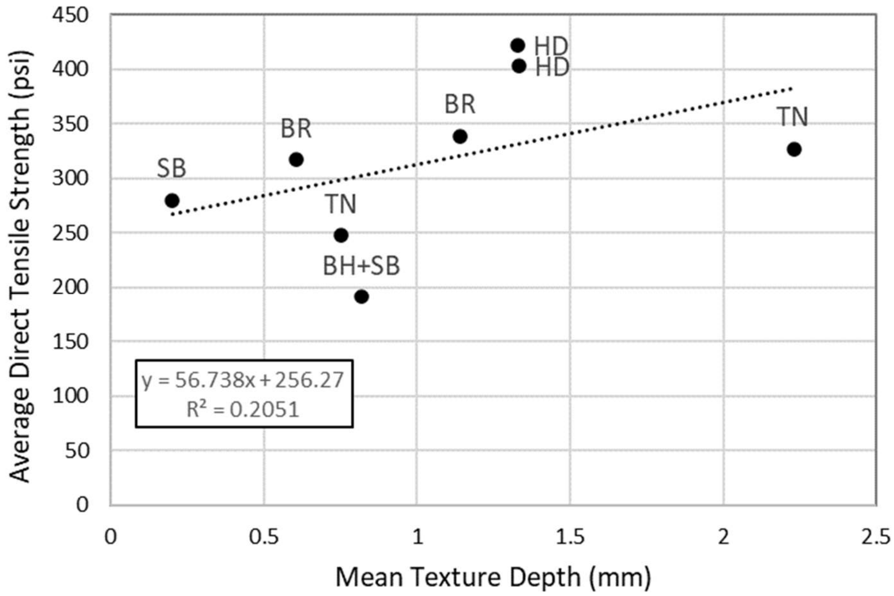

SB: Sandblast only
BH+SB: Bush hammer + sandblast
HD: Hydrodemolition
BR: Broom
TN: Tine

Figure 8-3: Lack of correlation between mean texture depth and direct tensile pull-off strength.

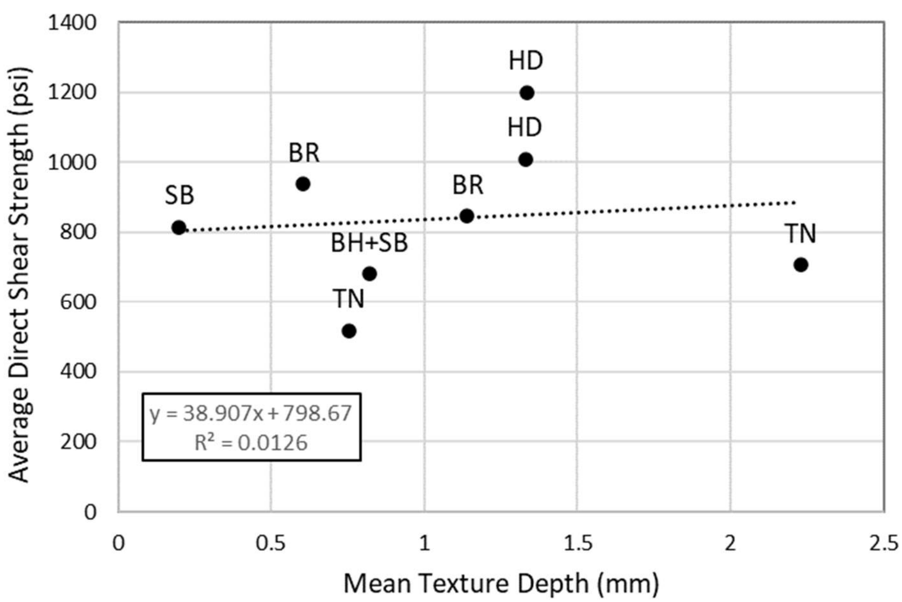

SB: Sandblast only
BH+SB: Bush hammer + sandblast
HD: Hydrodemolition
BR: Broom
TN: Tine

Figure 8-4: Lack of correlation between mean texture depth and direct shear strength.

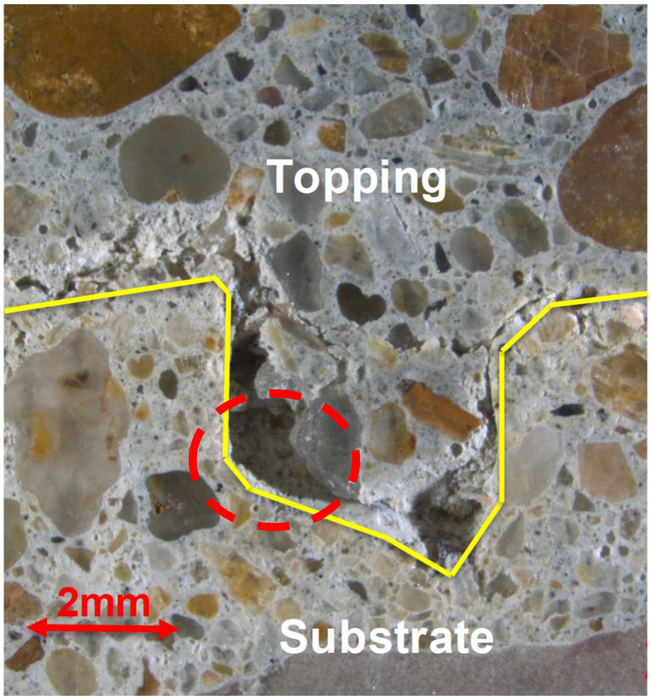

Figure 8-5. Precast Series Tine Interface (Phase 1): Close-up view of topping consolidation in substrate groove created by tining rake.

8.4. Comparison of Direct Shear Results to Direct Tensile Pull-off Test Results

The correlation between direct shear strength and direct tensile pull-off strength is often discussed in the context of repair design. The direct shear strength results in the current study (tested using the guillotine shear method) were consistently greater than direct tensile pull-off strength results.

8.4.1. Ratio of Shear-to-Tensile Strength for All Data

The correlation between average direct shear strength determined by guillotine shear test and average direct tensile pull-off strength is shown in Figure 8-6 for all Phase 1 and Phase 2 data. Ratios of interface shear-to-tensile pull-off strength for each interface type tested are listed in Table 8-2 and are plotted as a function of MTD in Figure 8-7. Note that the average results used to create this table and these figures were based on a sizeable data set of 156 direct shear guillotine tests and 105 direct tensile pull-off test results.

The ratios of shear-to-tensile strength range from 2.09 to 3.57, with an average value of 2.70 and standard deviation of 0.47. Figure 8-6 includes a linear regression trendline and indicates a good linear correlation between interface shear and tensile strength with a slope of 2.64 and a coefficient of determination (R^2) value of 0.98. Note that the regression trendline is based on a zero y-intercept; correlation is decreased using a non-zero y-intercept.

Table 8-2. Ratio of average interface direct shear strength to direct tensile pull-off strength.

Category	Interface Preparation Technique	Mean Texture Depth, MTD (mm)	Average Shear Strength (psi)	Average Tensile Strength (psi)	Ratio of Shear-to-Tensile Strength
Repair	Sandblast-Phase 1	0.20	815	280	**2.91**
	Bush Hammer+Sandblast-Phase 1	0.82	682	191	**3.57**
	Hydrodemolition-Phase 1	1.33	1009	422	**2.39**
	Hydrodemolition-Phase 2	1.33	1207	404	**2.99**
Precast	Broom-Phase 1	1.14	848	339	**2.50**
	Broom-Phase 2	0.60	939	317	**2.96**
	Tine-Phase 1	2.23	707	327	**2.16**
	Tine-Phase 2	0.75	518	248	**2.09**
				Average	**2.70**

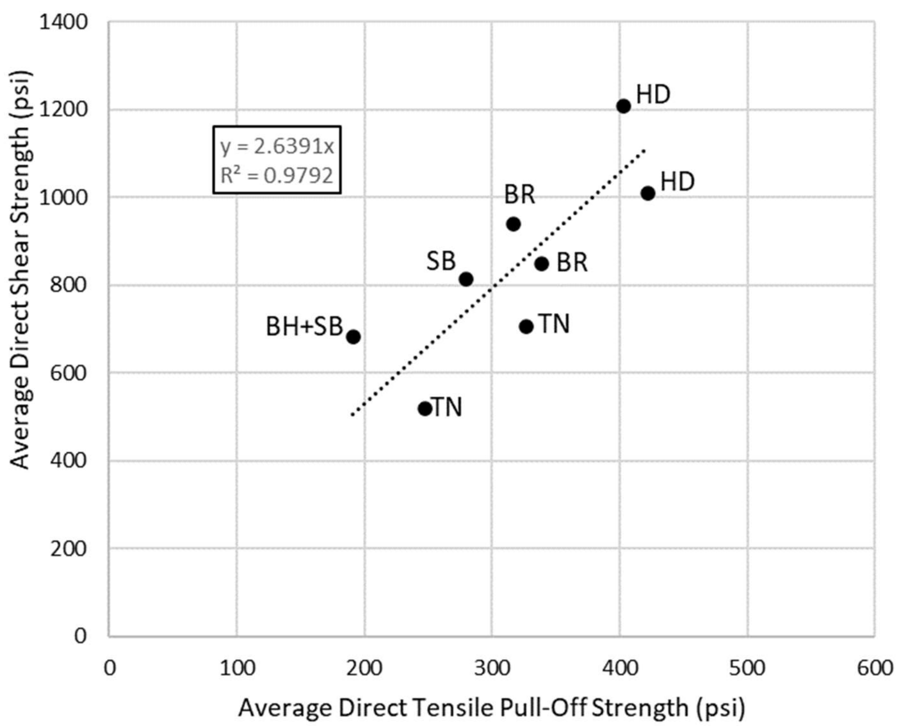

SB: Sandblast only
BH+SB: Bush hammer + sandblast
HD: Hydrodemolition
BR: Broom
TN: Tine

Figure 8-6: Correlation between interface direct shear strength and direct tensile pull-off strength.

The ratios of shear-to-tensile strength do not appear to correlate with surface roughness measured using MTD (Figure 8-7). A linear regression shows a slight decreasing trend in strength ratio with increasing MTD, although the coefficient of determination is low (R^2 = 0.21). The results for the repair series bush hammer + sandblast interface have the highest ratio of shear-to-tensile strength of 3.57, while having an MTD less than the average value for the interfaces tested.

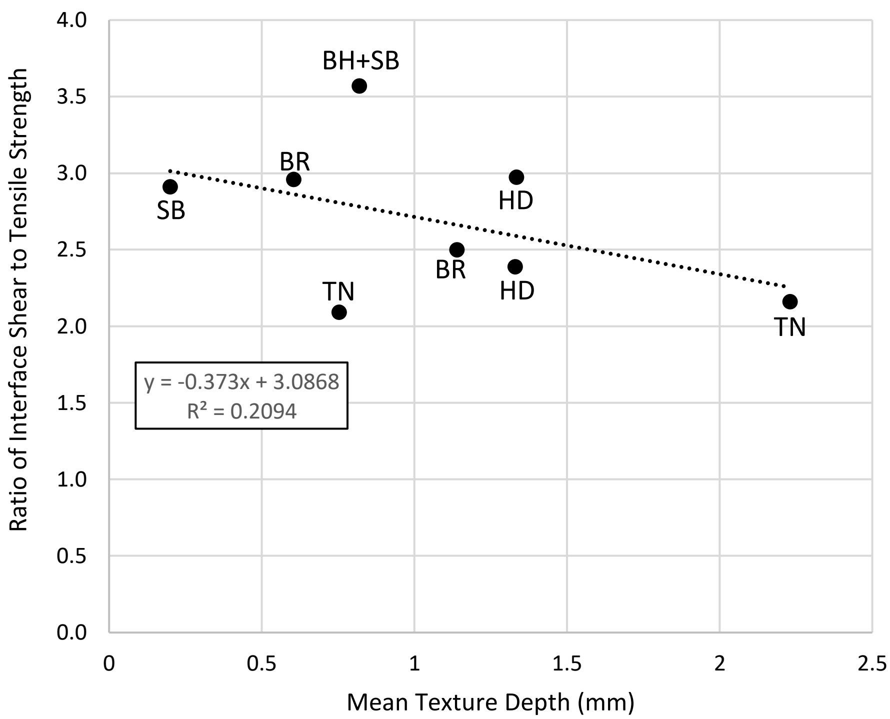

SB: Sandblast only
BH+SB: Bush hammer + sandblast
HD: Hydrodemolition
BR: Broom
TN: Tine

Figure 8-7. Variation of ratio of shear-to-tensile bond strength with respect to mean texture depth.

8.4.2. Comparison of Shear-to-Tensile Strength Ratios from Current Study to Published Results

Numerous previous research studies have explored the correlation between different test methods used to assess interface shear bond strength, and some have examined the correlation between interface shear strength and interface tensile bond pull-off strength. A limited review of previous research reveals that the actual correlation is dependent on the test methods used and interface parameters investigated, as described in Sections 3.3 and 3.3.7. Table 8-3 presents a summary of ratios of interface shear strength to direct tensile pull-off strength for various shear test methods reported in the literature.

Table 8-3. Comparison of published ratios of interface shear strength to direct tensile pull-off strength.

Reference	Shear Test Method	Ratio of Shear-to-Tensile* Strength
Silfwerbrand (2003)	In-situ torsion test	1.9 to 3.1
Rosen (2016)	Guillotine direct shear test	1.3 to 2.2
	Slant shear test	7.6 to 10.2
Momayez et al. (2005)	Single-shear test w/ rectangular prisms (low roughness interfaces)	1.6 to 2.2
	Single-shear test w/ rectangular prisms (high roughness interfaces)	1.7 to 2.4
	Slant shear test (low roughness interfaces)	5.1 to 7.5
	Slant shear test (high roughness interfaces)	5.4 to 8.8
Santos (2009)	Slant shear test	5.1 to 6.3

** Tensile strength as measured by direct tensile pull-off test.*

The shear-to-tensile pull-off strength results from the current study are consistent with or slightly higher than the range of values for direct shear or torsion shear tests from previous studies. The slant shear test produces significantly higher apparent shear strengths due to the effect of normal force across the interface tested.

Many research studies and repair design guides conclude that tensile bond pull-off testing is the preferred method for assessing in-situ interface bond conditions in practice based on its relative simplicity and ability to be performed entirely in the field. ACI 562-21 Clause 7.4.3 requires the use of quantitative bond strength testing to verify performance of cementitious repairs for unreinforced interfaces where the factored shear stress (demand) is between 30 and 60 psi. Direct tension pull-off tests are one method permitted by ACI 562 for this purpose. The commentary for Clause 7.4.3 states that "typically direct shear strengths are larger than direct tension strengths," although it goes on to indicate that "it is generally adequate to assume that the repair to substrate bond will resist an interface shear equal to the direct tensile pull-off test result." The ratios of measured interface direct shear strength to tensile pull-off strength are consistently greater than the assumed ratio of 1:1 noted in the ACI 562 commentary; presumably the commentary is intended to provide a conservative lower bound.

The data from the current study and other published research show that the ratio of shear strength to tensile pull-off strength is influenced by the interface preparation condition including surface roughness and mean texture depth. This observation, in combination with the dependence of the shear-to-tensile strength ratio on test methods used to obtain the strength results and the general variability of shear and tensile bond strength results, indicates that a generally applicable single value, or even a range of values, for ratio of shear-to-tensile strength suitable for quality control purposes may not achievable. Rather, the ratio would likely need to be determined based on test data on a case-by-case basis to effectively use it for quality control purposes in a performance-based design approach for interface shear.

8.5. Comparison of Shear Strength Results to Design Values

The average direct shear strengths determined by guillotine shear testing were significantly higher than the nominal interface shear strength for design of 80 psi per ACI 318 and ACI 562 for all interface preparation techniques investigated. It is important to note that average material strength test results are not typically appropriate for use in structural design or evaluation.

8.5.1. Estimated Characteristic Shear Strength Based on Direct Shear Strength Tests

The Tolerance Factor Method is one approach that that can be used to estimate equivalent specified, or characteristic, material strengths for design based on test data. The results of the current study suggest that shear bond strength may vary significantly depending on the interface preparation techniques, topping or repair material used, placement and consolidation, and other factors; the results do not support recommending a "universal" interface shear strength for design. Alternatively, estimating the characteristic shear strength using the Tolerance Factor Method with the test results obtained for various conditions provides an indication of the potential for increased shear strength values for use in design.

Characteristic design interface shear strengths were estimated by applying the Tolerance Factor Method to the direct shear (guillotine) test results. Results are presented in Table 8-4 for 10 percent and 5 percent fractile values at a confidence level of 90 percent. The 10 percent fractile (i.e., 90 percent probability of exceedance) is commonly used for evaluating concrete strength test data (ACI 214.4-21, ACI 228.1-19) while the 5 percent fractile is used to establish characteristic values for post-installed anchors in concrete (ACI 355.4-19). The 90 percent confidence level is commonly used for evaluating concrete strength data and is specified in ACI 355.4 for establishing design strengths for post-installed anchors based on tests.

The data presented in Table 8-4 include all Phase 1 and Phase 2 results. Note that the Phase 1 data for the precast series have been combined for the moderate slump concrete placed by hand consolidation and vibration since these data sets were not shown to be statistically different. Furthermore, the table does not include the results for precast specimens with lower slump topping placed by screed only, as the variability of these results was too large to provide meaningful results.

Table 8-4. Characteristic design interface shear strengths based on Tolerance Factor Method (90% Confidence).

Slab Category	Interface Preparation Technique	Direct Shear Strength – Test Data*				Characteristic Strength (psi)	
		Average (psi)	Std. Dev. (psi)	CoV	Sample Size	10% Fractile	5% Fractile
Repair	Sandblast	815	209	26%	19	443	350
	Bush Hammer + Sandblast	682	237	35%	18	255	149
	Hydrodemolition	1063	259	24%	33	634	524
Precast	Broom	861	232	27%	40	490	395
	Tine	667	244	37%	46	282	182

Std. Dev.: Sample standard deviation
CoV: Coefficient of variation
**Note: All data from Phase 1 and 2.*

The characteristic design shear strengths estimated by the Tolerance Factor Method reflect the significant influence of variability in the test results on the resulting design strength. Notably, the characteristic interface shear strength for the broom finish is about double that for tine finish, while the mean strength of the broom finish was only 30 percent higher than that of the tine finish. In this case, the tine finish had a greater coefficient of variation than the broom finish (Table 8-4), which results in a larger difference between the mean and characteristic strengths. A similar punitive result occurs for the bush hammer + sandblast repair interface, which had a coefficient of variation of 35 percent, resulting in a characteristic strength less than half of the mean strength.

The estimated characteristic design shear strengths based on a 5 percent fractile range from 1.9 to 6.6 times higher than the current 80 psi nominal interface shear strength in ACI 318 and ACI 562. These results suggest that partial-depth repairs and precast topping applications with good interface surface preparation and well-consolidated repair or topping concrete may justify the use of a higher interface shear bond strength for design.

8.5.2. Comparison of Shear Strength from Beam Tests to ACI Horizontal Shear Provisions

ACI 318-19 requirements for horizontal shear transfer in composite members in Clause 16.4 are based on the simplified elastic method (see Section 3.1.2) to estimate the interface shear demand. ACI 318 also permits an alternative method, known as the segment method, to estimate horizontal shear demand (see Section 3.1.3).

The estimated horizontal shear stress at interface shear failure was calculated using the segment method and the simplified method for each of the three beams tested (Table 8-5). The results for the segment method are shown for each segment considered, including the maximum shear stress (based on segment S3) and average shear stress (based on segment S4). The compression resultants used in the segment method were estimated using Method C as described in Section 7.3.6. As discussed in Sections 7.3.6.6 and 7.5.2.1, the selection of segment length and variation of shear stress along the length of the interface will influence the estimated maximum shear stress, particularly for situations where the topping or repair (i.e., composite section) is stopped before the end of the member. Based on the experimental data and strain gauge layout used, the maximum shear stress based on segment S3 is expected to be more representative of the shear strength of the interface than the average shear stress based on segment S4.

The three composite beam specimen tests experienced an interface shear failure at a maximum horizontal shear stress (based on the segment method using Method C) between 1073 psi and 1108 psi, or more than 13 times the nominal horizontal shear stress limit of 80 psi in ACI 318-19. The average shear stress at failure based on the segment method ranged between 547 psi and 647 psi, or about 7 times the nominal horizontal shear stress limit in ACI 318-19. The interface shear stress at failure calculated using the simplified method was 346 psi to 360 psi, or 4.3 to 4.5 times the ACI 318-19 nominal horizontal shear stress limit. While these results illustrate that the estimated horizontal shear stresses may vary significantly depending on the analysis approach used, in all cases the interface shear stress corresponding to the occurrence of debonding failure in the beams exceeded the nominal stress limit of 80 psi in ACI 318-19 by a significant margin. Further discussion of the methods to estimate shear stress demand is included in the following section.

Table 8-5. Summary of estimated horizontal shear stress at interface shear failure from beam tests.

Interface Preparation Technique	Applied Load at Interface Shear Failure	Segment Along Beam Length Considered	Segment Method* (psi)		Simplified Elastic Method	
			$\frac{C_1 - C_2}{l * b_v}$		$\frac{V_u}{b_v * d}$	
	(kips)		$V_{uh} = (C_1 - C_2)$ (kips)	v_{uh} (psi)	V_u (kips)	v_u (psi)
Broom	89.9	S1	50.8	397	45.0	360
		S2	50.9	397		
		S3 (max.)	88.7	1108		
		S4 (average)	190.4	567		
Tine	86.6	S1	49	383	43.3	346
		S2	49	383		
		S3 (max.)	85.8	1073		
		S4 (average)	183.8	547		
Hydro-demolition	86.8	S1	49	383	43.4	347
		S2	49	383		
		S3 (max.)	86.2	1078		
		S4 (average)	184.2	548		

**Note:* *Based on section analysis Method C (strain compatibility analysis). Note that V_{uh} and v_{uh} will be lower using Method A or B. See Table 7-10 for comparison of analysis methods.*

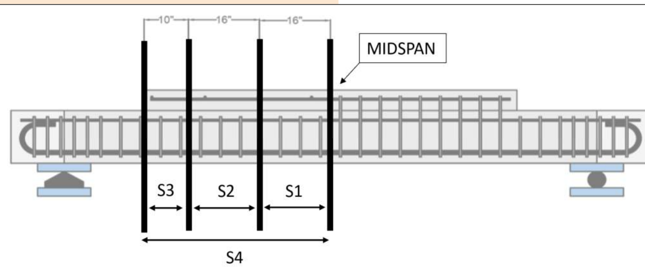

8.5.3. Estimation of Shear Stress Demand Using ACI 318

The estimated horizontal shear stresses in Table 8-5 using the ACI 318 simplified and segment methods illustrate that the interface shear demand used for design could vary significantly depending on the analysis method used. If the beam loads at interface shear failure (89.9 kips, 86.6 kips and 86.8 kips for the broom, tine and hydrodemolition beams, respectively) were assumed to be factored loads for design, the estimated horizontal shear stress demand using the simplified elastic method ranges from would have been less than 50 percent of the maximum demand estimated using the segment method.

The significant difference between the estimated interface shear stresses using the segment method and simplified method for the beam specimen is due to the composite condition wherein the topping slab (or section enlargement for repair) does not extend to the end of the beam. In this situation, the maximum shear stress near the end of the topping is significantly higher than the shear stresses along the length of the interface since the compression resultant in the topping decreases to zero at the end of the topping. In this situation, the shear stress in segment S3 (i.e., the last 10 inches of the topping) is more representative of the peak shear stress that will be developed and should be used for design. Using the simplified method would significantly underestimate the shear stress demand in this case.

The segment method requires selection of the segment length for the analysis. ACI 318-19 Clause 16.4.5 does not specify segment length; this is left to the discretion of the designer. In the situation where the topping or repair does not extend to the end of the member or a location of zero moment, the length selected for the analysis segment at the end of the topping or repair will affect the maximum estimated shear stress; short segment lengths will tend towards very high interface shear stresses in the end segment, while long segment may underestimate the maximum shear stress that may be developed. Since an unreinforced interface will typically be unable to redistribute interface shear stresses once the bond strength is exceeded at a peak stress location, a brittle debonding failure is likely. Thus, estimation of the peak shear stress is critical, and using average values may not be appropriate. For the beam specimens tested, the use of a segment length of 8 to 10 inches (effective depth of composite beam is just over 15 inches) results in an estimated peak shear stress at interface failure that is similar in magnitude to the direct shear strength of the interfaces tested using the guillotine shear test for the broom and hydrodemolition interfaces.

The simplified elastic method is implied by ACI 318-19 Clause 16.4.4. This method does not account for bonded interface length or the topping (or repair) depth relative to the full section depth or neutral axis depth. The simplified method is also presented in Article 5.7.4.5 of the AASHTO LRFD Bridge Design Specifications (AASHTO 2020). The commentary for this clause includes the derivation of the simplified interface shear stress formula, which demonstrates that this approach was intended for use for composite concrete slabs on girders where the horizontal interface is close to the neutral axis for the composite section. That is, the compression resultant in the slab is essentially equal to the total compression resultant. For this condition, and assuming the topping slab extends to the end of the member, the simplified and segment methods will estimate very similar, if not equivalent, interface shear demands. However, if the topping or repair does not extend to the end of the beam (or zero moment location), or if the depth of the topping does not correspond to the neutral axis depth, the difference between the estimated shear stresses obtained using the two methods may be non-trivial. In the former case, the peak stresses will be likely be higher using the segment method as discussed above. In the case where the topping depth is less than the neutral axis depth, the simplified method will overestimate the interface shear demand.

Lastly, it is noted that the AASHTO LRFD requirement for the simplified method uses d_v (distance between the centroid of the tension steel and the mid-thickness of the slab) to compute a factored interface shear stress while ACI 318 uses d (distance from extreme compression fiber for the entire composite section to the centroid of tension reinforcement). The use of d_v is consistent with the derivation shown in AASHTO LRFD C5.7.4.5 and will result in interface shear demands that are larger than using d per ACI 318. The difference between predictions using d_v and d will be small for deeper composite sections like concrete slabs on girders or a topping slab on a precast double-T beam. However, the difference between the two methods may be more significant for topping or repairs on shallow members like slabs.

In summary, the design of interface shear transfer for composite sections should be based on the segment method to estimate interface shear stress demands for situations where the topping or repair does not extend the full length of the member, or where the depth of the topping or repair is less than the neutral axis depth for the section. The segment method should consider the effects of flexural cracking of the composite section and non-linear section behavior when estimating the compression (or tension) resultants in the topping or repair.

8.6. Comparison of Guillotine Test to Other Direct Shear Test Methods

Currently there is no industry standard test method to measure shear bond strength for unreinforced interfaces in repair or new construction. Research studies have evaluated various shear test methods including the slant shear test, torsion or friction-transfer test, bi-surface or triplet test, and single-shear tests including the guillotine test, as summarized previously in Section 3.4. Most of these studies have compared different shear test methods to one another or to tensile bond strength by pull-off test or splitting tensile test. Results from shear-to-tensile comparisons were summarized previously in this report. A brief comparison of shear strength results for different test methods is summarized below.

Rosen (2016) reported ratios of average slant shear strengths to average guillotine shear strengths ranging from 3.8 to 6.4. Momayez et al. (2005) reported ratios of average slant shear strengths to average bi-surface shear strengths ranging from 3.2 to 3.5 and 3.3 to 3.7 for low and high roughness interfaces, respectively. The results indicate that slant shear strengths are consistently higher (on the order of at least three times higher) than direct shear strengths determined using the guillotine test or bi-surface shear test. These results illustrate the significant effect of compression across the interface in the slant shear test on the resulting shear strength. Since many repair and new construction topping applications do not have sustained compression across the unreinforced interface, the use of slant shear tests to establish interface shear strength for design is not appropriate.

The variability of the strength results for the different test methods is illustrated by the reported CoV values. The CoV for the guillotine shear tests from the current study ranged from 21 percent to 34 percent for specimens with moderate slump toppings. This range of CoV is comparable to the guillotine shear tests reported by others. Sprinkel (2016) tested two groups of cores with samples sizes of 10 and 7 and reported CoV of 30 percent and 23 percent. Rosen (2016) tested six groups of cores, each group with a sample size of 2, in guillotine shear and reported CoV ranging from 14.3 percent to 36.9 percent.

The CoV values for slant shear tests and bi-surface shear tests from previous studies are also variable. Santos (2009) reported CoV from slant shear tests from 2.0 percent to 38.3 percent for laboratory-cured specimens and from 6.7 percent to 28.4 percent for exterior cured specimens. Momayez et al. (2005) reported CoV for slant shear specimens ranging from 4.7 percent to 15.8 percent and CoV from bi-surface shear tests ranging from 6.5 percent to 13.3 percent.

The CoV for shear strength results in the current study and other research are higher than those normally associated with concrete compressive strength or splitting tensile strength results in new construction. However, this this not unexpected given the complex nature of interface shear failure and tests performed on samples obtained by coring. The limited comparison of guillotine shear strength results to other shear strength test methods does not indicate that the guillotine test is more variable than the slant shear test or bi-surface shear test.

9. OVERALL SUMMARY AND CONCLUSIONS

This project comprised two phases to investigate the bond of composite concrete-to-concrete interfaces. Phase 1 included 20 composite slabs with a series of direct shear and direct tensile bond tests. Within this phase, the use of the guillotine shear test method was explored while testing various interface surface preparations representative of repair and precast members. Phase 2 studied interface shear failure in composite beam specimens along with additional direct shear and direct tensile bond tests. Key observations from this research study are presented below.

- The guillotine shear test appears to be an appropriate method to assess interface bond strength for composite concrete members (new construction and repairs).
- The ratio of direct shear strengths obtained by the guillotine shear test and direct tensile strengths from pull-off tests are between 2.1 to 3.6.
- The ratio of direct shear strengths obtained by the guillotine shear test and maximum horizontal shear strengths from flexural tests area are between 0.5 to 1.1.
- Sound, tightly-adhered concrete-to-concrete bond is dependent on many factors including moderate topping slump, good topping consolidation, and moderate substrate roughness.
- Concrete-to-concrete bond strength is not consistently related to the degree of roughness measured by mean texture depth.
- Average direct shear strength results ranged from 8 to 13 times greater than the nominal value of 80 psi specified by ACI 318-19 and ACI 562-19 for design of unreinforced interfaces for shear.
- Maximum horizontal shear stresses at interface shear failure in beam tests were more than 13 times greater than the nominal value of 80 psi specified by ACI 318-19 and ACI 562-19 for design of unreinforced interfaces for shear.

9.1. Phase 1 Summary and Conclusions

Phase 1 of this experimental program comprised 192 direct shear tests and 84 direct tensile pull-off tests performed on slab specimens with six different interface conditions. The interface conditions were defined in two series; the repair series considered sandblast only, bush hammer + sandblast, and hydrodemolition interface preparation techniques, while the precast series considered float, broom, and tine (rake) finishes. The interface preparation types were selected to provide a range of surface roughness conditions. The surface texture was quantified using mean texture depth measured using laser line scanning.

The topping or repair concrete for the repair series was placed with a moderate slump (5 inches) and was consolidated in two lifts by hand. The topping concrete for the precast series was placed with lower slump (< 4 inches) and with moderate slump (> 5 inches). The lower slump concrete was consolidated by screed only, while the moderate slump concrete considered two consolidation methods: hand consolidation (2 lifts) and vibration.

The primary objectives of the Phase 1 study were as follows:

- To collect data on interface shear strength for a range of interface conditions using the guillotine direct shear test method performed on core samples.

- To study the correlation between direct shear strength from the guillotine shear test method and direct tensile pull-off strength.
- To determine whether the ACI nominal interface shear stress limits for unreinforced interfaces in repair and new construction should be redefined.

Although the intent of the research was not to determine the optimal surface or interface preparation technique and concrete placement method for repair and new construction, the direct shear and tensile pull-off strength test data collected also provide some insight to the effects of interface type and concrete placement on interface bond strength. The primary findings of Phase 1 are summarized below.

9.1.1. Effect of Interface Preparation - Repair Series

- The substrate interface prepared by hydrodemolition had the highest direct shear and tensile pull-off strengths in the repair series specimens. Hydrodemolition produces a surface profile with a high degree of surface roughness with a low risk for microcracking or bruising.
- The bush hammer + sandblast interface had the lowest shear and tensile bond strengths in the repair series. The results suggest that microfractures in the cement paste and loosening of the coarse aggregate occurred at the substrate surface, creating a weakened or bruised layer that was not removed by subsequent sandblasting. This surface preparation type had the highest ratio of shear-to-tensile bond strength of all interfaces investigated, suggesting that the microcracking had a more significant effect on the tensile pull-off strength than on the direct shear strength.
- The sandblast only interface achieved higher direct shear and tensile pull-off strengths than the bush hammer + sandblast interface and had comparable strength results to the broom and tine interfaces in the precast series. These results illustrate the benefits of limited “intentional roughening” that removes laitance and minor surface defects while opening the paste pore structure at the repair interface. Note that while good performance of the sandblast interface was observed in Phase 1, beam and slab specimens with sandblast only preparation debonded in Phase 2, likely due to differential shrinkage.

9.1.2. Effect of Interface Preparation - Precast Series

- The broom interface developed an average direct shear strength approximately 20 percent higher than the tine interface. The average tensile pull-off strength was similar for the two interfaces. The broom interface shear strength results were slightly less variable than the results for the tine surface, although the opposite trend was noted for the tensile pull-off strength results.
- While it is generally assumed that a tine or rake finish will provide more surface roughness than a broom finish and thus improve interface bond strength, the results of this study do not indicate a consistent improvement in bond strength for the tine finish. This finding suggests that bond strength is less influenced by surface roughness than interface strength due to friction. The uniform roughness provided by the broom finish appears to be as, or more, effective as the deep, widely spaced grooves created by the rake tines in terms of interface shear bond strength.
- The loading direction relative to the broom or tine orientation (parallel or perpendicular) did not provide a meaningful effect on interface shear strength results.

9.1.3. Effect of Consolidation Method

- Consolidation of moderate slump topping in the precast series by hand consolidation or vibration did not have a meaningful effect on interface direct shear strength results.
- Consolidation of lower slump topping in one layer without mechanical vibration resulted in low interface direct shear strength results and debonding of the topping.

9.2. Phase 2 Summary and Conclusions

Phase 2 of the experimental program comprised five composite beams with different interface preparations and one monolithic beam. The experimental program also included direct shear (guillotine) tests and direct tensile pull-off tests on samples from companion composite slabs. The interface preparation techniques considered were broom, tine, sandblast, hydrodemolition, float, and monolithic. The broom and tine specimens were representative of precast or new construction, the sandblast and hydrodemolition specimens were representative of repair practice, and the float and monolithic specimens were included to compliment the experimental program as a low and high boundary for composite beam behavior.

The surface texture was quantified by mean texture depth which determined by an analysis of 3D data obtained by laser scanning. The topping or repair concrete for all specimens was placed with a moderate slump (5.75 inches) and was vibrated for consolidation.

The monolithic beam developed its full flexural capacity while three of the composite beams failed due to horizontal shear at their unreinforced interface (as designed), and two of the composite beams exhibited interface delaminations prior to testing resulting in non-composite behavior (the companion slabs to these beams also delaminated).

The primary objectives of the Phase 2 study were as follows:

- To test the behavior of an unreinforced interface when subject to high horizontal shear stresses caused by bending.
- To study the correlation between interface horizontal shear strengths determined from flexural tests and direct shear strength from the guillotine shear test method.
- To further study the correlation between direct shear strength from guillotine shear tests and direct tensile pull-off strength.
- To compare interface shear strengths from two test methods to the ACI nominal interface horizontal shear stress limits for unreinforced interfaces in repair and new construction.

Phase 2 of this study was intended to complement the Phase 1 findings on concrete-to-concrete interface shear strength. The main goal of this project to find an appropriate method to assess bond strength with the possibility of increasing the nominal shear limit when proven capable. The primary findings of Phase 2 are summarized below.

9.2.1. Effect of Interface Preparation Technique on Debonding

- The beam and slab specimens with substrates prepared by sandblast and float delaminated prior to testing resulting in no horizontal shear strength. The likely cause of this failure was differential shrinkage between the substrate and topping.

- The occurrence of debonding in these specimens was likely due to the very low surface roughness in comparison to the other interface preparation techniques (hydrodemolition, broom and tine) that did not debond.

9.2.2. Effect of Interface Preparation Technique – Precast Series

- The Phase 2 direct shear tests indicated that the broom interface developed higher average direct shear strength than the tine interface, and comparable average tensile pull-off strength. This is consistent with the Phase 1 findings.
- Although the tine or rake finish typically provides more surface roughness than a broom finish, this does not appear to correlate with a consistent improvement in bond strength for the tine finish.

9.2.3. Effectiveness of the Beam Test to Study Interface Shear

- The beam tests were included in Phase 2 to provide an evaluation of bond strength in composite beams where interface shear is developed due to bending rather than direct shear. The beam tests require substantial experimental effort to prepare and conduct, and the experimental results do not provide a direct measurement of the interface shear strength at failure. The measured load, vertical deflection, interface slip, and reinforcement strain response from the beams was interpreted to estimate the maximum and average interface shear stresses corresponding to interface shear failure. Three different analysis approaches were used to estimate the interface shear forces and stresses.
- The composite beam specimens with interfaces prepared by broom, tine, and hydrodemolition presented a consistent response: the differences in interface preparation technique and surface roughness did not have a meaningful effect on the beam load that caused interface shear failure; failure loads were between 86.6 kips and 89.9 kips.
- The measured reinforcement strain response indicates that the interface shear stresses are maximum near the end of the topping region in the composite beam. This occurs because the topping does not extend to the end of the beam or a location of zero moment, creating a region of higher shear stresses near the end of the topping. The estimated peak interface shear stresses at failure was on the order of 1,000 psi, while the average shear stress at failure was about 550 psi for the interfaces tested.
- The ratio of average direct shear strength to maximum horizontal shear strength from flexural testing is 0.85 and 1.1 for broom and hydrodemolition, respectively. The ratio of average direct shear strength to average horizontal shear strength from flexural testing is 1.7 and 2.2 for broom and hydrodemolition, respectively.
- While the data suggest that the maximum horizontal shear strength from beam tests is lower than that measured from direct shear testing, it is noted that the shear strengths from the beam test are estimated using reinforcement strain data. The section analysis procedure used, related assumptions, and the locations of the strain gauges may influence the apparent interface shear stress at failure. That is, the apparent interface shear strength from the beam tests could be higher or lower than the values reported herein.

9.3. Findings Based on Results from Both Phases

The primary aspects and parameters of the experimental program were the same between the two phases. The findings based on the combined results from the two phases are summarized below.

9.3.1. Effect of Interface Surface Roughness on Shear and Tensile Bond Strength

- The combined Phase 1 and Phase 2 shear and tensile bond strengths of the unreinforced interfaces considered in this study do not indicate a consistent correlation with degree of surface macrotexture roughness quantified by MTD.
- The surface roughness, measured using MTD, was more consistent between phases and specimen types for repair surface preparations (hydrodemolition) than for precast surface preparations. This may reflect variability of concrete finishing by broom and tining rake due to finishing practices and personnel.
- The results suggest that the interface bond strength in shear may be less dependent on degree or magnitude of surface roughness, and more dependent on having a uniformly roughened surface that is sound (i.e., no laitance or surface defects) and having well consolidated repair or topping concrete.
- Finishes without intentional roughening, including floated or as-cast surfaces and sandblast only surfaces, may be prone to debonding due to differential shrinkage.

9.3.2. Correlation Between Direct Shear Strength and Tensile Pull-off Strength

- The ratio of direct shear strength to tensile pull-off strength ranged from 2.1 to 3.6 for the interfaces considered in this study, with an average of 2.70. The data indicate a good linear correlation between interface shear and tensile strength with a coefficient of determination (R^2) value of 0.98 (assuming y-intercept of zero; correlation is decreased for a non-zero y-intercept).
- The test results from the current study and published research indicate that the ratio of interface shear to tensile strength is dependent on several factors, including interface surface preparation and roughness, material properties and test methods used. These findings suggest that if tensile pull-off tests are intended to provide an indication of shear bond strength for quality control purposes, the ratio of interface shear strength to tensile pull-off strength should be determined based on test data on a project-by-project basis.
- The ACI 562-19 Clause R7.4.3 (Commentary) statement that "it is generally adequate to assume that the repair to substrate bond will resist an interface shear equal to the direct tensile pull-off test result" appears to provide a conservative lower bound to the relationship between interface shear and tensile bond strength.

9.3.3. Horizontal Shear Demand Provisions in ACI 318-19

- The ACI 318 provisions for horizontal shear transfer in composite members permit the use of a simplified method or an alternative (segment method) to estimate the shear demand at the interface between connected elements. These methods are expected to produce similar shear stress demands for typical composite construction applications such as concrete slabs on girders or a topping slab on a precast double-T beam where the neutral axis depth in the composite member coincides with the interface between the two materials.

- The analysis of the Phase 2 beam test results illustrates that the simplified and segment methods may estimate significantly different interface shear demands depending on the configuration of the composite member. In particular, the simplified method may substantially underestimate the maximum interface shear stress in situations where the composite topping or repair does not extend to the end of the member or to a location of zero moment.
- The design of interface shear transfer for composite sections should be based on the segment method to estimate interface shear stress demands for situations where the topping or repair does not extend the full length of the member, or where the depth of the topping or repair is less than the neutral axis depth for the section. The segment method should consider the effect of the segment length on the estimated peak shear and account for the effects of flexural cracking of the composite section and non-linear section behavior when estimating the compression (or tension) resultants in the topping or repair.

9.3.4. Interface Shear Bond Strength for Design

- The combined results for all Phase 1 and 2 interface conditions (repair and precast) investigated with a moderate slump and well consolidated topping achieved average direct shear (guillotine) strengths approximately 8 to 13 times higher than the nominal horizontal shear strength limit of 80 psi specified in ACI 318-19 and ACI 562-19.
- Phase 2 beam test results achieved bond strengths more than 10 times higher than the nominal horizontal shear strength limit of 80 psi specified in ACI 318-19 and ACI 562-19.
- A summary of published research investigating bond strength of unreinforced interfaces using beam tests, bond tests, and other types of shear tests consistently reported average shear strengths in excess of the nominal horizontal shear strength limit of 80 psi specified in ACI 318-19 and ACI 562-19.
- Characteristic design strengths estimated based on the test data using the Tolerance Factor Method (5 percent fractile at 90 percent confidence) ranged from 1.9 to more than 6.6 times higher than the ACI nominal shear strength of 80 psi.

9.3.5. Guillotine Shear Test Method

- The guillotine direct shear test is a practical method to assess interface bond shear strength using cores from laboratory specimens, new construction, and existing structures. The core is subjected to direct (single) shear, which allows assessment of the bond strength without a normal force acting on the interface. The test can be readily performed in a concrete compression testing frame or universal testing frame using a simple guillotine shear jig.
- A comparison of direct shear (guillotine) strength results with maximum estimated shear stresses at interface failure in composite beam specimens indicates similar, but higher shear strengths from the guillotine test. The beam test data in the current study is very limited; additional testing would be required to establish the relationship between the test methods.

10. APPLICATION OF RESEARCH FINDINGS

The research results indicate that a sound (i.e., not bruised or microcracked by concrete removal), laitance and defect free interface with moderate and uniform surface texture in combination with good consolidation of the repair or topping materials are keys to good shear and tensile bond strengths. The results show that interfaces with these characteristics can achieve average and characteristic interface shear strengths significantly higher than the ACI nominal shear strength of 80 psi.

The current research study and published research indicates that bond strength may vary significantly due to substrate surface preparation, substrate and topping or repair material properties, topping or repair material placement, consolidation and curing procedures, and the effects of differential volume changes (e.g., shrinkage and thermal).

Many of the findings from the current study and other published research can be applied to improve design and construction for unreinforced interfaces in new construction and partial depth repairs. The following recommendations are proposed for consideration.

10.1. Qualitative Requirements or Commentary

The following factors have been demonstrated as important for bond strength in unreinforced interfaces:

- Uniform intentional roughness.
- Sound substrate free from laitance and microcracking.
- Well consolidated topping or repair concrete.
- While not directly related to bond strength, the use of moist curing and low shrinkage topping or repair concrete will reduce differential shrinkage and reduce the likelihood of debonding due to volume changes.

The first two factors listed above are qualitatively addressed by ACI 318-19 Clause 16.4.4; however, no specific recommendations or requirements for consolidation of the topping, curing, or use of low shrinkage materials in composite construction are included in ACI 318 or ACI 301. Consideration should be given to adding requirements or commentary language to convey the importance of these factors.

The factors listed above are not explicitly addressed in ACI 562-21 Clause 7.4, although the quantitative bond strength testing requirements will identify poor bond conditions in concrete repair construction. Consideration should be given to adding commentary language to convey the importance of these factors and reduce the likelihood of poor bond strength results.

10.2. Performance-Based Approach for Interface Design Shear Strength

The research suggests that a performance-based methodology could be considered to establish a design (i.e., nominal or characteristic) interface shear bond strength based on direct shear tests performed using project-specific material, interface, and construction parameters.

The following is suggested as a possible performance-based approach to shear design strength for unreinforced interfaces:

1. Retain a lower bound nominal interface shear bond strength of 80 psi for situations where project-specific testing to establish a characteristic bond strength is not justified.

2. Where project circumstances justify a performance-based approach:
   a. Prepare mockups of project conditions, including interface preparation techniques, substrate and topping or repair materials, substrate conditioning, and topping or repair material placement and consolidation.
   b. Perform testing[1] on the mockups to determine the interface shear strength. The sample size can be adjusted based on the observed variability of the results obtained and the outcome of the characteristic strength calculation in 2c.
   c. Establish a characteristic shear strength for design using the Tolerance Factor Method based on the test data collected. A 5 percent fractile (95 percent probability of exceedance) and 90 percent confidence level is recommended (consistent with requirements for anchorage to concrete).
   d. Perform direct tensile pull-off testing on the mockups to establish the expected tensile bond strength for the project conditions. Implement quality control testing using direct tensile pull-off tests to verify that as-constructed conditions are consistent with those in the mockups used to establish the characteristic shear design strength.

[1] Direct shear (guillotine) tests on cores extracted from the mockups could be used for this purpose. Other direct shear or torsional shear tests may be appropriate. Slant shear tests are not appropriate for this purpose due to the effect of compression across the interface in the test specimen that may overestimate the in-situ shear strength.

11. REFERENCES

AASHTO (2020). "LRFD Bridge Design Specifications," 9th Edition, American Association of State Highway and Transportation Officials. Washington, DC.

ACI-ASCE Committee 333, (1960). "Tentative Recommendations for Design of Composite Beams and Girders, for Buildings." ACI Journal, 57(6), 609 – 628.

ACI 214.4R-10, (2010), "Guide for Obtaining Cores and Interpreting Compressive Strength Results." American Concrete Institute. Farmington Hills, MI.

ACI 228.1R-19, (2019), "In-Place Methods to Estimate Concrete Strength." American Concrete Institute. Farmington Hills, MI.

ACI 318-63, (1963). "Building Code Requirements for Structural Concrete and Commentary." American Concrete Institute. Farmington Hills, MI.

ACI 318-71, (1971). "Building Code Requirements for Structural Concrete and Commentary." American Concrete Institute. Farmington Hills, MI.

ACI 318-19, (2019). "Building Code Requirements for Structural Concrete and Commentary." American Concrete Institute. Farmington Hills, MI.

ACI 562-19, (2019). "Code Requirements for Assessment, Repair, and Rehabilitation of Existing Concrete Structures and Commentary." American Concrete Institute. Farmington Hills, MI.

ACI 355.4R-19, (2019). "Qualification of Post-Installed Adhesive Anchors in Concrete." American Concrete Institute. Farmington Hills, MI.

ASTM Standard C39/ C39M, (2020). "Standard Test Method for Compressive Strength of Cylindrical Concrete Specimens.". ASTM International. West Conshohocken, PA.

ASTM C143-15, (2015). "Standard Test Method for Slump of Hydraulic-Cement Concrete." ASTM International. West Conshohocken, PA.

ASTM C1583-20, (2020). "Standard Test Method for Tensile Strength of Concrete Surfaces and the Bond Strength or Tensile Strength of Concrete Repair and Overlay Materials by Direct Tension (Pull-off Method)." ASTM International. West Conshohocken, PA.

ASTM C496/ C496M-17, (2017). "Standard Test Method for Splitting Tensile Strength of Cylindrical Concrete Specimens." ASTM International. West Conshohocken, PA.

ASTM E965-15, (2015). "Standard Test Method for Measuring Pavement Macrotexture Depth Using a Volumetric Technique." ASTM International. West Conshohocken, PA.

Becker, M.E., (2020). "Investigation of Bond in Unreinforced Concrete Interfaces for Partial Depth Repairs and New Construction." M.S. Thesis, University of Texas at Austin, 160 pp.

BS EN 1504-10 (2017). "Products and systems for the protection and repair of concrete structures. Definition, requirements, quality control and evaluation of conformity. Site application of products and systems and quality control of the works." British Standards Institution, London, UK.

El Hachem, Y., (2019). "The UTexas Seal Coat Design Method Using 3D Laser Technology." M.S. Thesis, University of Texas at Austin, 318 pp.

fib Model Code 2010, (2013). "fib Model Code for Concrete Structures 2010." International Federation for Structural Concrete (fib). Berlin, Germany.

Hanson, N. W., 1960, "Precast-Prestressed Concrete Bridges: Horizontal Shear Connections," Bulletin, PCA Research and Development Laboratories, V. 2, No. 2, May, pp. 38-58. doi: 10.14359/16708

ICRI 310.2R-2013, (2013). "Selecting and Specifying Concrete Surface Preparation for Sealers, Coatings, Polymer Overlays, and Concrete Repair," International Concrete Repair Institute.

ICRI 210.3R-2013, (2022). "Guide for Using In-Situ Tensile Pull-off Tests to Evaluate Bond of Concrete Surface Materials," International Concrete Repair Institute.

Kaar, P. H., Kriz, L. B., and Hognestad, E., (1960). "Precast Prestressed Concrete Bridges: (1) Pilot Tests of Continuous Girders," PCA Research and Development Laboratories Bulletin, V. 2, No. 2, May, pp. 21-37. doi: 10.14359/51685340

Kovach, J. D. & Naito, C., (2008). "Horizontal Shear Capacity of Composite Concrete Beams without Interface Ties" Advanced Technology for Large Structural Systems (ATLSS) Report No. 08-05. Bethlehem, PA.

Loov, R. E., & Patnaik, A. K., (1994). "Horizontal Shear Strength of Composite Concrete Beams with a Rough Interface". PCI Journal, 39(1), 48 - 69.

Momayez, A., Ramezanianpour, A.A., Raijai, H. and Ehsani, M.R., (2004). "Bi-surface shear test for evaluating bond between existing and new concrete, American Concrete Institute, ACI Materials Journal, Vol. 101, No. 2, pp. 99-106, March-April 2004.

Momayez, A., Ehsani, M.R., Ramezanianpour, A.A. and Rajaie, H., (2005) "Comparison of methods for evaluating bond strength between concrete substrate and repair materials", Elsevier, Cement and Concrete Research, Vol. 35, No. 4, pp. 748-757, April 2005.

Mones, R. M., & Brena, S. F., (2013). "Hollow-core Slabs with Cast-in-place Concrete Toppings: A Study of Interfacial Shear Strength." PCI Journal 58(3):124-141.

Ozell, A. M., & Cochran, J. W., (1956). "Behavior of Composite Lintel Beams in Bending." PCI Journal, 1(1), 38-48.

Revesz, S., (1953). "Behavior of Composite T-Beams with Prestressed and Unprestressed Reinforcement." ACI Journal, 24(6), 585 – 592.

Rosen, C., (2016). "Shear Strength at the Interface of Bonded Concrete Overlays" M.S. Thesis submitted to the University of Colorado. The University of Colorado. Denver, Colorado

Saemann, J. C., & Washa, G. W., (1964). "Horizontal Shear Connections between Precast Beams and Cast-inPlace Slabs," ACI Journal Proceedings, V. 61, No. 11, Nov., pp. 1383-1409. doi: 10.14359/7832.

Santos, P., (2009). "Assessment of the Shear Strength between Concrete Layers." Thesis for Doctor of Philosophy in Civil Engineering, University of Coimbra. Coimbra, Portugal.

Seible, F., & Latham, C., (1990). "Horizontal Load Transfer in Structural Concrete Bridge Deck Overlays." Journal of Structural Engineering ASCE, 116(10), 2691-2709.

Silfwerbrand, J., (2003). "Shear Bond Strength in Repaired Concrete structures". Materials & Structures, Vol. 36, July 2003, pp. 419-424.

Sprinkel, M. (2016) "Bond Strength Between Shotcrete Overlay and Reinforced Concrete Base." Concrete Repair Bulletin, January/February 2016.

Swan, A. (2016). "Alternate Methods for Testing Shear Strength at a Bonded Concrete Interface." M.S. Thesis submitted to the University of Colorado. Denver, Colorado.